

## ABSTRACT

Title of Dissertation:                   **QUANTIFYING FIRE-INDUCED SURFACE  
FORCING IN SIBERIAN LARCH FORESTS**

  Dong Chen, Doctor of Philosophy, 2017

Dissertation directed by:            Dr. Tatiana V. Loboda, Associate Professor,  
  Department of Geographical Sciences

Wildfires are a common disturbance agent in the global boreal forests. In the North American boreal forests, they have been shown to exert a strong cooling effect through post-fire changes in surface albedo that has a larger overall impact on the climate system than associated carbon emissions. However, these findings are not directly applicable to the Siberian larch forests, a major component of the boreal biome where species composition are dominated by a deciduous needleleaf species and fire regimes are characterized by the common occurrence of both stand-replacing and less-severe surface fires. This dissertation quantifies the post-fire surface forcing imposed by both fire types in these forests over 14 years since fire, and determines that both surface and stand replacing fires impose cooling effects through increased albedo during snow season. The magnitude of the cooling effect from stand replacing fires is much larger than that of surface fires, and this is likely a consequence of higher levels of canopy damage after stand-replacing fires. At its peak (~ year 11 after

fire occurrence), the cooling magnitude is similar to that of the North American boreal fires. Strong cooling effect and the wide-spread occurrence of stand-replacing fires lead to a net negative surface forcing over the entire region between 2002 and 2013. Based on the extended albedo trajectory which was made possible by developing a 24-year stand age map, it was shown that the cooling effect of stand-replacing fires lasts for more than 26 years. The overall cooling effect of surface fires is of lower magnitude and is likely indicative of damages not only to the canopies but also the shrubs in the understory. Based on the identified difference in their influences on post-fire energy budget, this dissertation also identified a remote sensing method to separate surface fires from stand-replacing fires in Siberian larch forests with an 88% accuracy. The insights gained from this dissertation will allow for accurate representation of wildfires in the regional or global climate models in the future.

QUANTIFYING FIRE-INDUCED SURFACE FORCING IN SIBERIAN LARCH  
FORESTS

by

Dong Chen

Dissertation submitted to the Faculty of the Graduate School of the  
University of Maryland, College Park, in partial fulfillment  
of the requirements for the degree of  
Doctor of Philosophy  
2017

Advisory Committee:

Associate Professor Tatiana V. Loboda, Chair  
Professor Shunlin Liang  
Dr. Ivan Csiszar  
Professor Zhanqing Li  
Associate Research Professor Dongdong Wang

© Copyright by  
Dong Chen  
2017

## **Dedication**

To my parents, Xuxu Ren, Tieping Chen, and my wife Tingting Zhong.

## **Acknowledgements**

I would first like to thank my advisor Dr. Tatiana Loboda. Thank you for offering me this wonderful opportunity to work with you in one of the best geography programs in the world. Over the past six years, you have taught me so much that any descriptive words are understatement. You helped me understand the qualities that a scientist should possess: perseverance, diligence, passion, and many others. And you did that not by telling me, but by showing me through your daily work routine. Under your guidance, my other abilities have been considerably improved as well, such as my communicational skills and creative thinking. I am truly proud to be your student and hopefully one day I can be a good scientist and mentor as you are.

I would also like to thank my committee members. Thank you, Dr. Shunlin Liang, Dr. Ivan Csiszar, Dr. Zhanqing Li, Dr. Dongdong Wang, and Dr. Guoqing Sun, for all the guidance and advice that you have given me throughout my dissertation project. Without them, this dissertation work would be lackluster and I would not be able to present it with confidence. With your encouragement, I will continue working passionately on my path of seeking truth in science.

I would like to thank all my friends and colleagues, especially my lab mates, for the support you have given me over the past six years. They meant a lot to me and without them I would not have reached this far.

To my family, especially my parents and my wife, thank you for standing behind me and supporting me unconditionally every single day. I love you!

# Table of Contents

Dedication.....	ii
Acknowledgements.....	iii
Table of Contents.....	iv
List of Tables.....	vi
List of Figures.....	vii
Chapter 1: Introduction.....	1
1.1. Background and Motivation.....	1
1.2. Research Questions and Dissertation Structure.....	9
1.2.1. Question 1: What is the stand age distribution of the Siberian larch forests over the past 24 years?.....	9
1.2.2. Question 2: What is the surface forcing imposed by stand-replacing fires in the Siberian larch forests since 2000?.....	10
1.2.3. Question 3: What is the surface forcing imposed by surface fires and how does it differ from stand-replacing fires?.....	10
Chapter 2: Mapping stand age dynamics of Siberian larch forests from recent Landsat observations using an innovative approach.....	12
2.1. Introduction.....	12
2.2. Study area.....	16
2.3. Data.....	18
2.4. Methodology.....	21
2.4.1. Training a random forest.....	22
2.4.2. Applying the random forest.....	24
2.4.3. Accuracy assessments.....	25
2.5. Results.....	27
2.5.1. Selected random forest model.....	27
2.5.2. Accuracy assessment results.....	28
2.5.3. Stand age map.....	31
2.6. Discussion.....	33
2.6.1. Accuracy of the produced map.....	33
2.6.2. 24-year stand age distribution in the Siberian larch forests.....	38
2.7. Conclusion.....	39
Chapter 3: Strong cooling induced by stand-replacing fires through albedo in Siberian larch forests.....	41
3.1. Introduction.....	41
3.2. Data and Methods.....	44
3.3. Results.....	49
Figure.....	60
3.4. Discussion.....	61
3.4.1. Strong fire-induced cooling effect in the Siberian larch forests.....	61
3.4.2. Mechanism of the fire-induced cooling effect.....	63
3.4.3. Spatial distribution of 12-year SF and its implications.....	65
3.5. Conclusion.....	67
Chapter 4: Surface fires in Siberian larch forests and associated surface forcing.....	68
4.1. Introduction.....	68

4.2. Materials and methods .....	72
4.3. Results.....	75
4.4. Discussion.....	81
4.4.1. Temporal and spatial distribution of surface fires in the Siberian larch forests between 2001 and 2012.....	81
4.4.2. Surface forcing trajectory of surface fires.....	82
4.4.3. Identifying surface and stand-replacing fires using remote sensing-based burn severity indices .....	84
4.5. Conclusion .....	86
Chapter 5: Conclusion.....	88
5.1. Major findings.....	88
5.1.1. Cooling effects of wildfires in the Siberian larch forests through fire-induced albedo changes .....	88
5.1.2. Effectiveness of dNBR as a measure differentiating stand-replacing fires from surface fires .....	89
5.1.3. The stand age dynamics of the Siberian larch forests.....	90
5.2. Implications for climate science .....	90
5.3. Future work.....	93
References.....	95



## List of Tables

Table 2-1 Summary of the datasets.....	19
Table 2-2 Confusion matrix for the 1989-2000 era. ....	29
Table 2-3 Confusion matrix for the 2001-2012 era. ....	29
Table 2-4 Estimated area of unburned and burned forests at the 95% confidence level. .....	29

## List of Figures

Figure 1-1 Distribution of the Siberian larch forests (diagonally striped area) in relation to the global boreal biome (shaded area), southern boundaries of the continuous permafrost (thick dashed line) and discontinuous permafrost (thin dashed line). Figure is adopted from Osawa and Zyryanova (2010). .....	6
Figure 2-1 Location of the study area, as indicated in light green. This study area reflects a conservative estimate of the Siberian larch forest distribution focusing on stands dominated by larch species. The study area presented is not intended to be used as a definitive boundary of the Siberian larch forests. ....	17
Figure 2-2 General workflow of the proposed method.....	22
Figure 2-3 Variable importance ranking according to the produced random forest model. From left to right the variable importance decreases.....	28
Figure 2-4 Assessment results generated based on the active fire component of the ABFM product. Each histogram corresponds to a fire polygon group for a separate year. The ESA values (defined in Section 2.4.3) are represented by the blue bars in the background.....	30
Figure 2-5 Assessment results generated based on the burn scar component of the ABFM product. Each histogram corresponds to a fire polygon group for a separate year. The ESA values (defined in Section 2.4.3) are represented by the blue bars in the background.....	31
Figure 2-6 (a) The produced 24-year stand age distribution map for the Siberian larch forests in 2012 with 30-m resolution. Insets (b)-(d) show detailed views of three subsets of the stand age map. ....	32
Figure 2-7 Inter-annual burned area distribution calculated based on the produced stand age map and the associated accuracy statistics. Blue and yellow represent the pre-2000 and post-2000 components of the produced map, respectively. Dashed lines represent the mean annual burned area during the corresponding 12-year period. ....	33
Figure 2-8 An example fire event: a) Landsat image on 7/31/1999, b) Landsat image on 8/10/2000, c) dNBR calculated based on a) and b), d) estimated year of burn according to the produced map (black indicates unclassified area).....	37
Figure 3-1 The statistical relationship between annual mean BSA and WSA between 2001 and 2015 within the study area. ....	47
Figure 3-2 Annual mean SF trajectory for burned forests. Grey area denotes $\pm 1$ standard deviation range. ....	50
Figure 3-3 Mean BSA trajectories for the burned forests generated using the MODIS albedo data for 2001-2015. The vertical dashed line represents the year of fire occurrence. The negative “year since fire” range represents pre-fire conditions. The horizontal dashed lines represent the mean pre-fire BSA for the corresponding trajectories. Uncertainties are represented by shaded areas within $\pm 1$ standard deviation.....	51
Figure 3-4 Mean annual mean BSA trajectory (red) compared with the BSA uncertainty range calculated based on $\pm 1$ year variation in the assumed timing of disturbance within the pre-2000 stand age values in the 24-year stand age map. ....	52
Figure 3-5 Monthly SF trajectories for the burned forests. Uncertainty is represented by $\pm 1$ standard deviation.....	53

Figure 3-6 Monthly mean total downward shortwave surface flux between 2001 and 2015. Error bars represent $\pm 1$ standard deviation. ....	54
Figure 3-7 The 8-day BSA anomalies calculated for the forests that burned between 2001 and 2012. Green and red represent albedo increase and decrease, respectively, relative to the forests that did not experience stand-replacing fires during 2001-2012. In each graph, the x-axis is Julian Day and the y-axis is year (from 2001 to 2015)...	55
Figure 3-8 SF between 2001 and 2013 for the Siberian larch forests. Black color represents unclassified area or missing data. Six $10^\circ \times 7.5^\circ$ zones are superimposed on top of the distribution map and are labeled sequentially. ....	58
Figure 3-9 Area proportion of the five SF ( $Wm^{-2}$ ) classes within (a) burned and (b) unburned forests between 2001 and 2012.....	59
Figure 3-10 Results of the zonal analysis: (a) Mean 2001-2013 SF calculated for all 6 zones based on burned forests only, unburned forests (between 2001 and 2012) only and burned and unburned forests combined. The dashed line represents mean 2001-2013 SF calculated based on all forests (burned + unburned) across the entire study area. Uncertainties are represented by $\pm 1.96 \times$ standard error. (b) Areal distribution of burned and unburned forests across the 6 zones. Labels show the proportions of burned forest area out of all forests area in the corresponding zones. ....	60
Figure 3-11 Mean snowmelt and snow onset dates in the study area between 2001 and 2015 determined based on the MODIS MOD10A1 daily snow cover product. The dashed lines represent linear trends. ....	61
Figure 4-1 Comparison of (a) annual area distribution and (b) total area between surface and stand-replacing fires between 2001 and 2011. ....	76
Figure 4-2 Distribution of surface fires in the Siberian larch forests between 2001 and 2012.....	76
Figure 4-3 Comparison of mean SF trajectories of surface (this chapter) and stand-replacing (see chapter 3 for details) fires. Solid red and blue lines represent the mean SF trajectories of stand-replacing and surface fires, respectively. Uncertainties are represented by shaded areas within $\pm 1$ standard deviation. ....	77
Figure 4-4 Mean BSA trajectories for the burned forests generated using the MODIS albedo data for 2001-2015. The vertical dashed line represents the year of fire occurrence. The negative “year since fire” range presents pre-fire conditions over two years before fires. The horizontal dashed lines represent the mean pre-fire BSA for the corresponding trajectories. Uncertainties are represented by shaded areas within $\pm 1$ standard deviation. ....	78
Figure 4-5 Classification accuracy of first post-fire (a) snow season dBSA, (b) summer dNBR, and (c) summer dNDVI in differentiating surface fires from stand-replacing fires. Each bar represents the classification accuracy associated with a single threshold value. The red bar in each graph represents the threshold value with the most optimal classification accuracy for the corresponding index. ....	80

# Chapter 1: Introduction

## 1.1. Background and Motivation

The Earth's climate system is essentially driven by solar radiation through the net balance of incoming solar radiation and outgoing shortwave radiation reflected by the atmosphere and the Earth's surface and longwave radiation emitted by the Earth (Cubasch et al. 2013; Liang 2004). The climate system is stable when the incoming and outgoing radiation is balanced, i.e. the global net radiation is zero. On the contrary, imbalances in incoming and outgoing radiation destabilize global climate system, resulting in climate change. The three major components that influence radiation balance include the amount of the incoming solar radiation, the fraction of the incoming solar radiation that is reflected from the atmosphere and the Earth's surface, and the ability of atmosphere to trap the outgoing longwave radiation. The role of the latter has been most prominently discussed in the scientific literature and is linked to the atmospheric concentration of greenhouse gases (e.g. CO<sub>2</sub> and CH<sub>4</sub>). The greenhouse gases are capable of retaining longwave radiation that is otherwise emitted into space, resulting in a warming effect (i.e. the greenhouse effect) (Cubasch et al. 2013; Myhre 2013). Due to the continuous increase of atmospheric concentration of the greenhouse gases, the global mean surface temperature has been experiencing a persistent increase since the late 19<sup>th</sup> century (Bindoff 2013). The influence of the increased concentration of greenhouse gases on the climate system is modified by other components of the radiation balance that influence the amount of incoming radiation that the Earth absorbs. These variations in the fraction of absorbed

solar radiation strengthen or offset the impact of increasing greenhouse gas concentrations in the atmosphere through positive or negative feedback loops to the climate system and require careful consideration in climate change research and climate modeling (Cubasch et al. 2013).

Albedo is the ratio of the reflected shortwave solar radiation to the incoming shortwave solar radiation (Liang 2004). It is one of the main components of the energy budget, in that it controls the net shortwave radiation absorbed by the Earth (Cubasch et al. 2013; Liang 2004; Myhre 2013):

$$K^* = (1 - \alpha) \cdot S_{\downarrow}$$

where  $\alpha$  represents albedo,  $K^*$  is the net shortwave radiation ( $\text{Wm}^{-2}$ ) and  $S_{\downarrow}$  is the downward shortwave solar radiation ( $\text{Wm}^{-2}$ ). Influenced by albedo (both surface and top of atmosphere combined), about 30% of the incoming solar shortwave radiation is reflected back to space (Cubasch et al. 2013). Because albedo directly determines the amount of solar radiation absorbed by the Earth, which powers climate, albedo thus possesses a strong control over local, regional and global climate (Liang 2004; Lucht et al. 2000) and is a key input variable in climate models (Liang 2004; Lucht et al. 2000). Due to the strong influence of albedo on climate, any driver that considerably alters albedo over large spatial scales has the potential to impose significant climatic impacts. The immediate climatic impacts of both anthropogenic and natural drivers that alter surface albedo can be quantified using surface forcing (also known as surface shortwave forcing), which represents instantaneous change in net radiative flux at the surface (Barnes and Roy 2008). Surface forcing can be converted to radiative forcing, defined as the changes in net radiative flux at the tropopause

allowing for the adjustments of the stratospheric temperature (Hansen et al. 1997; Myhre 2013), which can be used for direct comparison between multiple forcing agents.

Located in the high northern latitudes, the global boreal biome is one of the largest terrestrial biomes in the world (Chapin et al. 2006; Malhi et al. 1999; Melillo et al. 1993). It plays a pivotal role in influencing regional and global climate, mainly through two sets of mechanisms: the biogeochemical effects and the biogeophysical effects (Bala et al. 2007; Bathiany et al. 2010; Betts 2000; Chapin et al. 2000). The former refer to those that are related to carbon emissions, since there is an exceptional amount of carbon stored in the boreal region (Kasischke and Stocks 2000). And the latter refer to those that are related to the biophysical aspects of the boreal forest, such as albedo, evapotranspiration, surface roughness. Among these, albedo has been suggested to be the most climatically influential factor of the boreal forest (Bala et al. 2007). The important role of albedo is largely attributable to the drastic difference between the high albedo of snow and low albedo of the forest canopy during the long snow seasons in the boreal forest (Bala et al. 2007; Bonan 2008; Bonan et al. 1992). Specifically, although the albedo of the snow cover is high, the canopy of the boreal forest can effectively mask out snow on the ground (Bonan 2008; Bonan et al. 1992; Hall et al. 1993; Ni and Woodcock 2000). According to Hall et al. (1993), the albedo of dense coniferous stands can stay at a relatively low level ( $< 0.3$ ) even with snow on the ground. The relatively low albedo of the boreal forest allows it to be more efficient in absorbing incoming shortwave radiation compared to other land cover types such as steppe and tundra and thus imposes a warming effect. Through

comparisons between simulated scenarios where the boreal forest is present and replaced by bare ground, Bonan et al. (1992) demonstrated the warming effect the boreal forest, and pointed out that this effect exists not only in the winter, but also in the summer. Betts (2000) indicated that the positive forcing resulting from the albedo-caused warming of the boreal forest may be large enough to completely offset the negative forcing induced by carbon sequestration, and that the net effect of the boreal forest may be accelerating climate change instead of mitigating it. These studies, together with many others (e.g. Bala et al. 2007, Anderson et al. 2010, Bathiany et al. 2010, Betts et al. 2007, Claussen et al. 2001 and Robert et al. 2008), directly or indirectly indicated that the biogeophysical effects, especially the albedo effect, are potentially larger than the biogeochemical effects over the high-latitude boreal region in influencing the climate, and the net effect of the boreal forest is expected to increase regional and global temperatures.

Wildfires have been shown to exert strong influences on the regional and global climatic feedbacks in the boreal forests in North America. Although they impose a warming effect through carbon-related emissions, this warming effect is largely outweighed by the cooling effect, which is imposed through the fire-induced changes in forest albedo (Randerson et al. 2006). There are two mechanisms involved acting at different temporal scales. The first mechanism is through the removal of forest canopy. Stand-replacing fires effectively remove canopy cover, resulting in much higher levels of ground exposure, which when covered by snow, leads to much higher albedo of the forests in the winter (Amiro et al. 2006; Randerson et al. 2006). The second mechanism involves the temporary change of dominant species in the

regrowing forests. During the early successional stage of the forests, there is usually a period with broadleaf deciduous species dominance (Amiro et al. 2006; Liu and Randerson 2008; Lyons et al. 2008; McMillan and Goulden 2008; Viereck 1973). Because the albedo of these broadleaf species is usually higher than that of the evergreen species, forest albedo typically remains elevated in the summer for a considerable amount of time, followed by a gradual return to the pre-fire level with evergreen species resume dominance (Liu and Randerson 2008; McMillan and Goulden 2008). The combination of these two mechanisms leads to a strong cooling effect imposed by wildfires that may last for decades. According to Randerson et al. (2006), taken into account all major positive forcings imposed by wildfires, including those caused by the long-lived greenhouse gases (CH<sub>4</sub> and CO<sub>2</sub>) and black carbon, the net forcing of the wildfires is still negative and can remain so for more than 150 years.

Approximately 20% of the global boreal forests are located in the eastern half of the Siberian region of Russia (Figure 1-1; Osawa and Zyryanova 2010) and these forests are characterized by several features. The boreal forests of North America and European Russia mostly consist of a mixture of several evergreen coniferous, including spruce (*Picea* spp.), pine (*Pinus* spp.) and fir (*Abies* spp.) (Osawa and Zyryanova 2010; Wallenius et al. 2011). However, in eastern Siberia, the boreal forests are dominated by larch (*Larix* spp.), which are deciduous needleleaf species (Abaimov 2010; Osawa and Zyryanova 2010). As in other boreal zones, wildfires are a common disturbance agent in the Siberian larch forests and they impose direct influences on the regeneration and growth of forests (Shorohova et al. 2009).



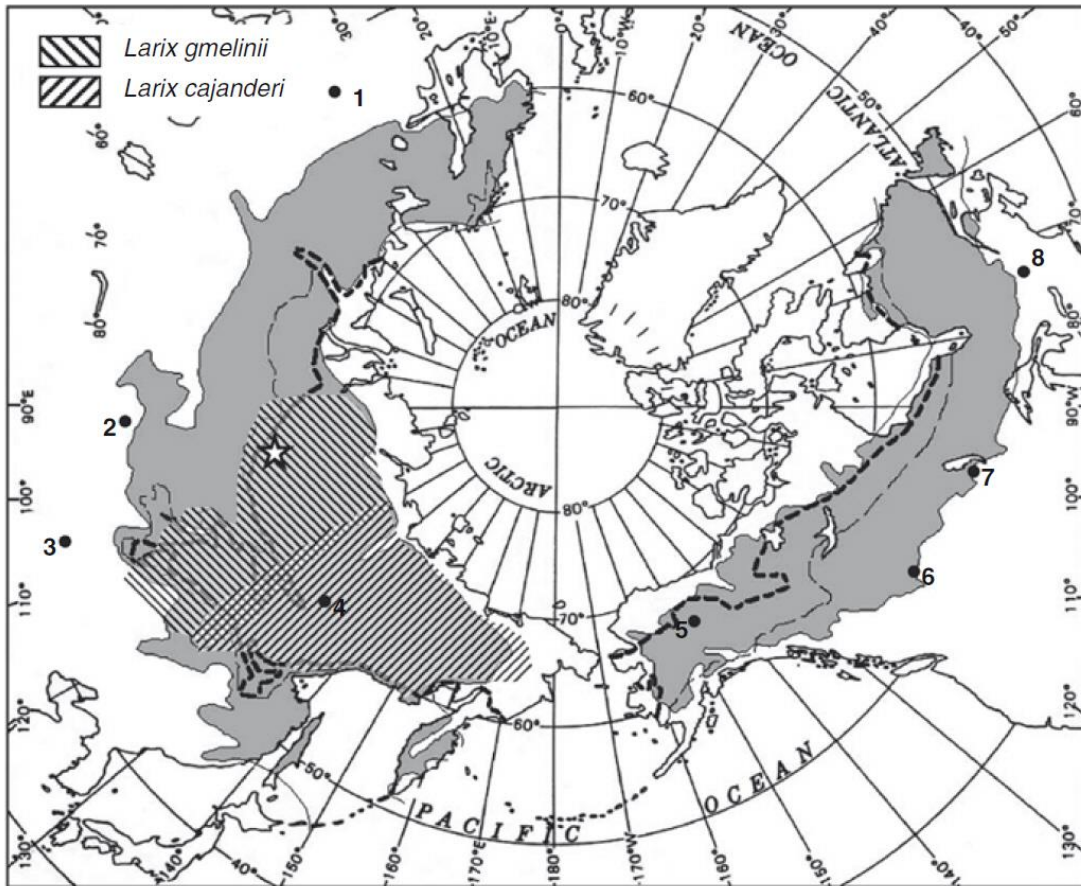


**Figure 1-1 Distribution of the Siberian larch forests (diagonally striped area) in relation to the global boreal biome (shaded area), southern boundaries of the continuous permafrost (thick dashed line) and discontinuous permafrost (thin dashed line). Figure is adopted from Osawa and Zyryanova (2010).**

However, the fire regimes and the resultant successional patterns are strikingly different from those in the North American boreal forests in two important aspects. First, there is a much higher proportion of surface fire in the region. In the boreal forests of North America, fires are generally stand-replacing, as tree species are mostly susceptible to fire (Wirth 2005). In great contrast, larch is known to be less prone to fire by possessing a series of fire-resisting adaptations. For example, they have thick bark which can effectively prevent them from being damaged by low

severity fires (Kharuk et al. 2010; Schulze et al. 2012; Wirth 2005). They also shed low hanging branches before the formation of fuel ladders which facilitate the occurrence of high-severity crown fires (Wirth 2005). These adaptations, together with generally lower canopy closure of the larch forests (Kharuk et al. 2011; Sofronov and Volokitina 2010), effectively limit the severity of most fires in the region to a low level, resulting in the wide occurrence of surface fires, which generally cause a much lower level of tree mortality (Wirth 2005). Second, the forest succession in the Siberian larch forests generally occurs without temporary dominance of secondary tree species. After stand-replacing fire events, larch regenerates quickly in the post-fire sites and although there may be other co-existing shrub and tree species, they are soon overwhelmed by larch (Babintseva and Titova 1996). Consequently, larch resumes dominance even in the early successional stage (Babintseva and Titova 1996; Zyryanova et al. 2010). As Kobak et al. (1996) pointed out, the apparent difference between larch stands of early and late successional stages may be no more than the degree of closure of the canopies.

Although there has been an abundance of research confirming the cooling effect of the wildfires in the North American boreal forests, it is still largely uncertain whether wildfires impose a similar effect in the Siberian larch forests. Located in interior Eastern Siberia, where environmental conditions are extremely severe, the Siberian larch forests are mostly free of human activities and difficult to access (Sofronov and Volokitina 2010). Most of the area in this region is beyond the limit of the Russian aerial fire monitoring service and remote sensing-based analysis has been mostly limited to 1995-2002 using the Advanced Very High Resolution Radiometer

(AVHRR) data (Sukhinin et al. 2004) and after 2000 using the Moderate Resolution Imaging Spectroradiometer (MODIS) and Landsat Enhanced Thematic Mapper Plus (ETM+) observations. Few research studies have focused specifically on the climatic impacts of these forests, especially at the regional scale. The knowledge gained from the North American boreal forests is not applicable to these forests, due to the substantial differences in many aspects of these forests. Specifically, there are several key science questions that have not been addressed, including how albedo reacts immediately after fire and over longer time spans, especially in the post-fire winters since larch is deciduous; how surface fires impact albedo since they are of lower severity than stand-replacing fires; what impacts wildfires in these larch forests impose through surface forcing, and whether they are different from those imposed by the North American boreal fires. Without the answers to these questions, our understanding of the land-atmosphere interaction in the boreal zone is incomplete, which carries even stronger implications in the context of global climate change. Having experienced the highest level of warming in the world over the past decades, the high-latitude boreal forests are at the frontier of global warming (Hartmann 2013). This warming trend will likely persist in the region, resulting in intensified fire regimes with more severe and frequent wildfires (Collins 2013; Groisman et al. 2007). In order to better predict how wildfires, the forests and climate will interact with each other in the future, we need to know how wildfires are affecting the climate currently. Motivated by this need, this dissertation attempts to quantify the climatic impacts of wildfires exerted through fire-induced albedo changes, which is expected to be a major element of the fire-climate interactions in these forests.

## 1.2. Research Questions and Dissertation Structure

The overarching question that this dissertation aims to address is: **How do fires (both stand-replacing and surface) impact surface shortwave forcing in the Siberian larch forests?** This question has been broken down into three specific questions and each of these three questions is addressed in a separate chapter in this dissertation from Chapter 2 to Chapter 4. Chapter 5 offers a summary of the findings, discusses their implications, and outlines potential directions for future research.

*1.2.1. Question 1: What is the stand age distribution of the Siberian larch forests over the past 24 years?*

In order to quantify the post-fire surface forcing, the locations and timing of the fire events is of critical importance. Although there is an existing dataset that provides this information about the stand-replacing fires since 2001 (Krylov et al. 2014), this dataset is limited in that it allows for neither the examination of associated albedo trajectory over longer time span nor the comparison with the control group (i.e. the forests that have not been impacted by fire in the recent past). Another available dataset that was considered for this dissertation is the AVHRR-based fire mapping product (Sukhinin et al. 2004) developed by using both active fire and burned area for Russia between 1995 and 2002. However, initial evaluation suggested that this dataset lacked the accuracy in identifying fire events and the spatial continuity that were required by this dissertation, thus was not applicable. Due to this lack of available datasets that suited my need, in this chapter a stand age map mapping the stand-replacing fire events in the Siberian larch forests between 1989 and 2012 is produced based on a novel method. It serves as the foundation based on

which the surface forcing of stand-replacing fires can be quantified and the associated surface forcing patterns can be explained.

Question 1 is addressed in Chapter 2, and it has been published in October 2016 in *Remote Sensing of Environment*.

*1.2.2. Question 2: What is the surface forcing imposed by stand-replacing fires in the Siberian larch forests since 2000?*

Because stand-replacing fires and surface fires are two major components of the fire regime in the Siberian larch forests and it is expected that they show different post-fire surface forcing patterns, these two fire types are separated and examined in two different chapters. Chapter 3 focuses on stand-replacing fires only, and it is designed based on the stand age map produced in Chapter 2. This study not only quantifies the surface forcing after stand-replacing fires, but also explains the mechanisms of the revealed patterns. In addition, the results are compared with those obtained previously in different spatial and temporal domains based on which a better understanding of the impacts that stand-replacing fires impose is developed.

*1.2.3. Question 3: What is the surface forcing imposed by surface fires and how does it differ from stand-replacing fires?*

This question is addressed in Chapter 4, which examines the surface forcing of surface fires, the other major component of the fire regimes in the Siberian larch forests. The results reveal the direction and magnitude of the surface forcing that surface fires impose on a regional scale. Together with the results obtained in Chapter 3, they draw a relatively complete picture of the climatic impacts of fires in the region

through associated albedo changes and surface forcing. In addition, this study also explores the feasibility of using several remote sensing-based indices to differentiate surface fires from stand-replacing fires. The results reveal a cost-effective solution to reliably separating these two fire types, which has a strong potential to be adopted by various studies involving wildfires in the Siberian larch forests.

Finally, in Chapter 5, the implications of this dissertation, especially those for the climate modeling community, are discussed. In short, the findings of this dissertation will greatly enhance our overall understanding of the influences of wildfires on post-fire energy budget in the Siberian larch forests, which will, in turn, allow for accurate representation of wildfires in the future climate models.

# **Chapter 2: Mapping stand age dynamics of Siberian larch forests from recent Landsat observations using an innovative approach<sup>1</sup>**

## **2.1. Introduction**

Covering more than 15 million km<sup>2</sup> of land, containing the amount of carbon that is comparable to the combined carbon storage in tropical and temperate forests, boreal forests are a vital global biome (Dixon et al. 1994; Kasischke 2000). Stand age is a crucial parameter related to carbon cycling (Bond-Lamberty et al. 2004; Goulden et al. 2006; Gower et al. 1996; Harden et al. 2000; O'Neill et al. 2003) and the energy budget (Amiro et al. 2006; Bright et al. 2013; Liu and Randerson 2008) in boreal forests and is the central component in the atmosphere-land interactions of the global climate system (Bonan 2008; Randerson et al. 2006). Previous studies in boreal forests of Alaska (Randerson et al.) showed that over the short-term (within 20 years) following the disturbance events the fire-induced carbon emissions produce a positive climatic forcing, which outweighs the negative forcing resulting from the increase in surface albedo. However, over a longer time span (~ 80 years), the net forcing of stand-replacing fires is negative due to the long-lasting effect of increased forest albedo resulting from slow rates of forest recovery. Therefore, understanding stand

---

<sup>1</sup> This chapter has been published: Chen, D., Loboda, T.V., Krylov, A., & Potapov, P.V. (2016). Mapping stand age dynamics of the Siberian larch forests from recent Landsat observations. *Remote Sensing of Environment*, 187, 320-331. <http://dx.doi.org/10.1016/j.rse.2016.10.033>

age dynamics in the boreal forests is highly important for quantifying and modeling the net climatic impacts of the boreal biome.

Approximately 20% of the boreal forests in the world are located in Eastern Siberia and the Russian Far East (Osawa and Zyryanova 2010). In contrast to boreal forests of North America and Europe, dominated by evergreen coniferous species (e.g. spruce, pine and fir), boreal forests of Eastern Siberia are covered by larch (Abaimov 2010; Osawa and Zyryanova 2010; Shuman et al. 2011). Larch forests differ from other boreal forests considerably in two very important aspects. First, unlike other coniferous species, larch is deciduous which has large and unique implications for nutrient cycling and surface albedo. And second, the successional pattern of larch forests usually does not include an early stage of dominance by the broadleaf species (Abaimov and Sofronov 1996; Furyaev et al. 2001; Zyryanova et al. 2010). Comparatively little is known about dynamics of the Siberian larch forests at the regional scale in the English-language peer-reviewed publications. In recent decades Eastern Siberia, particularly the regions above 55 °N, has experienced the most significant level of warming which is expected to continue under the projected scenarios of climate change (Balzter et al. 2010; Collins 2013; Groisman et al. 2007; Hartmann 2013; Kirtman 2013; Stocks et al. 1998). One of the likely immediate consequences of the continuing warming trend is a substantial increase in wildfire occurrence and severity (Kharuk et al. 2011; Krylov et al. 2014; Schimel et al. 2001). Wildfires are the dominant disturbance agent in Siberian forests and exert a strong control on stand age distribution (Goldammer and Furyaev 1996; Kharuk et al. 2011; Shorohova et al. 2009; Sofronov and Volokitina 2010). Therefore, a changing fire



regime is likely to lead to changes in stand age dynamics in the region with large implications for biogeochemical and biogeophysical properties of the region. However, it is difficult to quantify the change in forest dynamics or fire regimes without a baseline stand age assessment that precedes the year 2000.

Traditionally stand age assessment is conducted using field observations as part of the forest inventory survey (e.g. USDA 2014). Although the results of these surveys are highly accurate and detailed, they are strongly limited by the accessibility of specific forest stands and the cost of field surveys. For large inaccessible regions, remote sensing offers a substantial advantage due to the capacity for observing remote areas with a high degree of consistency over time. Depending on the availability of the remotely sensed data, there are two general approaches for estimating stand age in the boreal forests. When annual observations are available, stand age can be derived by mapping and tracking stand-replacing events such as fires or forest harvest which reset the stand age to zero. This has been accomplished, particularly in North America, using dense stacks of high quality Landsat images (Hansen et al. 2013; Huang et al. 2009; Huang et al. 2010; Masek et al. 2008; Schroeder et al. 2011; Thomas et al. 2011). When frequent satellite observations are unavailable, stand age can be inferred from the overall distribution of forests at varying stages of regrowth across the landscape. The comparatively slow recovery of boreal forest stands after disturbances provides a ~30 year window during which young forests can be reliably mapped (Loboda et al. 2012). For example, Zhang et al. (2004) produced a stand age map for the boreal forests in Ontario, Canada, employing a regression method built on the relationship between stand age and the Normalized

Difference Water Index (NDWI) using fire inventory data, Satellite Pour l'Observation de la Terre (SPOT) VEGETATION and Advanced Very High Resolution Radiometer (AVHRR) images. Loboda et al. (2012) developed a Moderate Resolution Imaging Spectroradiometer (MODIS)-based method that used a decision tree classifier driven by available samples from multi-temporal Landsat imagery in the Russian Far East to model the timing of disturbances based on forest regrowth patterns. This method was later modified by Loboda and Chen (2016) who mapped the spatial distribution of young forests in Russia at 500-m resolution. These existing approaches rely on availability of some historical imagery that can be used to train algorithms and hindcast forest age from a later-date distribution of regrowing forests on the landscape.

Since 2000, multiple satellite imaging platforms, including Landsat TM and ETM+ and MODIS, have provided consistent coverage over Siberia which supports annual mapping of forest cover change in the region. However, before 2000 due to a combination of reasons including intermittent acquisition of Landsat TM data received by the international ground stations (Goward et al. 2006; Kim et al. 2014; Kovalskyy and Roy 2013), coverage of satellite observations of Eastern Siberia is neither spatially- nor temporally-contiguous. The small sample of acquired available imagery is spaced at very large time steps making it virtually impossible to date the age of disturbances in the images. This considerably limits the success rate of using existing methods and necessitates the development of new approaches to hindcasting stand age distribution of Siberian larch forests. In this work we present a new algorithm aimed at mapping stand age distribution of Siberian larch forests as a

function of changes in spectra of recovering forests over time at 30-m resolution. This algorithm capitalizes on the wealth of post-2000 observations of Siberian forests and allows for hindcasting the stand age distribution before 2000 at 30-m resolution based on the assumption of spectral stability of forest-age signature over the past 24 years. Using the resultant map we further quantify changes in the occurrence of stand-replacing fires in larch forests over the past 24 years as reflected in stand age distribution.

## **2.2. Study area**

The study is focused on the contiguous area of larch dominance in Siberia (Figure 2-1). We used the 500-m MODIS Land Cover Type Product (MCD12Q1; Friedl et al. 2002; Friedl et al. 2010) to define the larch forest mask as all pixels mapped as deciduous needleleaf forest according to the International Geosphere-Biosphere Programme (IGBP; Loveland et al. 2000) classification scheme layer of the MCD12Q1 product in Eastern Siberia at any time between 2001 and 2012. In doing this we aimed to maximize, to a reasonable extent, the potential coverage of the Siberian larch forests, to account for disturbances during the 2001-2012 period and allow for regrowth after the disturbance, considering that larch quickly regenerates after fires and dominates recovering stands even at early successional stages (Zyryanova et al. 2010). We then applied a majority filter (25 pixel kernel) to delineate a broad ecoregion of larch dominance that defines our study area and is located within 50 °66 °N and 94 °140 °E, encompassing a total area of  $1.93 \times 10^6$  km<sup>2</sup>.

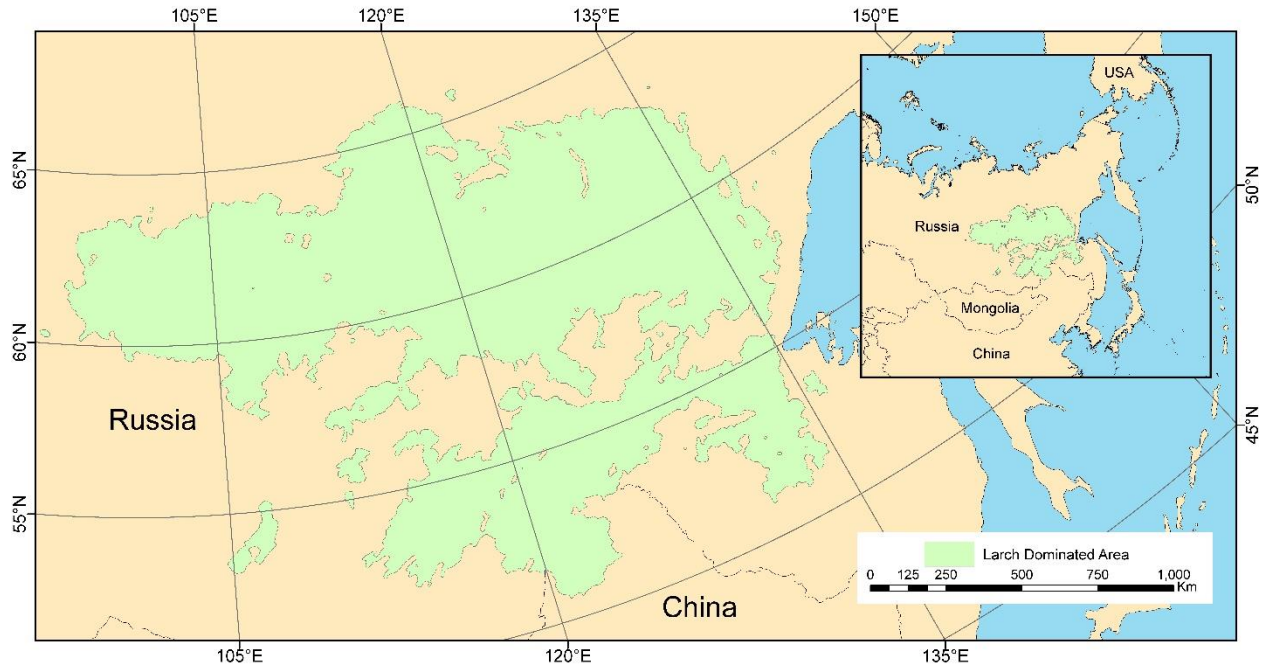


**Figure 2-1 Location of the study area, as indicated in light green. This study area reflects a conservative estimate of the Siberian larch forest distribution focusing on stands dominated by larch species. The study area presented is not intended to be used as a definitive boundary of the Siberian larch forests.**

Two larch species dominate this region: *Larix gmelinii* in the west and *Larix cajanderi* in the east (Abaimov 2010; Nikolov and Helmisaari 1992). The high dominance of larch species over such a vast area, which is largely underlain by permafrost, is a unique characteristic of these forests compared with other parts of the global boreal forests (Herzschuh et al. 2013; Kharuk et al. 2010; Osawa and Zyryanova 2010).

Wildfire is the dominant disturbance agent in the region (Goldammer and Furyaev 1996; Zyryanova et al. 2010). We conducted an initial analysis during which fire-driven forest loss, defined as areas of tree cover loss within the known burns (Krylov et al. 2014), was compared with the total tree cover loss (Hansen et al. 2013)

in the study area between 2001 and 2012. The result suggested that wildfire accounted for about 87% of the total forest loss in the region. While other factors including pest infestation, plant disease, windstorms and timber harvesting contribute to forest loss, their respective contributions are comparatively small and thus the analysis focuses on wildfire as the primary driver of stand age distribution.

### **2.3. Data**

In this study we used several datasets (shown in Table 2-1) developed by the Global Forest Change (GFC) project (Hansen et al. 2013) as data inputs. The GFC project produced a suite of remotely sensed datasets based on Landsat Enhanced Thematic Mapper Plus (ETM+) imagery. At 30-m spatial resolution and covering the global land surface, these datasets mapped a set of parameters that are either directly or indirectly related to the changes in forest cover since 2000, including forest gain and loss and tree canopy cover. The GFC datasets also include a set of cloud-free Landsat image composites for selected years (Hansen et al. 2013). In this project, we used the Landsat-based composites and tree cover for *circa* year 2000 and 2012. Generated based on images captured during the growing season (i.e. June-August), the composites included four spectral bands of the Landsat ETM+ (Band 3 - red, 4 - Near Infrared (NIR), 5 - short-wave infrared (SWIR<sub>1.6</sub>) and 7 – SWIR<sub>2.2</sub>), all of which were converted from original digital values to normalized top-of-atmosphere (TOA) reflectance. These composites are cloud-free and were produced by employing a gap-filling algorithm which replaced the pixels contaminated by clouds and cloud shadows with those from temporally adjacent clear observations (Hansen et al. 2013).

**Table 2-1 Summary of the datasets.**

Dataset Name	Used in	Original Spatial Coverage	Spatial Resolution	Temporal Span
GFC Landsat-based TOA reflectance composites	Map production	Global	30 m	<i>circa</i> 2000 and 2012
GFC Landsat-based tree cover	Map production	Global	30 m	<i>circa</i> 2000 and 2012
SRFM	Map production	Russia	30 m	2001-2012
Landsat images	Accuracy Assessment	Siberian larch forests	30 m	<i>circa</i> 1989, 2000 and 2012
ABFM	Accuracy Assessment	Russia	1 km	1995-2002

In addition, we used the stand-replacing fire mapping (SRFM) dataset produced by Krylov et al. (2014) to identify the areas of stand-replacing fires which occurred in the Russian boreal forests annually between 2001 and 2012 (year 2001 and 2012 were absent from the initial publication of the SRFM product and were later included into the dataset) at 30-m resolution. It is a regionally enhanced product which was derived based on a data fusion of the GFC tree cover and forest loss products (Hansen et al. 2013), 1-km MODIS active fire data (Giglio et al. 2003) and 500-m MODIS-based Regional Burned Area Mapping Product for Russia (Loboda et al. 2007; Loboda et al. 2011). The fusion of the Landsat-scale detail with the MODIS temporal scope allowed the SRFM product to identify the timing of fire events with great accuracy.

There are very few spatially explicit datasets in existence that provide information regarding the stand age information within the Siberian larch forests at the regional scale. To develop a robust accuracy assessment for our product, we sought out all datasets that could serve as references. We chose not to use the

historical government records of fire occurrence as they have been shown to be inaccurate in identifying both the location and extent of wildfire occurrence (Conard et al. 2002). Instead we focused on two available reference datasets for accuracy assessment. First, we used a set of Landsat images for three epochs, i.e. 1989, 2000 and 2012. In order to confidently identify the ground conditions at each epoch, an exhaustive image search across the study area for snow-free L1T images (including Landsat MSS, TM and ETM+ images) with no more than 10% cloud cover was conducted. In the end, 1597, 1317 and 793 Landsat images were acquired for 1989, 2000 and 2012 epochs, respectively. These images composed an image pool from which individual images were drawn when the analyst assessed the accuracy of the classification at each random sample point.

Our second reference dataset is the AVHRR-based fire mapping (ABFM) product (Sukhinin et al. 2004). This dataset is the only currently available spatially explicit fire detection and burned area data product that contains the exact timing information (i.e. year of fire) in the study area before 2000. It includes both active fire detections and burn scars that were mapped between 1995 and 2002. The burn scar polygons represent a set of subjectively selected and generally very large events which are distributed in clusters in a few subregions of the Russian forests (Sukhinin et al. 2004). They were mapped from a single clear image after the fire event was completed. In contrast, the active fire polygons are aggregations of the 1-km AVHRR pixels flagged by an automated fire detection algorithm applied to all available AVHRR scenes (Sukhinin et al. 2004).

## 2.4. Methodology

Previous remote sensing-based stand age estimation methods are based upon the premise that the spectral characteristics of forest stands of the same age are similar across space (Loboda and Chen 2016; Loboda et al. 2012). The method used within this study is innovative in that it is established based on the hypothesis that spectral characteristics of the forest stands with the same age and species composition are similar across space and also across time. In other words, training samples for the stand age classes can be obtained from a different era, as long as 1) the forest composition remains largely the same, which is true for the Siberian larch forests over the past few decades, and 2) there are reliable and consistent coverage of remotely sensed products based on which the training samples can be derived. Following this assumption, we developed a two-pronged approach to producing a 24-year record of fire-induced forest dynamics across the Siberian larch forests using only post-2000 Landsat observations. The general workflow of the map development is presented in Figure 2-2. This approach combines two different methods to produce a single map. Within the first method, SRFM (Krylov et al. 2014), an existing dataset mapping annual areas of forest loss due to stand-replacing fires between 2001 and 2012 was adopted to produce a post-2000 forest stand age map. Within the second method – the novel method introduced in this study - we used post-2000 imagery to: 1) define spectral signatures of recovering forests in year 2012 following known (in space and time) stand-replacing fire events from the post-2000 forest stand age map described above; 2) build a random forest-based algorithm that can reliably separate recovering forests of different ages; and 3) apply the developed algorithm to identify and map



areas with similar spectra in the year 2000, which would have resulted from disturbance events that occurred prior to year 2000. The outcome of the second method is the pre-2000 map of forest stand age. We then merged the pre-2000 map with the post-2000 map to produce a single continuous map of stand age distribution of young (<25 years old) Siberian larch forests.

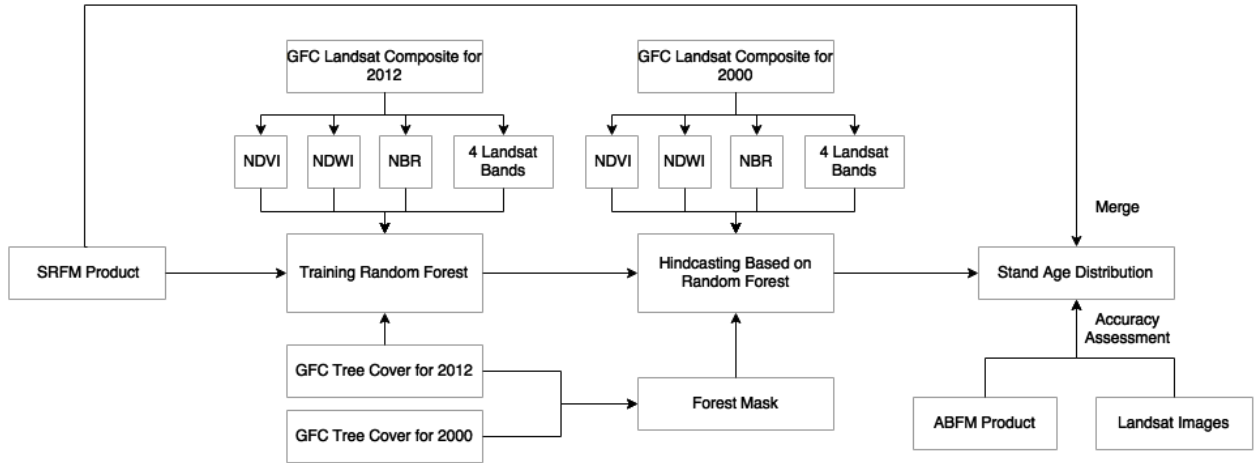


**Figure 2-2 General workflow of the proposed method.**

### 2.4.1. Training a random forest

During the pre-processing stage, all data inputs, including the GFC Landsat-based composites, GFC tree cover products, and the SRFM product, were clipped to a common extent based on the study area. Because all these datasets share the same origin and spatial information, geo-registration between data layers was not necessary.

Although the GFC Landsat-based composites contain only four bands, these four bands allow for the calculation of several spectral indices. In order to maximize the power of the image classifier, three commonly used spectral indices, namely the Normalized Difference Vegetation Index (NDVI, Tucker 1979), NDWI and the

Normalized Burn Ratio (NBR, Key and Benson 2006), were calculated based on the *circa* 2012 composite using the following equations:

$$\text{NDVI} = \frac{\text{NIR} - \text{red}}{\text{NIR} + \text{red}}$$

$$\text{NDWI} = \frac{\text{NIR} - \text{SWIR1.6}}{\text{NIR} + \text{SWIR1.6}}$$

$$\text{NBR} = \frac{\text{NIR} - \text{SWIR2.2}}{\text{NIR} + \text{SWIR2.2}}$$

Annual areas of fire-driven forest loss within the study area (defined in the SRFM dataset) were used as training data for the random forest classifier. Training data for 13 stand age classes, including 12 “burned forests” classes with stand age of 0-11 years, and one “unburned forests” class representing forests with stand age of  $\geq$  12 years, were then derived from the SRFM and GFC products. Specifically, the burn scars mapped by the SRFM dataset, which represented the stand-replacing fires between 2001 and 2012, was converted to the burned forests classes with stand age ranging from 0 to 11 years (as of 2012). For example, the scars that were burned in 2012 were assigned stand age of 0 years whereas those burned in 2001 were assigned stand age of 11 years. Each polygon in the resultant 12 classes was shrunk inward by 5 pixels to ensure the purity of the training samples. The unburned forests class was defined as the forested areas where no stand-replacing fire events occurred during the 12-year period (i.e. 2001-2012). To develop the training data for the unburned class, we selected all pixels within the study area that had tree cover greater than 10% in 2012. The SRFM burned area mask, expanded by 5 pixels outward was used to exclude any pixels partially impacted by fire from the training samples. The GFC composites are filled with data from adjacent years when clear surface observations for the year of interest (2012 in this case) were not available. Because the proposed

method is based on linking the age of recovering forest stands with spectral signature at a specific age, it is important that pixels from a single-year of acquisition are used for training to establish those relationships. Therefore, we removed all pixels which were present in the *circa* 2012 composite but were not acquired from the 2012 Landsat imagery.

For every one of the 12 burned forests classes we randomly selected 10,000 samples for a total of 120,000 sample points. Additional 120,000 samples were randomly selected for the unburned forests class, bringing the total number of training points to 240,000. For each training sample we extracted seven metrics from the input data layers (i.e. Landsat Band 3, 4, 5, 7 TOA reflectance and spectral indices NDVI, NDWI and NBR), linking these metrics (as the independent variables) to the stand age classes (as the dependent variable). The Random Forest algorithm (Breiman 2001) was employed to hindcast time since fire disturbances as a function of year 2012 spectral reflectance. Following the recommendation by Breiman and Cutler (2003), the number of variables that were randomly selected at each splitting node was set to 2 (square root of the total number of independent variables, i.e. 7). A series of random forests with increasing numbers of trees were produced and the suite with the strongest out-of-bag (OOB) score and the least amount of trees was selected. Random forests were generated in Python using the scikit-learn module (Pedregosa et al. 2011).

#### *2.4.2. Applying the random forest*

The same set of seven metrics, including TOA reflectance values from the four available Landsat bands and three spectral indices, were produced based on the

*circa* 2000 composite. We then used the selected random forest model to hindcast the forest age using the *circa* 2000 Landsat dataset. As a result each pixel in the study area was assigned one of the 13 stand age classes (12 burned classes and 1 unburned class), reflecting the forest stand age at that location in the year 2000. To exclude non-forested areas within the study area, a forest mask (different from the overall area of larch dominance defining the study area derived from the MCD12Q1 product) was generated based on the GFC tree cover data to include all pixels with tree cover of 10% or greater in either 2000 or 2012.

Finally, to extend stand age distribution into the 2000s era our 12-year stand age map for the year 2000 was fused with the annual disturbances between 2001 and 2012 in the SRFM product. In the fusion process the stand age values of all pixels where no stand-replacing fires occurred during the post-2000 period, according to the SRFM product, were set according to our prediction model. When a pixel was burned as indicated by the SRFM product, the stand age of that pixel was set to values calculated based on the most recent fire. The final output delivers a 24-year map presenting the stand age distribution of the Siberian larch forests for the period of 1989-2012.

#### *2.4.3. Accuracy assessments*

As described above, the final stand age map integrates two different methods for assessing forest stand age before (years 12 - 24) and after the year 2000 (years 0 - 11). In the first assessment, both components were assessed independently against the acquired Landsat images, following the practice described by Olofsson et al. (2014). The lack of Landsat TM data over the study region before 2000, which prompted the

development of the algorithm in the first place, also hinders our ability to validate the actual age since disturbance over this time period. Therefore, we were able to quantify accuracy only broadly over the two general time periods – pre-2000 and post-2000. First both components were converted into binary classification maps with two classes: burned and unburned forests. For the pre-2000 component, the 12-24 stand age classes as mapped by the produced data were grouped into a single burned forests class, whereas the unburned forests class remained unchanged. For the post-2000 component, the 0 – 11 stand age classes were converted to the burned forests class, and all the rest of the forested area, including the stand age classes 12 -24, were converted into unburned forests. Two separate sets of 500 random sample points, consisting of 150 and 350 points for the burned and unburned classes respectively, were generated to assess the pre-2000 and post-2000 map accuracy separately. For pre-2000 accuracy assessment at each sample point, the acquired Landsat images for *circa* 1989 and *circa* 2000 were visually compared to check if that location was burned during the 12-year period. For post-2000 accuracy assessment the same procedure was followed comparing *circa* 2000 and *circa* 2012 composites. The results were compiled within two confusion matrices to calculate associated statistics, including estimated area for both unburned and burned forests classes.

We also implemented an intercomparison between the estimated pre-2000 stand age distribution and an existing dataset: the ABFM product for Russia (Sukhinin et al. 2004). In this assessment, only the pre-2000 component was evaluated. Therefore, the fires and burn scars that were mapped after 2000 in the ABFM product were excluded. We visually compared ABFM active fires and burn

scars mapped before and in 2000 against the 2000 Landsat composite and excluded all ABFM polygons that showed no visible signs of disturbance in the Landsat composite. The results of this assessment led to exclusion of all ABFM polygons representing scars in 1998 and the active fires in 1997.

Acknowledging the dissimilarity between the active fire and burn scar components of the fire polygons (as described in Section 2.3), we used them separately during the assessment. All fire polygons of the ABFM product were divided into seven groups: three burn scar groups for 1995, 1996 and 2000, and four active fire groups for 1996, 1998, 1999 and 2000. Each of these groups was used to extract the pixels at the corresponding locations in the produced stand age map. The stand age values of the extracted pixels were then summarized and the resultant histogram was compared with the “expected stand age (ESA)” - a single stand age value assigned to each fire polygon group based on the year of fire event in relation to year 2000. For example, for the 1995 and 2000 burn scar groups, their ESAs are 5 and 0 years, respectively. The ESA serves as a reference mark which the mapped stand age distribution can be compared to intuitively.

## **2.5. Results**

### *2.5.1. Selected random forest model*

The random forest that was selected was built based on 500 trees and had an OOB error of 1.89% (i.e. OOB score of 98.11%). Figure 2-3 shows the importance ranking of all independent variables. As can be seen, three spectral indices, namely NBR, NDWI and NDVI, had larger contributions to the predicting power of the selected model compared with the four spectral bands.

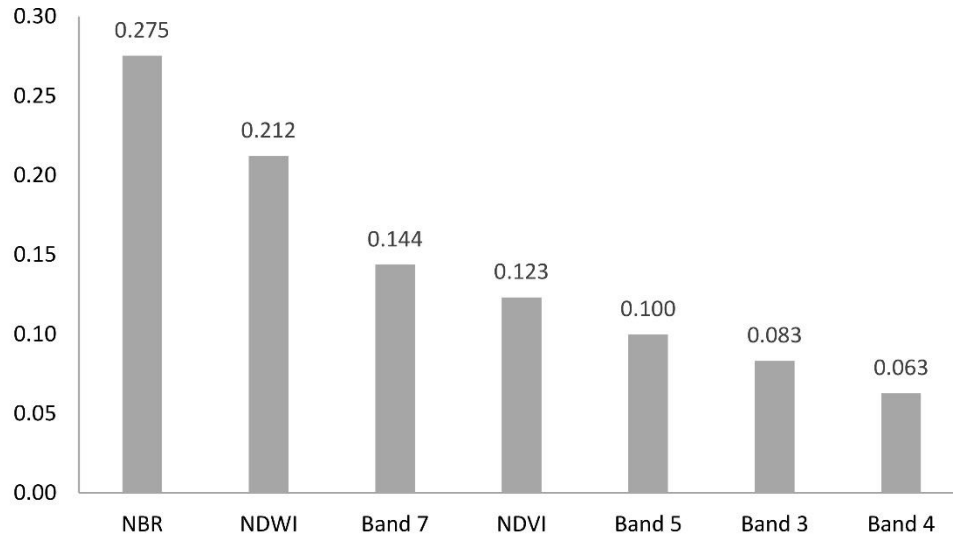


**Figure 2-3 Variable importance ranking according to the produced random forest model. From left to right the variable importance decreases.**

### 2.5.2. Accuracy assessment results

The confusion matrices generated in the first accuracy assessment are shown in Table 2-2 and Table 2-3. At the 95% confidence level, both the pre- and post-2000 components of the stand age map have high overall accuracies (i.e.  $0.97 \pm 0.02$  for the former and  $0.98 \pm 0.01$  for the latter). The pre-2000 component, which was the hindcasting result of the produced random forest model, has relatively lower accuracy, in terms of both the producer's ( $0.56 \pm 0.17$  versus  $0.80 \pm 0.16$ ) and user's ( $0.81 \pm 0.06$  versus  $0.92 \pm 0.04$ ) accuracies, in mapping the burned forests than the post-2000 component, which was inherited from the SRFM product. Based on the calculated accuracy statistics, the area of the unburned and burned forests within each era was estimated, as shown in Table 2-4.

**Table 2-2 Confusion matrix for the 1989-2000 era.**

		Reference			
		Unburned	Burned	Total	User's accuracy
Map	Unburned	0.94	0.02	0.97	0.98 ±0.02
	Burned	0.01	0.03	0.03	0.81 ±0.06
	Total	0.95	0.05	1	
	Producer's accuracy	0.99 ±0.00	0.56 ±0.17		
Overall accuracy: 0.97 ±0.02					

**Table 2-3 Confusion matrix for the 2001-2012 era.**

		Reference			
		Unburned	Burned	Total	User's accuracy
Map	Unburned	0.94	0.01	0.95	0.99 ±0.01
	Burned	0.00	0.04	0.05	0.92 ±0.04
	Total	0.95	0.05	1	
	Producer's accuracy	0.99 ±0.00	0.80 ±0.16		
Overall accuracy: 0.98 ±0.01					

**Table 2-4 Estimated area of unburned and burned forests at the 95% confidence level.**

	Area (km <sup>2</sup> )	
	1989-2000	2001-2012
Unburned	1,701,925 ±27,401	1,688,527 ±19,378
Burned	90,061 ±27,401	103,459 ±19,378

The results of the accuracy assessment against the ABFM product are shown in Figure 2-4 and 2-5, which correspond to the active fire and burn scar components, respectively. In each histogram, the expected stand age for that particular year is represented by the vertical bar in the background. As can be seen, in most histograms (i.e. Figure 2-4b-d, 2-5b-c), the highest or the second highest bars overlap with the



expected stand ages. Also, the later the reference data, the more concentrated the histograms are. In both Figures 2-4 and 2-5, histograms that are based on 1995 or 1996 fires show much weaker concentration than the later histograms do.

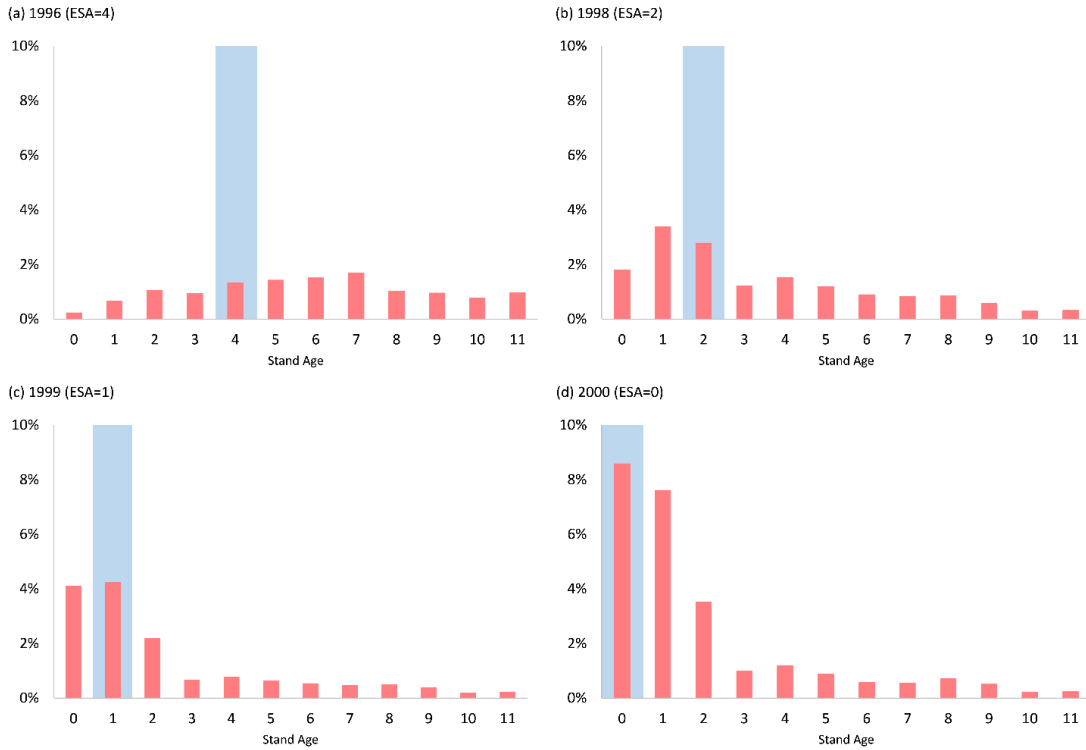


**Figure 2-4 Assessment results generated based on the active fire component of the ABFM product. Each histogram corresponds to a fire polygon group for a separate year. The ESA values (defined in Section 2.4.3) are represented by the blue bars in the background.**

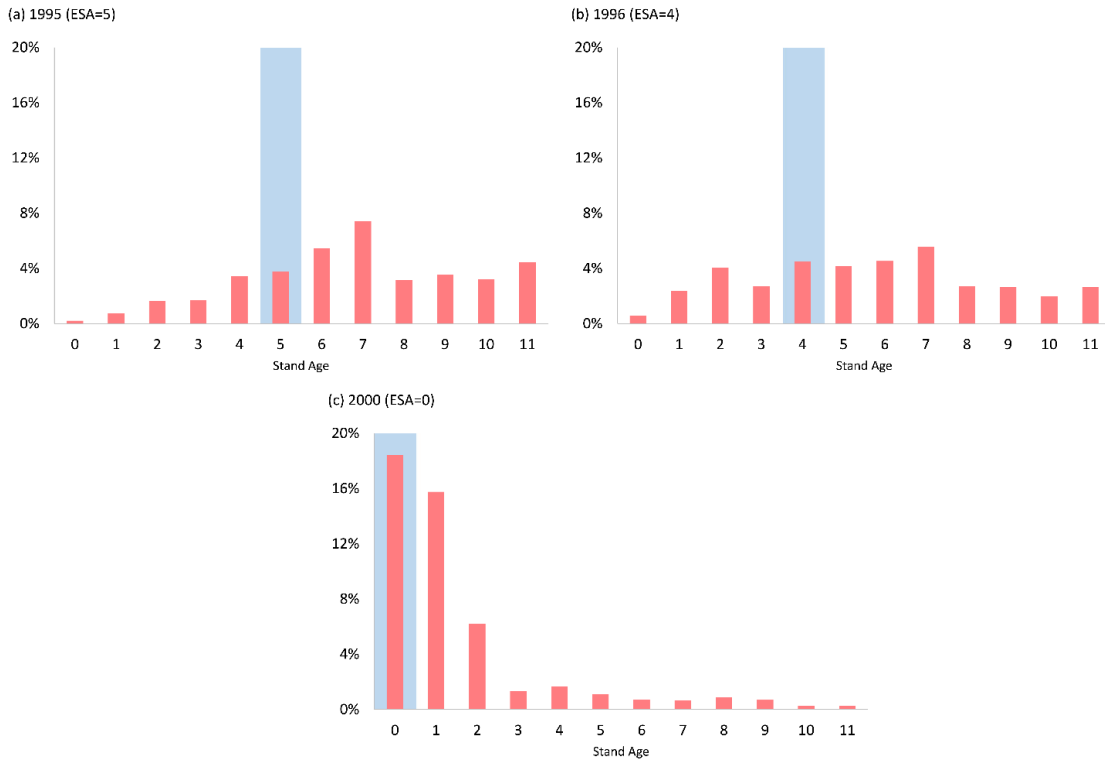
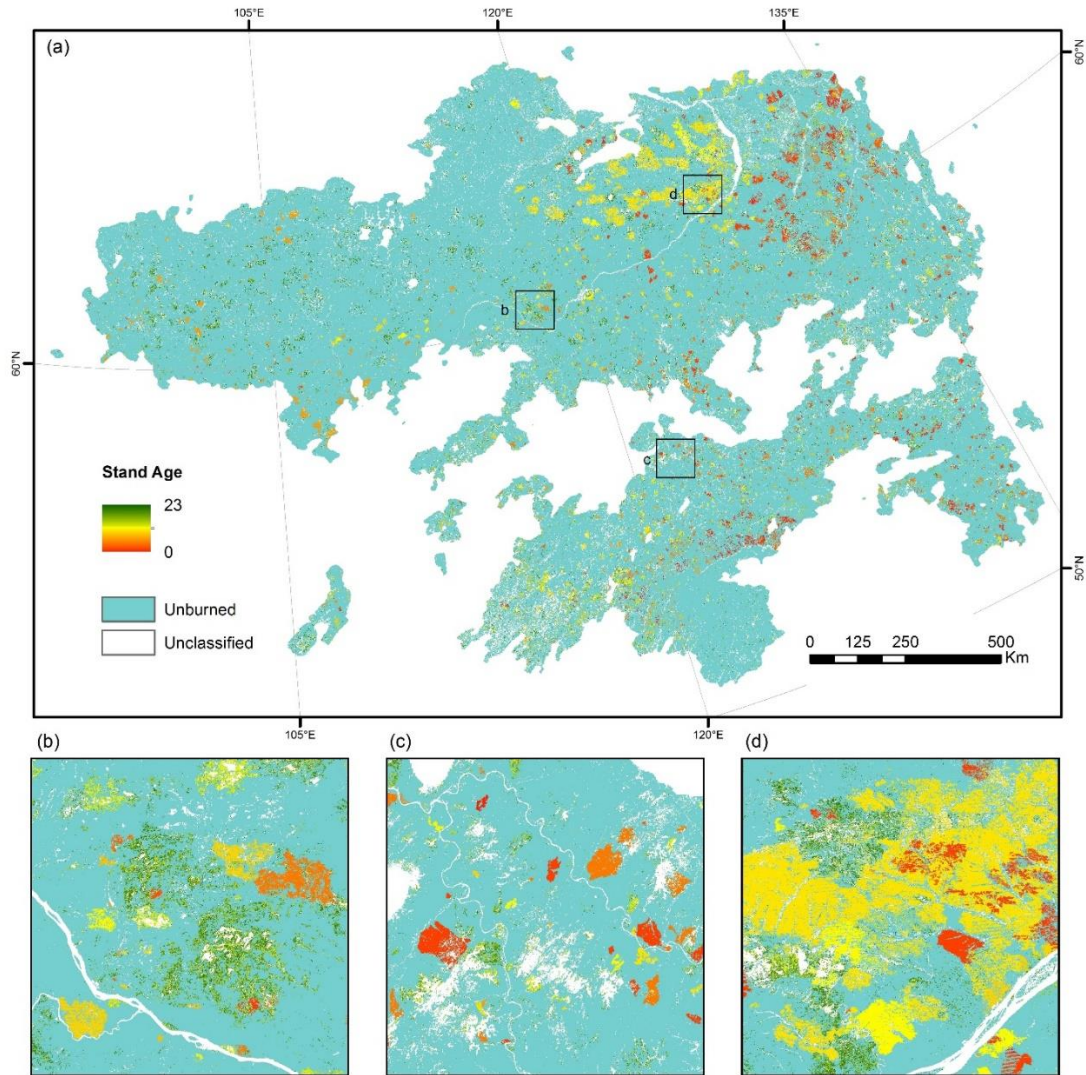


**Figure 2-5 Assessment results generated based on the burn scar component of the ABFM product. Each histogram corresponds to a fire polygon group for a separate year. The ESA values (defined in Section 2.4.3) are represented by the blue bars in the background.**

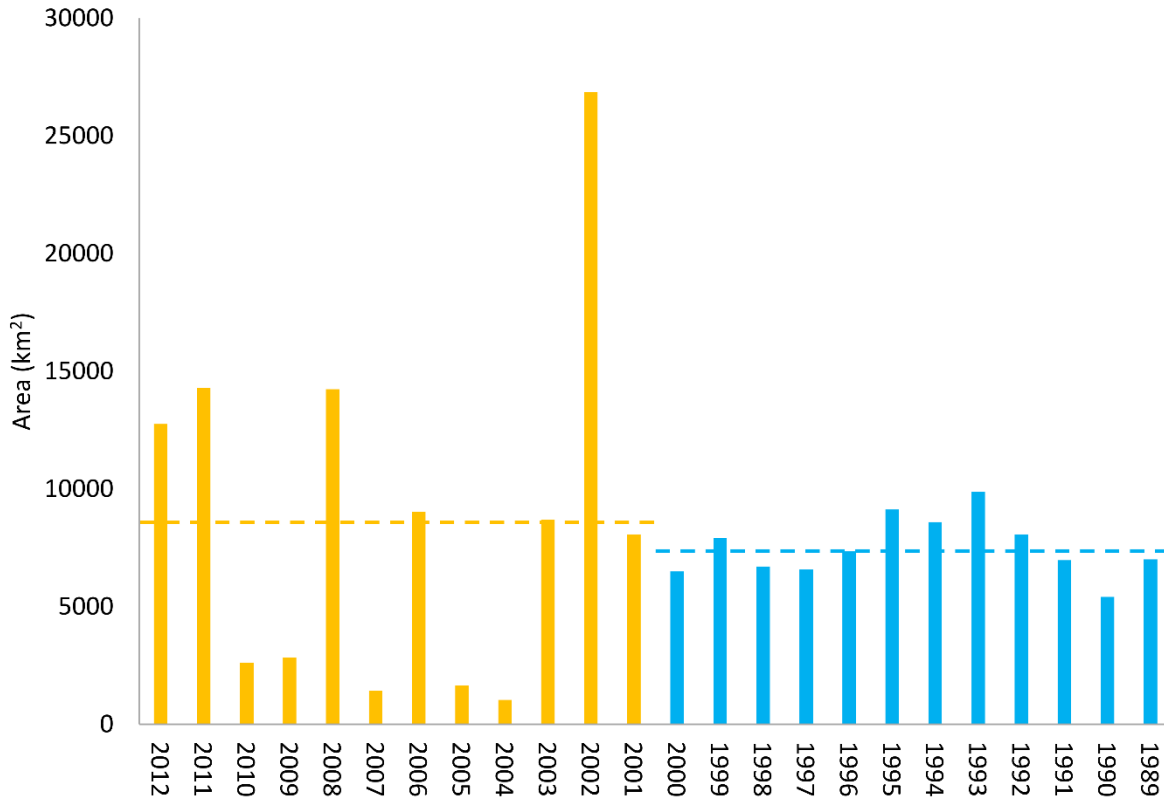
### 2.5.3. Stand age map

Figure 2-6 shows the produced 24-year stand age distribution map for the Siberian larch forests in 2012. The area of each class, as well as the annual burned area, was estimated based upon the mapped area and previously reported accuracy statistics. Across the study area, 89% (1,598,466 km<sup>2</sup>) and 11% (193,521 km<sup>2</sup>) of the forests were estimated to be unburned and burned, respectively. Out of the burned forests, approximately 53% (103,460 ± 19,378 km<sup>2</sup>) was burned during 2001-2012, compared with 47% (90,061 ± 27,401 km<sup>2</sup>) of the forests burned during 1989-2000. The inter-annual burned area distribution (Figure 2-7) indicates a higher level of

inter-annual variation in burned area during the post-2000 period than the pre-2000 period.



**Figure 2-6 (a) The produced 24-year stand age distribution map for the Siberian larch forests in 2012 with 30-m resolution. Insets (b)-(d) show detailed views of three subsets of the stand age map.**



**Figure 2-7 Inter-annual burned area distribution calculated based on the produced stand age map and the associated accuracy statistics. Blue and yellow represent the pre-2000 and post-2000 components of the produced map, respectively. Dashed lines represent the mean annual burned area during the corresponding 12-year period.**

## 2.6. Discussion

### 2.6.1. Accuracy of the produced map

Although our map depicts stand age at the annual time step, due to the lack of reference data prior to 2000, we were unable to assess its accuracy at this temporal resolution. Instead it was assessed in terms of the total burned/unburned categories. The results of the confusion matrices show that the two components of the stand age distribution map vary substantially in their mapping accuracy. This variation likely

stems from the difference in the mapping algorithms. It is not surprising that the SRFM map (our post-2000 component) that represents annual forest cover change detection assessment has higher user's and producer's accuracies. The pre-2000 component, which was estimated using a random forest classifier, shows lower accuracy for burned forest mapping, which was anticipated.

In addition to the ability to map the burned forests in general, the pre-2000 component represents the stand age of the burned forests within a ~3 year window with reasonable accuracy. As shown in Figures 2-4 and 2-5, in the assessments conducted against the ABFM product, the produced dataset shows good consistency, in most cases, with the expected stand age of each of the fire polygon groups. Admittedly, the peaks of the histograms do not match the expected stand age exactly in every instance and in some cases the histograms do not show obvious peaks; however, these mismatches are at least partially due to the mapping error in the reference dataset, including false detections. As stated in the Methodology section, visual examination of ABFM dataset showed a substantial number of false detections. In addition, it is not uncommon to identify mismatches between the preserved fire polygons in the ABFM product and actual burn scars in the 2000 imagery. These mismatches no doubt negatively affected the consistency between the histogram peaks and ESAs. Another factor which may negatively impact the consistency is the difference in spatial resolution between ABFM and our Landsat-based stand age map. Produced based on the AVHRR data, the ABFM dataset will likely miss fires that were too small at the scale of 1-km pixel size. However, those fires may be well

captured by our stand age map, considering that its spatial resolution is 30 m, much smaller than 1 km.

The accuracy of stand age estimation is subject to the influences of several main factors. Firstly, the existence of gaps in the GFC Landsat composite for *circa* 2000. Although gap-filling was implemented when producing the composite, it is not uncommon to identify artifacts in the composite images caused by the inconsistency in reflectance between the target and filled Landsat images. This will likely introduce some error to the produced map. Secondly, the inclusion of non-larch stands and non-burn-related disturbances in the study area. This study focuses on the Siberian larch forests based on the MODIS MCD12Q1 Land Cover Product. Although larch is expected to dominate the study area, due to a variety of reasons, including potential error of the MCD12Q1 product and changes in actual forest composition, it is expected that other forest types exist in the study area. In addition, while wildfires have been confirmed to be the most dominant disturbance agent in the region, other disturbances, such as insect and windstorm damage and forest harvesting also occur. The forest stands that are related to either one of these two factors may exhibit different stand age-reflectance relationships. Thirdly, the variability of age classes can be related to the difference in levels of burn severity. On the one hand, depending on fuel and environmental conditions, stand-replacing fires can exhibit variant levels of severity. High severity fires may lead to the delay of regeneration in the post-fire larch stands. In some cases, forest regeneration may completely fail after fires with very high severity because of recruitment failure. Although we have taken measures to limit the inclusion of these areas where regeneration had failed completely by

applying forest masks, the forest stands regenerated after less severe stand-replacing fires are likely to show slightly different spectral properties, thus affecting our stand age estimation. On the other hand, non-stand-replacing surface fires are common in the Siberian larch forests. That is because larch stands are relatively open and larch possess a series of fire-resistant adaptations, including thick bark and the ability to shed low-reaching branches to avoid the formation of fuel-ladders (Kharuk et al. 2010; Schulze et al. 2012; Wirth 2005). Due to the high fire resistance of larch, fire events in the Siberian larch forests usually lead to a mortality rate that is much lower than in North American boreal forests, where dominant tree species are much more vulnerable to fires (Wirth 2005). As a result of the difference in burn severity of both stand-replacing and non-stand-replacing fires, it is not uncommon for the burned larch stands to exhibit different levels of damage, even within the same burn scars. Figure 2-8 shows an example fire event in the study area. It occurred sometime between 7/31/1999 and 8/10/2000, as indicated by two temporally adjacent Landsat images (Figure 2-8a and 2-8b). Figure 2-8c shows a differenced Normalized Burned Ratio (dNBR) image based on the two Landsat images as dNBR is a commonly used measure to evaluate burn severity (Garcia and Caselles 1991). Although this fire event was successfully captured by the produced stand age map (Figure 2-8d) and, within the burn perimeter, most pixels were correctly assigned to values indicating the years of fire being either 2000 or 1999 (as indicated in red in Figure 2-8d), stands that were estimated to be burned in years before 1999 (as indicated in orange and yellow in Figure 2-8d) also exist within the same burn scar. When compared with the dNBR map, the variability in the estimated year of burn appears to be related to the

variation in burn severity. We believe the variation in fire-induced mortality rates associated with burn severity is a major source of uncertainty in the presented study, as partially damaged forest stands will recover more rapidly, thus spectrally resembling those burned by stand-replacing fires with longer post-disturbance time.

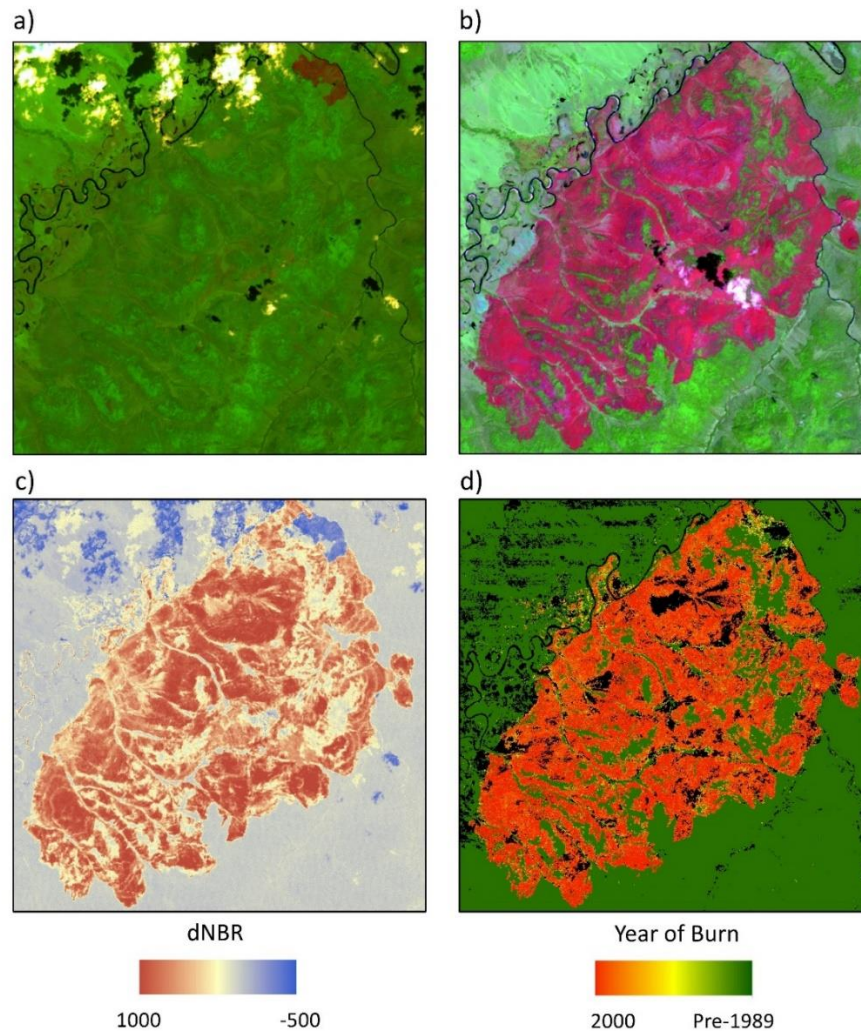


**Figure 2-8 An example fire event: a) Landsat image on 7/31/1999, b) Landsat image on 8/10/2000, c) dNBR calculated based on a) and b), d) estimated year of burn according to the produced map (black indicates unclassified area).**



### *2.6.2. 24-year stand age distribution in the Siberian larch forests*

According to the produced stand age distribution map, the inter-annual variation in burned area extent prior to 2000 seems to be substantially lower than that between 2001 and 2012. We suspect the actual variation before 2000 was larger than estimated here, however, since we are unable to assess the accuracy of annual disturbance estimates, we would caution against using these data to conduct assessments at the stand level and annual time-step, since the outcome may be more sensitive to inter-annual variation. However, as indicated by the results of the accuracy assessment at the landscape and regional scales and over longer time periods (e.g. pre-2000 vs post-2000) these comparisons are possible.

Our results show that the increase in burned area extent during the post-2000 era is primarily concentrated in a “hotspot” located in the northeastern part of the study area, along the midstream of the Lena River (approximately 59 °63 °N and 118 °135 °E). With only 10% forested area of the entire study area, this subregion experienced more than one third (36%) of the stand-replacing fires between 2001 and 2012. In addition, the sizes of individual recovering patches are also considerably larger than those in other parts of the Siberian larch forests. Higher concentration and larger individual fire sizes suggest there have been favorable conditions for wildfires in this subregion in the recent past.

During the development of the random forest model, the importance of the seven independent variables, in terms of their contribution to the overall predicting power of the final model, was revealed (Figure 2-3). Although the quantitative relationship between the spectral metrics and stand age in the Siberian larch forests

was unable to be provided by the current work due to the limitation of the random forest model in terms of model interpretability (Prasad et al. 2006), it is worth noting that the metrics that were shown to have the largest contributions were NBR and NDWI, which were not surprising since they have been shown to be highly correlated with post-fire forest recovery in boreal regions (Loboda et al. 2012; Zhang et al. 2004).

## **2.7. Conclusion**

The Siberian larch forests constitute a large proportion of the boreal forest biome and may potentially have a considerable impact on the regional and global climate through a series of biogeophysical and biogeochemical effects. The large spatial extent and remoteness of these forests make remote sensing the only feasible method to study the spatially explicit stand age dynamics of these forests at the regional scale. The lack of satellite observations over this region before year 2000 necessitates the development of new approaches to yield a better understanding of larch forest dynamics in the region. The method presented in this paper is novel in that it utilizes information gained from the data-rich post-2000 era about the spectral characteristics of forests of different ages and applies it to the study on the pre-2000 forest conditions. This approach is supported by a combination of factors including; the existence of high quality annual satellite observations since 2000, slow growing rates of larch forests, and the dominance of larch species in the region even during the early successional stage. The resultant map provides the first spatially comprehensive assessment of stand age distribution of young forests (< 25 years of age) within the Siberian larch domain. With the continuous acquisition of satellite imagery moving

forward, we have the opportunity to continue development of stand age assessments within boreal forests. The developed approach could be modified to take advantage of the available Landsat MSS imagery and extend the stand age distribution record further into the past. However, it will be extremely challenging to develop an accuracy assessment for an even earlier mapping period. In addition, with modification, the proposed method has potential to be applied in other parts of the boreal biome.

Being the first ever “wall-to-wall” stand age distribution map of the Siberian larch forests at a decadal temporal scale, this dataset possesses strong scientific significance as it can be used as the foundation of various studies examining forest dynamics of the Siberian larch forests as well as the resulting climatic impacts. Specifically, our results show that on average stand-replacing fires in Siberian larch forests impact over 8,000 km<sup>2</sup> per year. Over the 24-year period, the area covered by young forests has reached 10% of the total forested area. In our subsequent work, we aim to further explore the relationship between the remote sensing-based spectral metrics and the stand age in the Siberian larch forests and to examine the impact of regrowing larch forests on the radiative forcing and carbon stocks and fluxes in Siberia using the derived stand age distribution map.

# **Chapter 3: Strong cooling induced by stand-replacing fires through albedo in Siberian larch forests**

## **3.1. Introduction**

The boreal forest is one of the largest biomes in the world (Chapin et al. 2006; Melillo et al. 1993) and a key element in the global climate system that has the capacity to impact regional and global climate strongly (Bonan et al. 1992). Its influence on climate is exerted mainly through two sets of mechanisms: the biogeochemical effects, primarily through the carbon cycle, and the biogeophysical effects including albedo, evapotranspiration, and surface roughness. Boreal forest has a strong impact on global temperatures largely attributable to the increased absorption of solar radiation caused by considerably lower albedo of the boreal forest during the snow season, relative to other land cover types such as tundra and bare ground (Bonan 2008; Bonan et al. 1992). The albedo-driven warming effect likely overshadows the cooling resulting from the carbon sequestration in the boreal zone and is the dominant driver controlling the net climatic impact of the boreal forest (Bala et al. 2007; Betts 2000; Bonan 2008; Bonan et al. 1992).

Because albedo of the boreal biome exerts a strong control over the climate, any forces that significantly change forest albedo, including wildfire, can potentially carry strong climatic implications. Wildfire is a common natural disturbance agent in the boreal forest that controls species composition, stand age, and successional patterns (Bourgeau-Chavez et al. 2000; Chapin et al. 2006; Goldammer and Furyaev 1996; Kasischke 2000; Shvidenko and Nilsson 2000). Wildfire impacts have been

studied extensively in the boreal forests of North America, where wildfires have been found to impose a general cooling effect after fire (Amiro et al. 2006; Jin et al. 2012b; McMillan and Goulden 2008; Randerson et al. 2006; Rogers et al. 2015), for which two factors are responsible. First, wildfires in the North American boreal forests are generally stand-replacing. As a result, they remove forest canopy, causing higher level of ground exposure, and resulting in considerably higher albedo during the snow season (Amiro et al. 2006; Randerson et al. 2006). Second, in the post-fire forest stands, there is usually a prolonged successional period with high dominance of deciduous broadleaf species, which typically have higher albedo than needleleaf evergreen species (Amiro et al. 2006; Liu and Randerson 2008; Lyons et al. 2008; McMillan and Goulden 2008; Viereck 1973). Randerson et al. (2006) constructed a radiative forcing trajectory induced by post-fire albedo changes in the burned black spruce (*Picea mariana*) forest stands in interior Alaska. Their results indicated that albedo-induced radiative forcing in the burned forests became negative one year after fire and remained so for 50 years. During these 50 years, the magnitude of the cooling effect shifted from increasing to stable, then to decreasing, with the maximum level ( $-8 \pm 3 \text{ Wm}^{-2}$ ) reached 10 years after the fire. The cumulative cooling effect of the fire-induced albedo changes outweighed the combined warming effect of the CO<sub>2</sub> and CH<sub>4</sub> emissions, resulting in a net cooling effect estimates to last for more than 150 years. Rogers et al. (2015) also established an albedo-induced surface forcing (SF) trajectory for the burned forests in North America. Based on MODIS data, their results, although limited to an 11-year time span, were well-aligned with those of Randerson et al. (2006).

With the total area of about a fifth of the global boreal forest (Osawa and Zyryanova 2010), the forests of Eastern Siberia are an important component of the boreal biome. These forests are strikingly different from other boreal forests in that they are mostly underlain by continuous permafrost and dominated by larch - a deciduous needleleaf species (Abaimov 2010; Osawa and Zyryanova 2010). Moreover, unlike the boreal forests of North America, larch species dominate forest composition at all recovery stages and generally do not experience secondary broadleaf successional stages. These differences imply that the knowledge gained about the climatic impact of the fire-induced albedo changes in the North American boreal forests cannot be readily applied to the larch forests of Siberia. A recent study conducted by Rogers et al. (2015) indicates that the post-fire stands in boreal Northern Eurasia also produce a cooling effect although of a much smaller magnitude compared with those in the North American boreal forests. However, the mechanisms behind the apparent difference in the magnitude of fire-induced albedo forcing between North American and Siberian boreal forests are unclear. One of the likely contributing factors is the difference in the extent of stand-replacing fires and surface fires, which are also common in Siberia (Schulze et al. 2012; Wirth 2005). In this study I aim to isolate the impacts of stand-replacing fires within the Siberian larch forests on SF using a recently developed stand age map of the Siberian larch forests (Chen et al. 2016) along with the full record of high quality Collection 6 MODIS albedo product (Schaaf et al. 2002). I focus on understanding the temporal trajectory of SF resulting from stand-replacing fires as well as quantifying the impact of those

fires on the SF produced by the Siberian larch forests as a whole between 2001 and 2012.

### **3.2. Data and Methods**

This study is focused on the Siberian larch forests as they are defined in Chapter 2. It is a region in Eastern Siberia with high larch dominance, as derived from satellite-based datasets (see Section 2.2).

All good-quality (as indicated by the associated quality band) shortwave black-sky (BSA) and white-sky (WSA) albedo values between 2001 and 2015 within the study area were extracted from the MODIS albedo product (MCD43A3, Collection 6; Schaaf et al. 2002) and used to calculate annual mean BSA and WSA. The calculation of the annual mean albedo for each pixel was hierarchical, where the monthly mean values were calculated first, based on which the annual mean values were then calculated. The extremely low solar angles result in very few high quality albedo observations between November and February. Consequently, the mean albedo for those months would further hindered the calculation of the annual mean values. To compute the annual mean albedo across the study area, in cases when January and February monthly mean albedo was not available, I set the mean albedo values of those two months to the first high-quality albedo value in March of the corresponding year (e.g. January and February of 2015 received the mean monthly value of March 2015). Similarly, the mean albedo values for November and December, were set to the last high-quality albedo observation in October (e.g. November and December of 2014 received the mean monthly values of October 2014). After the annual mean albedo was calculated, following Rogers et al. (2015), a

three-year mean filter was applied to smooth the high inter-annual variability. The annual mean blue-sky albedo (BA) was then calculated by taking the mean of the annual mean BSA and WSA for each year.

I then calculated SF for the entire study area based on all possible year combinations allowing for the calculation of SF following the equation:

$$SF = (BA_{t1} - BA_{t2}) * S_{\downarrow}$$

where  $BA_{t1}$  and  $BA_{t2}$  represent annual mean BA for years  $t1$  and  $t2$  ( $t1 < t2$ ), respectively, and  $S_{\downarrow}$  stands for mean downward shortwave surface flux, calculated for all years between  $t1$  and  $t2$ . The clear-sky downward shortwave surface flux data produced by the Clouds and the Earth's Radiant Energy System (CERES) project (Kato et al. 2013) was used to compute  $S_{\downarrow}$ . This dataset was derived from the top-of-atmosphere (TOA) irradiance, which was acquired by the sensors on board the Terra and Aqua satellites, and calibrated using a set of independent data inputs including cloud properties identified by the MODIS products (Kato et al. 2013). Since the spatial resolution of the surface flux data is 1 ° it was resampled to 500-m to reconcile with the MODIS albedo data. The SF values were calculated for all areas that experienced stand-replacing fires between 2001 and 2012 (referred to as burned forests in this manuscript) as mapped in Chapter 2 (Chen et al. 2016, 2017). The extracted values were averaged according to year since fire based on which a post-fire SF trajectory was established. In order to show seasonal variation in SF changes, I also generated the monthly SF trajectories following the same methodology using corresponding monthly mean BA and downward shortwave surface flux. Monthly



mean total downward shortwave surface flux within the study area between 2001 and 2015 was also calculated to show the seasonal pattern of incoming solar radiation.

With the available datasets, the maximum range of the SF trajectories was 14 years. However, by using the 24-year stand age map, post-fire albedo dynamics can be assessed over a longer period. Therefore the albedo trajectories within all known burns as a function of time since burning were constructed and compared. In this analysis, BSA rather than BA was used to represent because of very high correlation between annual mean BSA and WSA within the study area during 2001-2015 ( $R^2 = 0.99$ , Figure 3-1). Three BSA trajectories (i.e. mean annual, snow-off and snow-on BSA) were established for all stand-replacing fires which occurred between 1989 and 2012 using all high-quality MODIS albedo data for 2001-2015. Snow-off BSA was calculated as the mean value for June, July and August and snow-on BSA was calculated based on October and March (because during these two months there are sufficient high-quality albedo observations in the region) in each year. BSA values for September, April, and May were not used in the mean snow-on and -off calculations because the extent of snow on the ground during these months varies and thus, if included in the averaging, would represent mixed signals for both snow-on and snow-off conditions. While no MODIS-based albedo data exists for fire-induced forest loss before 2001, I used 2001-2015 albedo values for those fire events to extend the BSA trajectories of burned forests beyond the MODIS 15-year record. For example, for stand-replacing events of 1989 and 2001, BSA values of 2015 were used to assess impacts on albedo 12 and 26 years since fire, respectively. The pre-fire albedo values for stand replacing fires that occurred between 2001 and 2012 were

utilized as the reference indicating the pre-fire baseline albedo dynamics. In addition to the post-fire BSA values, the pre-fire BSA values were also tracked for all burned forests and their corresponding “year since fire” values in the generated trajectories are negative.

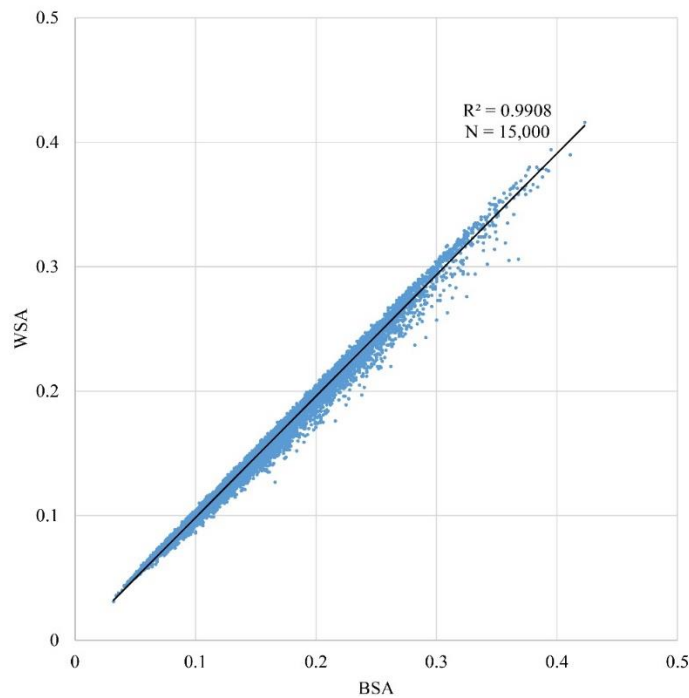


**Figure 3-1 The statistical relationship between annual mean BSA and WSA between 2001 and 2015 within the study area.**

To account for the inherent uncertainty in precision of disturbance timing translated into stand age for pre-2000 events in stand age distribution map (Chen et al. 2016), I generated suites of annual mean BSA trajectories iteratively. In each iteration, one stand age class in the pre-2000 component was allowed to vary  $\pm 1$  year of the stand age value, while other stand age classes remained unchanged. For example, the stand age class corresponding to stand-replacing fires occurred in 1998, was set to 1999 and 1997 in two iterations. This resulted in a total of 22 annual mean

albedo trajectories corresponding to 22 iterations (two for each year between 1990 and 1999 and, one for 1989 and 2000, respectively), and these trajectories were superimposed with the original annual mean BSA trajectory to represent the uncertainty resultant from the uncertainties in stand age estimations.

Subsequently, the BSA anomalies for forests that suffered stand-replacing fires in each year between 2001 and 2012 were calculated and examined. BSA anomalies were calculated within the mapped burns in each of the 12 years beginning with January 1 through 2001-2015 on an 8-day basis to minimize the influence of low-quality observations due to cloud cover. Similarly, mean BSA for each 8-day cycle across 15 years (i.e. 2001-2015) was calculated for all forests that did not experience stand-replacing fires between 2001 and 2012. The BSA anomalies were then computed by subtracting each of the 8-day mean BSA for the forests that did not burned during 2001-2012 from the corresponding 8-day burned BSA for each year.

Finally, I examined the spatial distribution of SF for the entire study area calculated between 2001 and 2013, which reflects the combined effect of all stand-replacing fires that occurred between 2001 and 2012. To summarize the findings, I divided the study area into 6 zones, each corresponding to 10 ° in longitude and 7.5 ° in latitude. I further compared SF for burned and unburned forests between 2001 and 2012 and all forests within each zone accounting for fraction of area burned. To aid the interpretation of revealed patterns of the spatial distribution of SF, I tracked the daily snow cover for each pixel within the study area between 2001 and 2015 using the MODIS MOD10A1 (Collection 6) daily snow cover product (Hall et al. 2006). Once a pixel switched from snow-on to snow-free and remained so for 7 consecutive

days, the first day of this 7-day window was considered the snow melt date for that pixel in that year. Due to the frequent occurrence of cloud cover, the qualified 7-day window was allowed to have no more than 5 cloudy days. The snow onset dates were calculated in a similar fashion, however, instead of searching for the snow-off windows, the algorithm searched for the snow-on windows. The first day of the identified 7-day window was considered the snow onset date for that pixel in that year. Generalized linear regression was fitted based on the snow onset and melt dates, respectively, of 150,000 (i.e. 10,000 for each year between 2001 and 2015) randomly selected sample points with respect to year.

### **3.3. Results**

The analysis of the SF trajectory for stand-replacing fires that occurred only between 2001 and 2012 (and thus can be linked directly to post-fire MODIS albedo observation at the annual time step) establishes that the mean annual SF of the burned forests is consistently below zero after fire for at least 14 years (which is the maximum temporal range that the SF trajectory could reach with the available datasets). During the first year after the fire event, the mean SF is slightly negative ( $-1.69 \pm 0.01 \text{ Wm}^{-2}$ ). The cooling effect, however, grows rapidly and continuously until the 11<sup>th</sup> year when it peaks at  $-9.60 \pm 0.03 \text{ Wm}^{-2}$ , after which it gradually lessens to reach  $-7.15 \pm 0.03 \text{ Wm}^{-2}$  by year 14 (Figure 3-2). The BSA trajectories (Figure 3-3) show that the mean albedo of the burned forests remained elevated compared with the pre-fire level for 26 years, suggesting that the cooling effect of the burned forests persisted during that period. The cooling effect remains virtually unchanged when the uncertainties resulting from the potential timing errors of the pre-2000 component of

the 24-year stand age map were taken into account. As shown in Figure 3-4, the annual mean BSA trajectory ensemble exhibits a higher level of variability beyond 12 years since fire. However, despite the increased variability forest albedo remains elevated compared to the pre-fire levels even in year 26. In terms of monthly distribution of SF (Figure 3-5), March shows the strongest post-fire cooling, followed by April. The cooling exists in all other months as well, but the magnitude is much smaller. In comparison, the monthly mean downwards shortwave surface flux exhibits a bell-shape pattern with a peak in June (Figure 3-6).

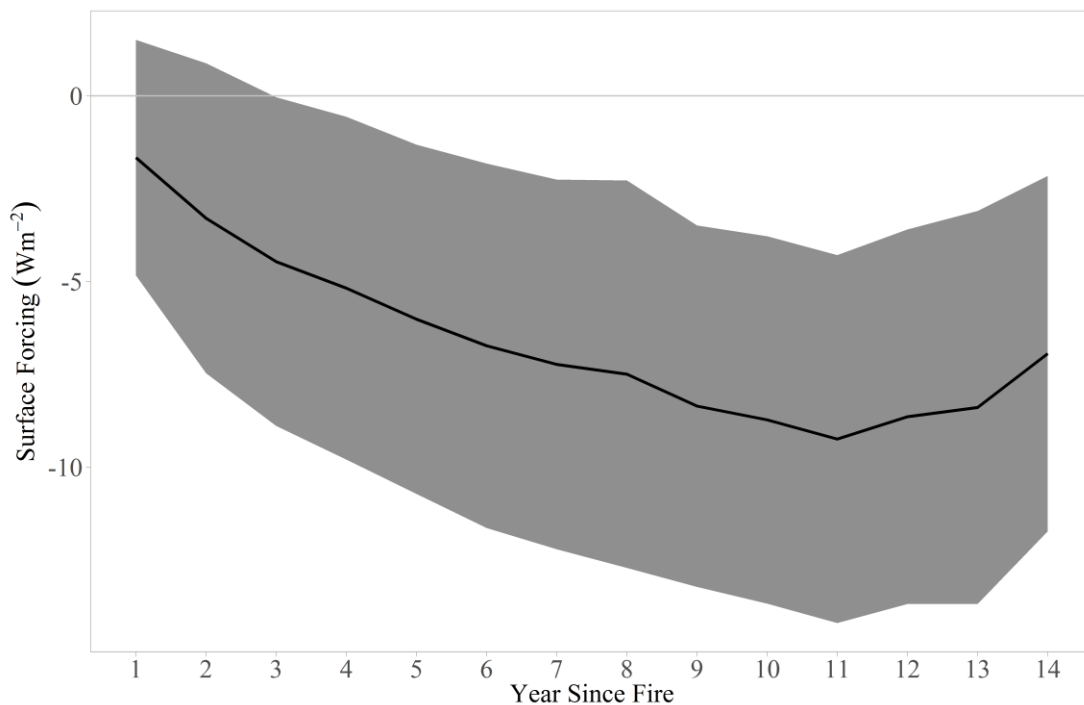


**Figure 3-2 Annual mean SF trajectory for burned forests. Grey area denotes  $\pm 1$  standard deviation range.**

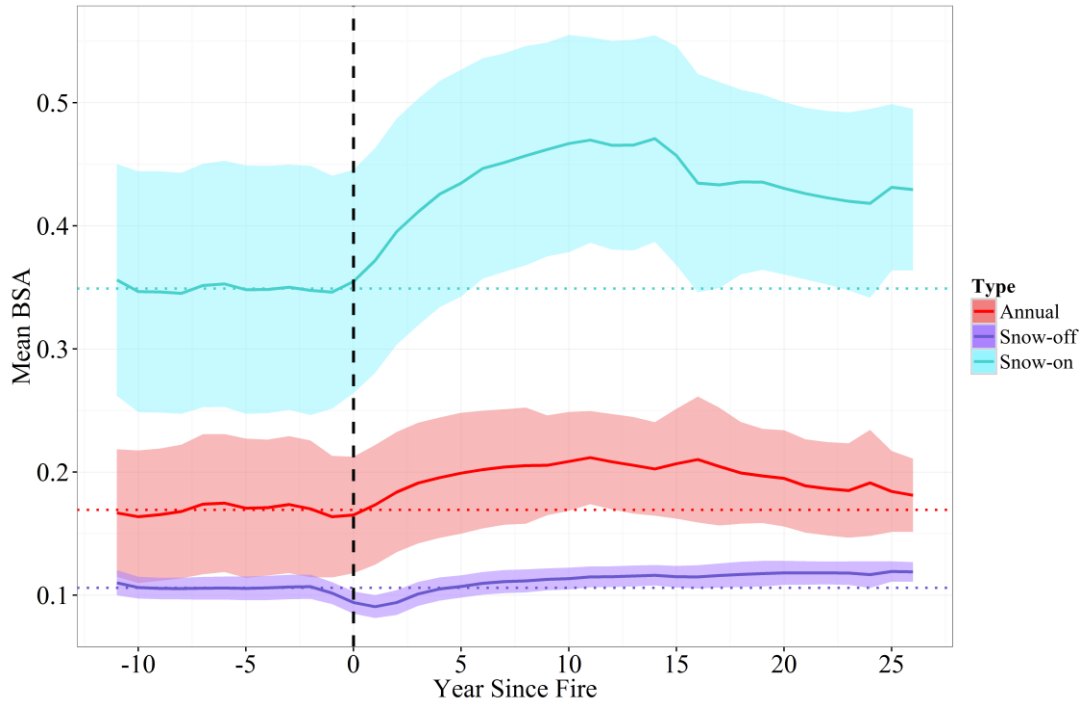


**Figure 3-3 Mean BSA trajectories for the burned forests generated using the MODIS albedo data for 2001-2015. The vertical dashed line represents the year of fire occurrence. The negative “year since fire” range represents pre-fire conditions. The horizontal dashed lines represent the mean pre-fire BSA for the corresponding trajectories. Uncertainties are represented by shaded areas within  $\pm 1$  standard deviation.**

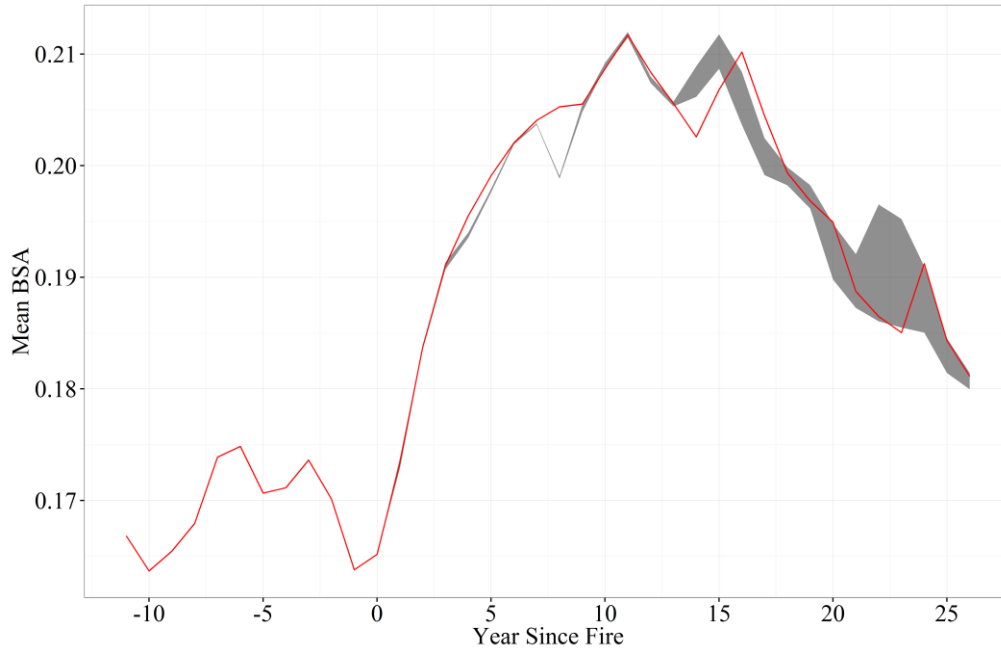


**Figure 3-4 Mean annual mean BSA trajectory (red) compared with the BSA uncertainty range calculated based on  $\pm 1$  year variation in the assumed timing of disturbance within the pre-2000 stand age values in the 24-year stand age map.**

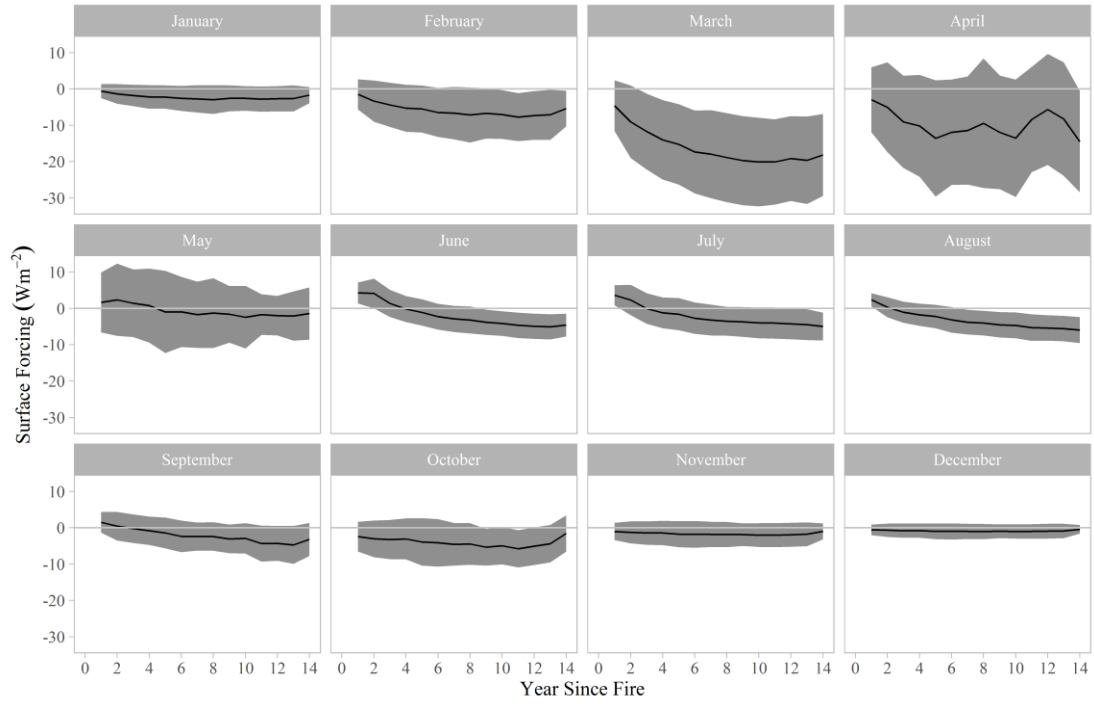


**Figure 3-5 Monthly SF trajectories for the burned forests. Uncertainty is represented by  $\pm 1$  standard deviation.**



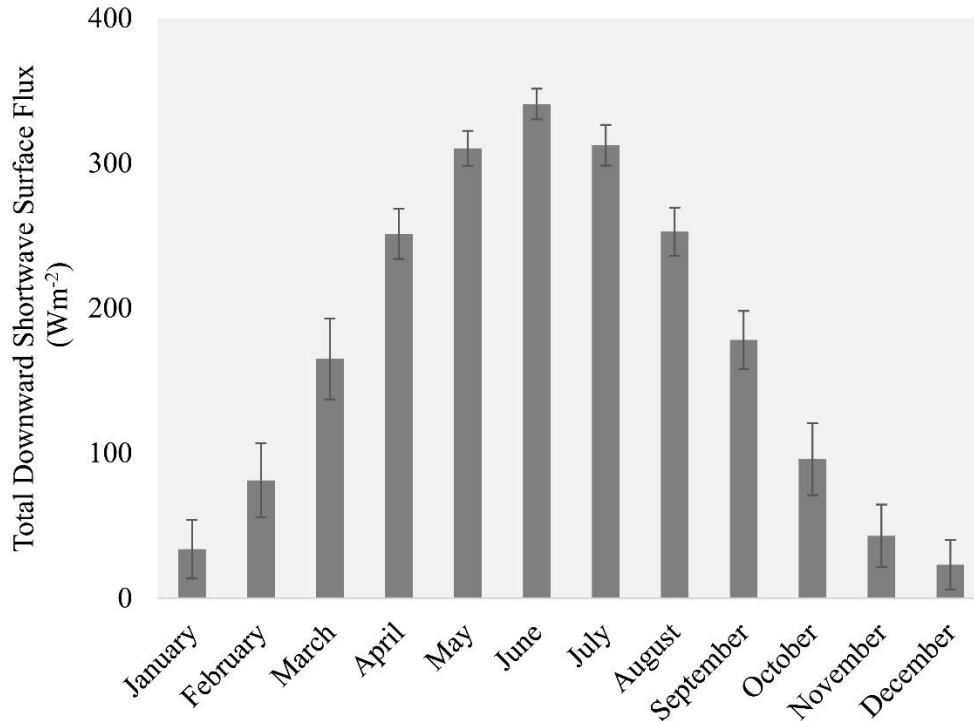


**Figure 3-6 Monthly mean total downward shortwave surface flux between 2001 and 2015. Error bars represent  $\pm 1$  standard deviation.**

Figure 3-3 and Figure 3-7 reveal the mechanism of the observed cooling effect in the burned forests. Mean albedo of the burned forests (Figure 3-3) increased considerably immediately after fire, and the increase was especially notable in the beginning and the end of each year (Figure 3-7), which together correspond to the snow season in the region. Figure 3-3 shows three trajectories corresponding to the mean annual, snow-off and snow-on BSA calculated for the burned forests over a longer time span. An inter-comparison between three trajectories reveals several interesting patterns. First, all three albedo trajectories show an overall increase in surface albedo after fire, but the magnitude of the increase is different, with the snow-on albedo being the most significant (up to an increase of 0.12 in year 14 relative to the mean pre-fire level). Second, the increase in mean snow-on BSA takes place

immediately after fire, whereas mean snow-off BSA shows an initial decrease the first year after fire, after which albedo begins to increase. Similar to mean snow-on BSA, the annual mean BSA trajectory begins increasing immediately after fire, which is likely because snow-on BSA has a stronger control over annual mean BSA than snow-off BSA. Third, the snow-off trajectory shows a small but seemingly continuous increase up to year 26, whereas the annual mean and winter trajectories

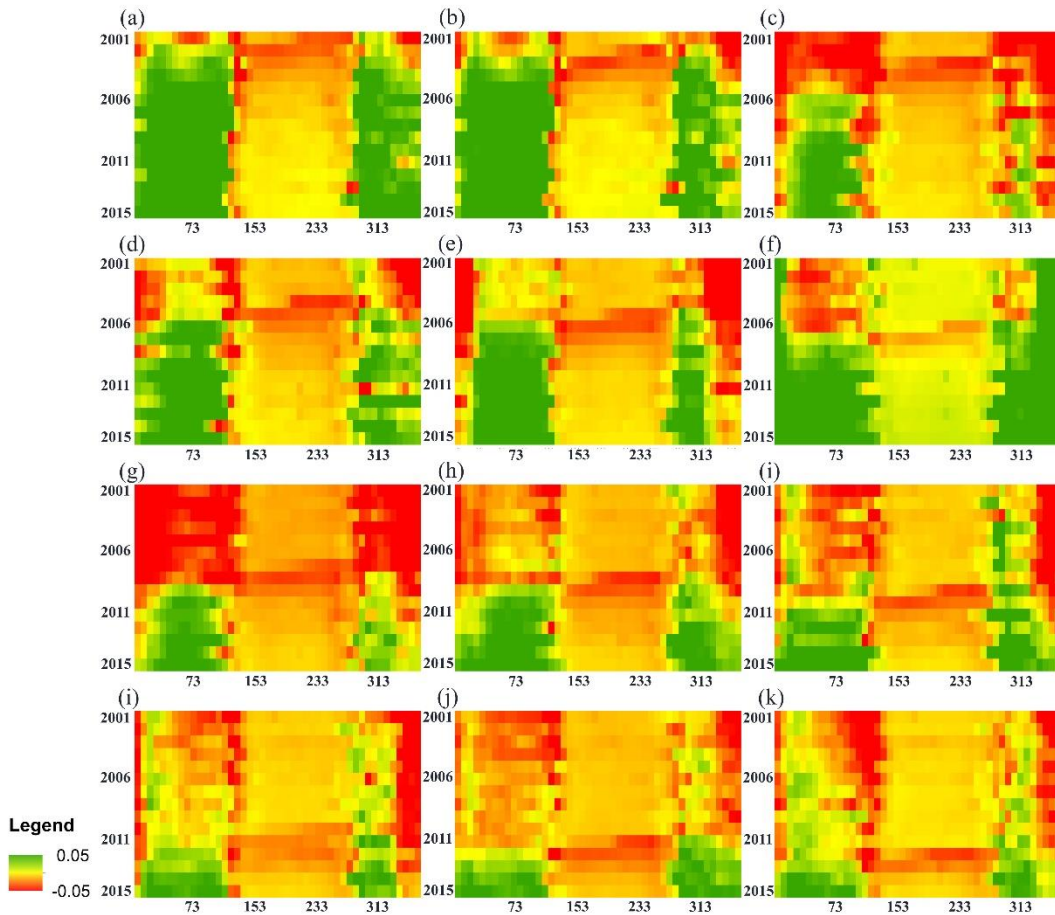


**Figure 3-7 The 8-day BSA anomalies calculated for the forests that burned between 2001 and 2012. Green and red represent albedo increase and decrease, respectively, relative to the forests that did not experience stand-replacing fires during 2001-2012. In each graph, the x-axis is Julian Day and the y-axis is year (from 2001 to 2015).**

reach maximum levels in year 11, followed by observable decreases. Despite the decreases, by year 26, annual mean and snow-off BSA is still at elevated levels compared with the pre-fire conditions.

The spatial distribution of albedo-induced SF calculated for 2001-2013 across the study area is heterogeneous (Figure 3-8). After classifying the total range of SF into 5 classes (1:  $SF > 5 \text{ Wm}^{-2}$ , 2:  $2 \text{ Wm}^{-2} < SF < 5 \text{ Wm}^{-2}$ , 3:  $-2 \text{ Wm}^{-2} < SF < 2 \text{ Wm}^{-2}$ , 4:  $-5 \text{ Wm}^{-2} < SF < -2 \text{ Wm}^{-2}$ , 5:  $SF < -5 \text{ Wm}^{-2}$ ), it appears that the distribution of areas with significant cooling effects ( $SF < -2 \text{ Wm}^{-2}$ ) is consistent with the areas that experienced stand-replacing fires between 2001 and 2012. This is well illustrated through the comparison in Figure 3-9: within the burned forests, 84% of the area consists of the two cooling classes (Classes 4 and 5), whereas the warming (Classes 1 and 2) and cooling (Classes 4 and 5) effects take up similar proportions within the unburned forests. The zonal analysis further confirms the dominance of the cooling effect of the burned forests over the region. Despite the fact that the net SF of the entire study area between 2001 and 2013 is estimated to be  $-0.78 \text{ Wm}^{-2}$ , the net 2001-2013 SF for three (i.e. Zones 1, 2 and 5) out of six zones is found to be positive (Figure 3-10a). I believe this is a combined effect of two causes: 1) these three zones have the three lowest burned area proportions (Figure 3-10b) and 2) the net SF of the forests that did not experience stand-replacing fires is positive. A closer examination on these three zones reveals that the warming effect of the unburned forests is likely caused by a decrease in albedo during the transitional period between the snow-on and snow-off seasons (i.e., Julian Days 113-145). The analysis of snow melt and onset dates (Figure 3-11) shows that over the 15 years, the snow melt in the entire

region occurred earlier and the trend is statistically significant ( $t = -246.56$ ,  $p < 0.001$ ). During the same time, the mean snow establishment was delayed ( $t = 43.30$ ,  $p < 0.001$ ), although the magnitude of the delay is much smaller. The changes in mean snow melt and establishment dates together lead to a general lengthening of snow-free seasons since 2001 by 10-15 days (Figure 3-11).

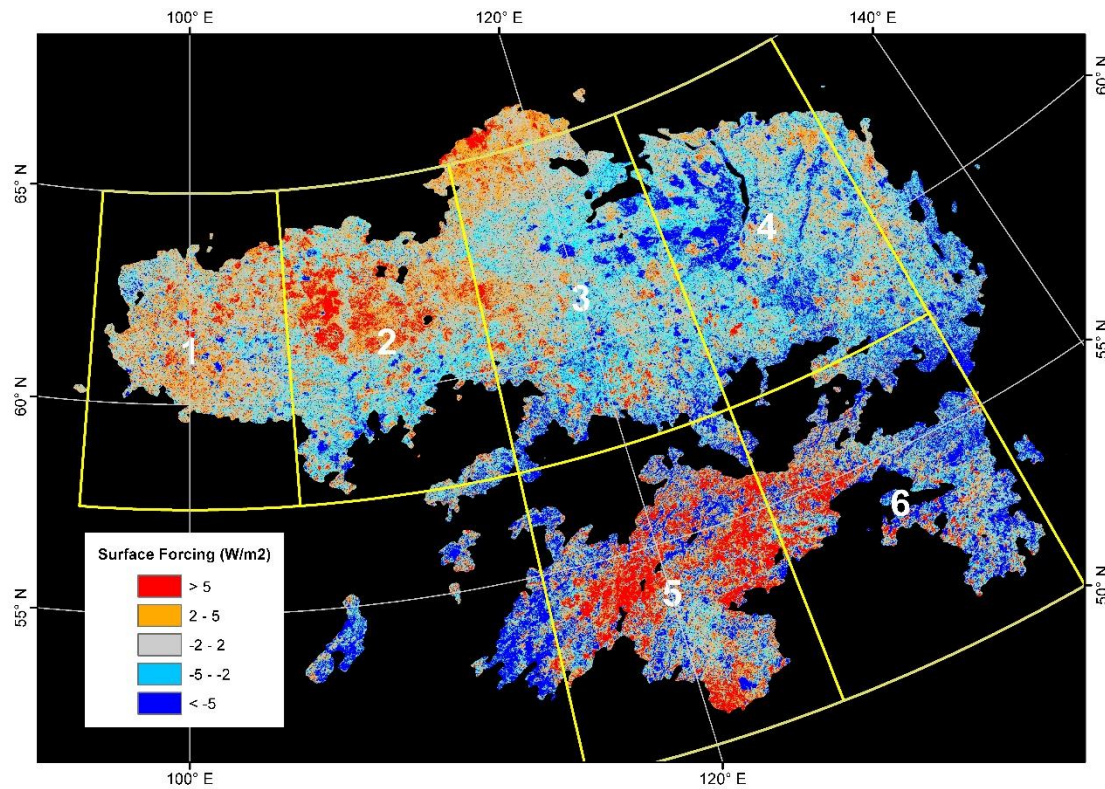


**Figure 3-8 SF between 2001 and 2013 for the Siberian larch forests. Black color represents unclassified area or missing data. Six 10°×7.5° zones are superimposed on top of the distribution map and are labeled sequentially.**

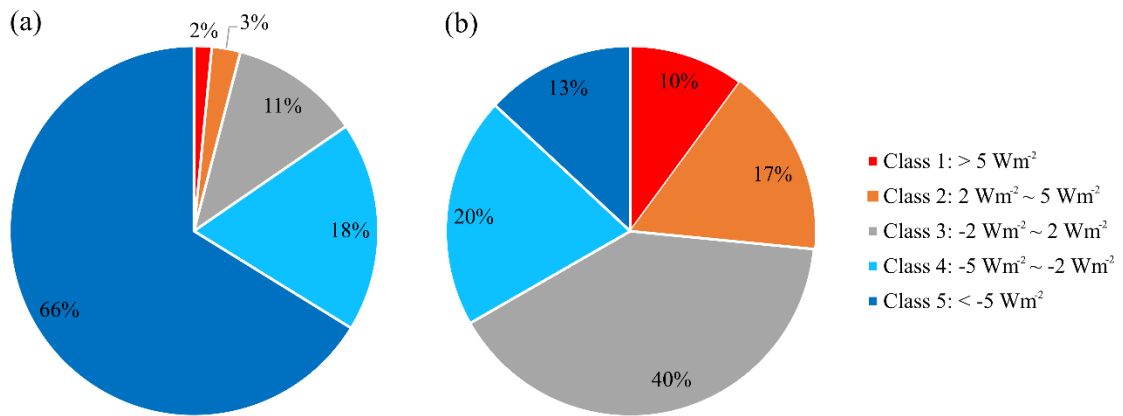


**Figure 3-9 Area proportion of the five SF ( $Wm^{-2}$ ) classes within (a) burned and (b) unburned forests between 2001 and 2012.**



**Figure 3-10 Results of the zonal analysis: (a) Mean 2001-2013 SF calculated for all 6 zones based on burned forests only, unburned forests (between 2001 and 2012) only and burned and unburned forests combined. The dashed line represents mean 2001-2013 SF calculated based on all forests (burned + unburned) across the entire study area. Uncertainties are represented by  $\pm 1.96 \times$  standard error. (b) Areal distribution of burned and unburned forests across the 6 zones. Labels show the proportions of burned forest area out of all forests area in the corresponding zones.**

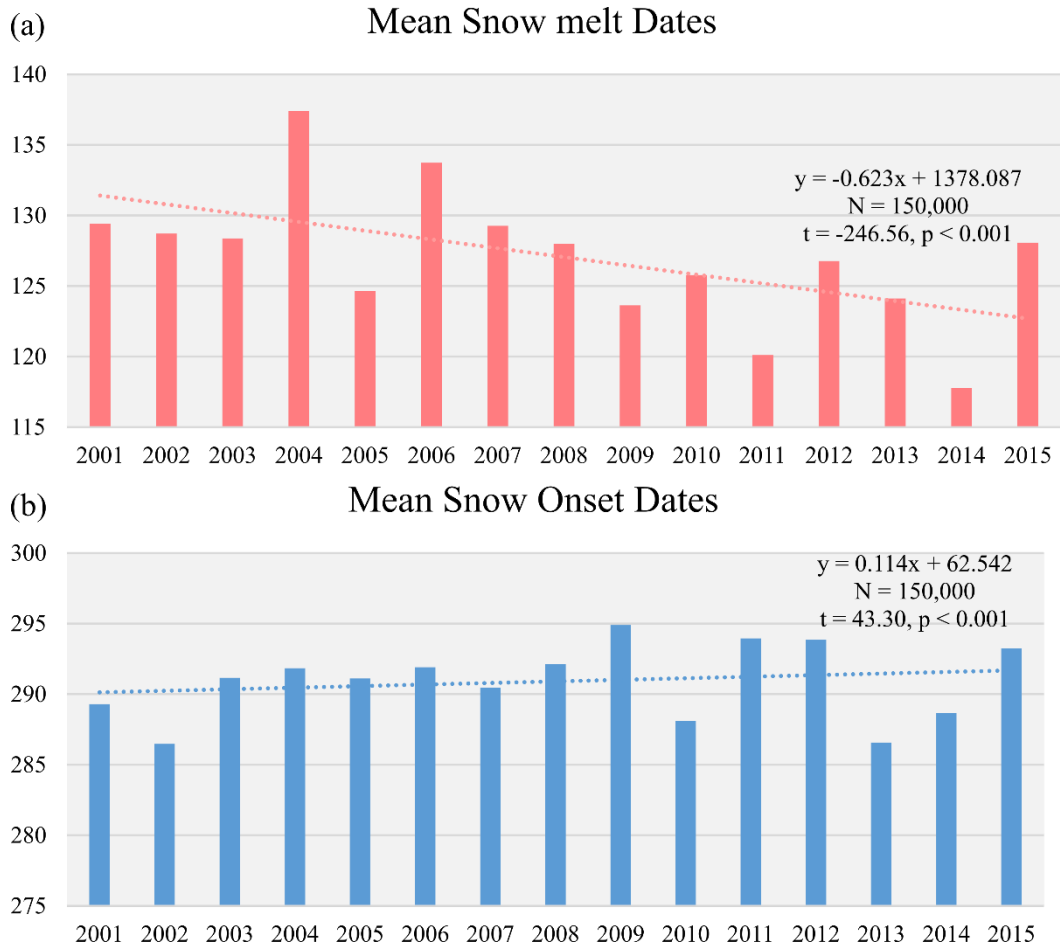


**Figure 3-11 Mean snowmelt and snow onset dates in the study area between 2001 and 2015 determined based on the MODIS MOD10A1 daily snow cover product. The dashed lines represent linear trends.**

### 3.4. Discussion

#### 3.4.1. Strong fire-induced cooling effect in the Siberian larch forests

The SF and albedo trajectories established for the forests that burned between 2001 and 2012 showed that stand-replacing fires in the region also impose a cooling effect for at least 26 years after fire. However, the magnitude of the fire-induced cooling effect estimated in the current study is much larger than what was suggested previously. According to my results, surface forcing of the forests that suffered stand-



replacing fires can exceed  $-9 \text{ Wm}^{-2}$ , which is about twice of the maximum magnitude indicated by Rogers et al. (2015). The difference, however, is not unexpected because the trajectory established in Rogers et al. (2015) did not differentiate stand-replacing fires from surface fires. As a result, the cooling effect of the forest stands recovering from stand-replacing fires may have been lessened by the potentially smaller climatic impacts imposed by surface fires which generally do not induce tree mortality (Goldammer and Furyaev 1996; Korovin 1996). The difference could also be attributable to the difference in forest species composition, as the study area within Rogers et al. (2015) covers not only the Siberian larch forests, but also western Siberia and the Russian Far East, where larch is not the dominant species (Larsen 1980). Another factor which may have contributed to the difference in magnitude of estimated post-fire SF is the difference in data inputs. The stand age map that I used to provide the locations of the stand-replacing fires was derived based on a series of Landsat-based remotely sensed datasets (Hansen et al. 2013; Krylov et al. 2014). Its spatial resolution is 30 m which may have translated into better delineation of stand-replacing fires than the MODIS-based burned area product employed by Rogers et al. (2015). In addition, Rogers et al. used the Collection 5 MCD43A3 albedo product, which has been reported to suffer from the degradation of MODIS Terra sensor (Wang et al. 2012). I encountered the impact of sensor degradation in a preliminary analysis, where the cooling effect of the burned forests estimated using the Collection 5 data was up to  $2 \text{ Wm}^{-2}$  smaller compared to estimates derived from the Collection 6 MODIS albedo product, which was corrected for the inconsistency and used in the current study. Moreover, the CERES downward shortwave surface flux data that I

used is more accurate than the reanalysis dataset (Kalnay et al. 1996) used by Rogers et al. in terms of both spatial resolution (i.e. 1 ° vs. 2.5 °) and production basis (i.e. observational vs modeled).

### *3.4.2. Mechanism of the fire-induced cooling effect*

The post-fire SF trajectory indicates that when comparing exclusively stand-replacing fires, the cooling effect induced by the post-fire albedo changes in the Siberian larch forests is similar, if not larger, to their North American counterparts as reported by previous studies (Randerson et al. 2006; Rogers et al. 2015). The similarity between two boreal zones in this regard likely reflects a common driver of cooling immediately after fire: damages to the forest canopy by stand-replacing fires. The analyses of albedo anomalies (Figure 3-7) and seasonal contribution to the albedo increase (Figure 3-3) confirm that the cooling effect of the burned forests in the Siberian larch forests is attributable to the elevated snow season albedo, which is indicative of higher exposure of snow on the forest floor resulting from canopy removal after fires. However, due to the difference in successional patterns stemming from different species composition, the change patterns of SF in two regions over a longer term are likely to diverge. In most North American boreal forests, there usually is a period of time at the early successional stages when the forest stands are dominated by deciduous broadleaf species (Amiro et al. 2006; Chapin et al. 2000; Kasischke et al. 2000; Lyons et al. 2008). As a result, forest albedo typically exceeds the pre-fire level and remains elevated for a considerable amount of time. According to Liu and Randerson (2008), it may take more than 60 years for forest albedo to recover to the pre-fire level in the black spruce forests in Alaska. In the Siberian larch

forests, however, there is typically no secondary succession, and larch remains a dominant genus very early in the burned sites (Abaimov and Sofronov 1996; Furyaev et al. 2001; Zyryanova et al. 2010). As a result, the duration of the fire-induced cooling is primarily determined by the time it takes for the larch stands to recover, especially in terms of canopy cover. The results show that forest albedo, especially the winter time albedo, is consistently higher than the pre-fire values over at least the first 26 years after fire. This suggests that the forest canopy in the study area has not fully recovered for at least 26 years, which is supported by several field-based studies stating that forest recovery in the Siberian larch forests is a multi-decadal process (Alexander et al. 2012; Berner et al. 2012; Zyryanova et al. 2010). According to Zyryanova et al. (2010), this process may take 50 to 90 years.

Although post-fire forests show strong cooling effects caused by the overall increase in albedo, it is worth noting that there is a small warming effect (shown in Figure 3-5) induced by the initial decreases in summer albedo represented by the purple dashed line in Figure 3-3. This may be due to the char deposition on the forest floor and boles, a consequence of combustion. With time char is gradually removed and within 4 years the summer albedo exceeds the pre-fire level.

The analysis of monthly distributions of the post-fire SF (Figure 3-5) and total downward shortwave surface flux (Figure 3-6) shows that the solar radiation input also plays a role in influencing the post-fire SF. Although forest albedo increases greatly after fire during the snow-on season, in the months when solar radiation input is low (e.g. January and December), the cooling effect is small. However, the significance of solar radiation is still outweighed by the increases in snow season

albedo. This is exemplified by the fact that during the snow-off months, solar radiation is considerably higher than in the snow-on months; nevertheless, the cooling effects during the snow-off months are much smaller, owing to the much smaller increases of snow-off albedo compared with those of snow-on albedo.

### *3.4.3. Spatial distribution of 12-year SF and its implications*

The region-wide analysis of albedo-induced SF calculated between 2001 and 2013 reveals a heterogeneous pattern of SF across the Siberian larch forests. The comparison of area proportions of the five SF classes between the burned and unburned forests (Figure 3-9) and a zonal analysis examining the 12-year SF in six different subsets of the entire study area (Figure 3-10) show that areas with significant cooling effects (i.e.  $SF < -2 \text{ Wm}^{-2}$ ) generally coincide spatially with stand-replacing fires. Within burned forests, the cooling effect dominates (Figure 3-9a), whereas in forests that did not experience stand-replacing burns between 2001 and 2012, warming and cooling effects are mixed in roughly similar proportions (Figure 3-9b). There are multiple potential explanations for the considerable existence of cooling in the latter group. First, within the forests that did not burn between 2001 and 2012, there is a considerable proportion that experienced stand-replacing fires during the past several decades before 2000, including those that have been estimated to be burned in the pre-2000 component of the stand age map (Chen et al. 2016, 2017). And since it has been shown that forest albedo is higher than the pre-fire level over at least 26 years since fire, the inclusion of these older burned forests results in the appearance of significant cooling effect. Second, the regional pattern also includes impacts from surface fires which were not examined in this study. It is generally

accepted that surface fires occur extensively in the Siberian larch forests (Abaimov and Sofronov 1996; Conard and Ivanova 1997; Goldammer and Furyaev 1996; Korovin 1996; Schulze et al. 2012; Wirth 2005), although there is a large uncertainty regarding both their spatial extent (Soja et al. 2004) and climatic impacts. However, I hypothesize that they could also impose a cooling effect because damages to the understory could also result in an increase, albeit smaller, in snow-on albedo. Finally, the error of the stand age map could also have caused the latter forest group to show negative forcing.

In addition to the strong relationship between areal proportion of stand-replacing fires and the net SF, the zonal analysis also reveals that the net 12-year SF in three zones that were less impacted by the stand-replacing fires is positive. Through subsequent analyses, I established that this increase appears to be related to the decreased albedo during the transitional periods between the snow-on and snow-off seasons, which is, in turn, a consequence of a considerable lengthening of snow-free period. This finding has major implications as it shows that a warmer climate has the potential to further augment the positive forcing imposed by undisturbed boreal forests as shown by Randerson et al. (2006) and to offset the cooling effect induced by wildfires. The climate in Siberia has been predicted to experience a further temperature increase in the future (Collins 2013; Groisman et al. 2007; Kirtman 2013), which is likely to result in even longer snow-free duration each year, leading to a stronger warming effect. Since fires may impose a stronger influence in a warmer climate, the net albedo-induced forcing of the whole Siberian larch forests would

hinge on the interaction between the fire-induced cooling effect and the climate-induced warming effect.

### **3.5. Conclusion**

Wildfires in the North American boreal forests have been shown to impose a strong cooling effect through the fire-induced albedo changes. However, whether this is the case in the Siberian larch forests, where species composition is different, has not been previously studied. In this paper, I focused explicitly on the stand-replacing fires in the Siberian larch forests which are directly comparable to the majority of fires in the North American boreal forests, and evaluated the relationship between albedo-induced SF and time since fire. The results confirm a strong fire-induced cooling effect that lasts for more than 26 years in the forests that experienced stand-replacing fires. The cooling is attributable to the increased albedo during the snow season and its magnitude is much larger than previously suggested. This study also reveals a warming effect imposed by the lengthening of snow-free season in the study area since 2000. Since the impacts of these two counteracting forces are both likely to amplify with the expected continuous increases in temperature in the region, the net surface forcing of the Siberian larch forests under the future climate is complex and thus deserves more attention from the scientific community.

## **Chapter 4: Surface fires in Siberian larch forests and associated surface forcing**

### **4.1. Introduction**

Boreal forests are a major biome on Earth with strong influences on global climate (Bonan et al. 1992; Chapin et al. 2006; Melillo et al. 1993). Among their influences, it has been shown that the albedo effect, i.e. its relatively lower albedo compared with tundra and other forest types during the snow seasons, is particularly important, as it may render the entire boreal zone to be a net heat sink (Bala et al. 2007; Betts 2000; Bonan 2008; Bonan et al. 1992). However, the albedo-induced warming effect of the boreal forests is considerably weakened by wildfires, which are a major disturbance agent throughout the global boreal biome (Bourgeau-Chavez et al. 2000; Kasischke 2000; Shvidenko and Nilsson 2000). Although wildfires can impose warming effects through carbon-related emissions, it has been suggested that at multi-decadal scales, their cooling effect may play a more dominant role, resulting in a net negative forcing to the climate (Randerson et al. 2006). This is because wildfires can considerably elevate forest albedo through different mechanisms, depending on the species compositions and temporal scales. Over shorter time spans, wildfires cause the increase in winter and spring albedo by damaging forest canopy (Amiro et al. 2006; Jin et al. 2012a; Randerson et al. 2006). Intact forest canopy effectively shields ground layer; when it is damaged or removed by wildfires, forest floor is exposed. And because snow albedo is very high and there are prolonged snow seasons in the boreal zone each year, the elevated snow season albedo in the burned

stands leads to an increase in annual mean albedo. Over longer time spans, as canopy gradually closes, most burned forests in North America still show elevated albedo which is driven by the dominance of broadleaf deciduous species, such as aspen (*Populus* spp.) and birch (*Betula* spp.), in the early successional stage (Amiro et al. 2006; Liu and Randerson 2008; Lyons et al. 2008; McMillan and Goulden 2008). Forests dominated by the deciduous species usually have higher albedo both in the summer (due to higher leaf reflectance) and winter (due to exposure of snow cover after senescence) (Betts and Ball 1997; Fuentes et al. 2001; Lyons et al. 2008).

Representing about a fifth of the global boreal forest (Osawa and Zyryanova 2010), the Siberian larch forests are a major component of the high-latitude boreal zone. Compared with other boreal forests, these forests in Eastern Siberia are unique in many aspects. For instance, they are dominated by larch (*Larix* spp.), which are deciduous needleleaf species (Abaimov 2010; Osawa and Zyryanova 2010). In addition, unlike many dominant tree species in the North American boreal forests which are susceptible to fire, larch are known as fire-resisting species in that they are highly adapted to wildfires (Wirth 2005). For example, their thick bark can effectively prevent larch trees from being damaged by low severity fires (Kharuk et al. 2010; Schulze et al. 2012; Wirth 2005). Larch also drop low hanging branches which limit the development of fuel ladders that facilitate spread of fire into the forest canopy (Wirth 2005). In addition, larch forests are less prone to high-severity fires because their canopy closure is relatively low (Babintseva and Titova 1996; Kharuk et al. 2010; Kharuk et al. 2011; Sofronov and Volokitina 2010). These factors together effectively lower the likelihood of the occurrence of stand-replacing fires



and result in extensive occurrence of surface fires which are generally low in severity (Wirth 2005). According to Korovin (1996), about 80% of fires in the Russian forests are surface fires. Kukavskaya et al. (2012), based on burned area estimated using both MODIS- and AVHRR-based fire mapping products, stated that the proportion of surface fires is higher than 50% in Siberia in most years. De Groot et al. (2013) suggested that surface fires account for more than 90% of total fires in the forests in Siberia, while Krylov et al. (2014) estimated that surface fires consist of more than 70% of fires in Russia and have a higher dominance over stand-replacing fires in the southern edge of the boreal forests than in the north. The large uncertainty of the areal estimates of surface fires is a consequence of several factors including the remoteness of the region, unreliable official statistics, and the mapping challenges from remotely-sensed data as many surface fires occur under the forest canopy and do not emit a thermal signal comparable in magnitude to stand-replacing fires (Conard and Ivanova 1997; de Groot et al. 2013; Kukavskaya et al. 2012; Sukhinin et al. 2004).

Most past research on surface fires in the region focused on the implications of surface fires for the carbon budget (e.g. Soja et al. 2004a, Schulze et al. 2012, Berner et al. 2012), while their potential climatic impacts through albedo have generally been overlooked. In Chapter 3, I have shown that stand-replacing fires in the Siberian larch forests impose a strong cooling effect through the post-fire albedo changes with magnitudes similar to those of the North American boreal fires. Since surface fires are much more frequent and may be much more extensive than stand-replacing fires, it is likely that they also exert significant climatic impacts through the

albedo effect. However, to the best of my knowledge, the direction and magnitude of their impacts have not yet been assessed independently of stand-replacing fires.

In addition, in this study I aim to identify a method that can be reliably used to differentiate two fire types as soon as possible after fire occurrence to enable projection of likely impacts of specific fire events on surface forcing (SF). Since one of the major differences between surface fires and stand-replacing fires lies in burn severity (Conard and Ivanova 1997; de Groot et al. 2013), this study examines several remotely sensed indices which may be used to differentiate stand-replacing and surface fires in terms of burn severity. There is an abundance of remote sensing-based indices that have been used as proxies for burn severity, among which the differenced normalized burn ratio (dNBR; Key and Benson 2006) is a prominent example. Built upon the rationale that fires usually result in substantial and opposite changes to surface reflectance in the near-infrared and shortwave infrared ranges of the electromagnetic spectrum (Verbyla et al. 2008), dNBR is calculated as the difference in normalized burn ratio (NBR; Garcia and Caselles 1991) which captures the fire-induced changes in these two wavelength ranges, and is a widely-used index in remote sensing-based research involving burn severity. In addition to dNBR, difference in snow season albedo and the differenced normalized difference vegetation index (dNDVI) have also been applied to indicate burn severity in boreal forests because they may be indicative of the damages caused to canopy and green vegetation, respectively (Isaev et al. 2002; Jin et al. 2012a). Since it has been suggested that the performance of the remotely sensed burn severity indices is usually inconsistent over different ecosystems and that they should be used selectively

(French et al. 2008; Jin et al. 2012a; Murphy et al. 2008; Rogers et al. 2015), this study aims to determine which of the three indices has the strongest predictive capability in the Siberian larch forests close in time to the occurrence of the fire events.

## **4.2. Materials and methods**

This project focuses on a region in Siberia with high larch dominance (see Section 2.2 for study area description). Two datasets were used as data inputs to map surface fires in the region. The first dataset is the MODIS-based regionally adjusted burned area mapping product (Loboda et al. 2007) developed for Russian forests, which was produced based on the combined information from MODIS active fire product (Giglio et al. 2003) and surface reflectance data (Vermote et al. 2002) with a spatial resolution of 500 m. The second dataset is the stand-replacing fire mapping product (SRFM, Krylov et al. 2014) which identifies stand-replacing fires that occurred between 2001 and 2012 in the Russian boreal forests based on forest loss as mapped by the Global Forest Change product (Hansen et al. 2013) at 30 m resolution. The SRFM product also uses the same MODIS-based burned area maps (Loboda et al. 2007) to confirm that forest loss was due to fire rather than other drivers. Surface fires in this study were identified by differencing the two datasets based on the assumption that fires that were mapped by the MODIS product but excluded by the SRFM product in the same year are likely to be surface fires. First, the SRFM data was resampled to 500 m to match the spatial resolution of the MODIS burned area product using a majority filter. As a result, stand-replacing fires that did not constitute “majority” within any given pixel were excluded from the resampled image. The

resampling is particularly likely to impact the edges of stand-replacing events adjacent to surface fires. To account for this potential misidentification, I buffered the resampled SRFM product outwards by 500 m to limit the inclusion of stand-replacing fires in the produced surface fire map. The resultant burned area maps were compared with the burned areas mapped in the MODIS-based burned area product for each year between 2001 and 2012. In some cases the uncertainty in timing of mapped forest loss in the SRFM, inherited from the Global Forest Change product, resulted in attributing forest loss to the fire events which occurred one year earlier or later (Hansen et al. 2013; Krylov et al. 2014; Linke et al. 2017). Because this uncertainty impacts my ability to differentiate surface and stand-replacing fires, I re-evaluated the timing of all stand replacing fires so that the fire polygons of year  $x$  from the MODIS-based burned area product were compared with those from three consecutive years (i.e. years  $x-1$ ,  $x$  and  $x+1$ ) in the processed SRFM product, and the areas included in the former but not by the latter were considered surface fires. For example, fires mapped by the MODIS burned area product in 2003 were compared with those identified by the SRFM products to occur in 2002, 2003 and 2004.

SF was computed for all areas that were mapped as surface fires using the MODIS MCD43A3 albedo product and CERES clear-sky downward shortwave surface flux data following the methodology described in detail in Chapter 3. To analyze the seasonal contribution of albedo changes to total SF, good-quality black-sky albedo (BSA) with full bidirectional reflectance distribution function (BRDF) conversions (as represented by the numeric value of zero in the associated quality band) from the MODIS albedo product for forests that experienced surface fires was

extracted and the annual, snow-off (June, July and August) and snow-on (October and March) mean BSA trajectories were constructed. For reference, forest albedo over two years before the fire events was tracked and used to represent the pre-fire condition.

Finally, three indices - snow season dBSA, summer dNBR, and summer dNDVI - were examined to quantify their success rate at differentiating surface fires from stand-replacing fires in the region. Snow season dBSA was calculated as the difference in mean October/March BSA. As previously mentioned in Chapter 3, very few good-quality observations are acquired from November through February in most of the study area and that October and March are generally still within snow season in the region. The difference was measured between the BSA of the first post-fire snow season and the last pre-fire snow season. For example, snow season dBSA for a fire event that occurred in year  $x$  would be calculated as

$$dBSA_X = \frac{BSA_{\text{October},X} + BSA_{\text{March},X+1}}{2} - \frac{BSA_{\text{October},X-1} + BSA_{\text{March},X}}{2}$$

Summer dNBR and dNDVI were calculated as the difference in mean summer (i.e. June, July and August) NBR and NDVI. For example, summer dNBR and dNDVI for a fire event that occurred in year  $x$  would be calculated as

$$dNBR_X = \frac{NBR_{\text{June},X-1} + NBR_{\text{July},X-1} + NBR_{\text{August},X-1}}{3} - \frac{NBR_{\text{June},X+1} + NBR_{\text{July},X+1} + NBR_{\text{August},X+1}}{3}$$

$$dNDVI_X = \frac{NDVI_{\text{June},X-1} + NDVI_{\text{July},X-1} + NDVI_{\text{August},X-1}}{3} - \frac{NDVI_{\text{June},X+1} + NDVI_{\text{July},X+1} + NDVI_{\text{August},X+1}}{3}$$

where NBR and NDVI were, in turn, calculated based on different combinations of two bands from the MODIS MCD43A4 reflectance data (Schaaf et al. 2002):  $NBR = (\text{Band } 2 - \text{Band } 7) / (\text{Band } 2 + \text{Band } 7)$ ,  $NDVI = (\text{Band } 2 - \text{Band } 1) / (\text{Band } 2 + \text{Band } 1)$ . All three indices were calculated for all surface fires identified in this project and

stand-replacing fires mapped in Chapter 3 based on the years immediately before and after the years of fires to develop a consistent method that is not impacted by the specific timing of fire occurrence within a given fire season. Then each of the three indices was examined through a series of binary classifications to differentiate stand-replacing and surface fires. To identify the classification threshold with the most optimal classification accuracy for each index objectively, the entire range of the distribution of each index was divided into 100 equal intervals which were used iteratively to determine the threshold with the best binary classification accuracy.

### **4.3. Results**

The total area that experienced surface fires between 2001 and 2012, including repeated burns, was 122,407 km<sup>2</sup>, which is ~20% greater than the total area of stand-replacing fires (103,460 km<sup>2</sup>) that occurred during 2001-2012. Averaged over the 12 years, the annual area impacted by surface fires in the study area is 10,200 km<sup>2</sup>, however, the amount of area burned in surface fires in individual year varies very substantially. More than 75% of area burned in surface fires occurred in 2003 and 2012 combined (Figure 4-1). The spatial distribution of surface fires in the study area shows strong clustering patterns. Surface fires in the study area are clustered in two regions (Figure 4-2): 1) the area (59 °N-63 °N and 129 °E-136 °E) along the mid- to down-stream of the Aldan River, a tributary of the Lena River, and 2) the southern edge of the study area (52 °N-55 °N and 111 °E-127 °E) along the Chinese border in the east and the temperate grasslands in southern Zabaykalsky Krai in the west.

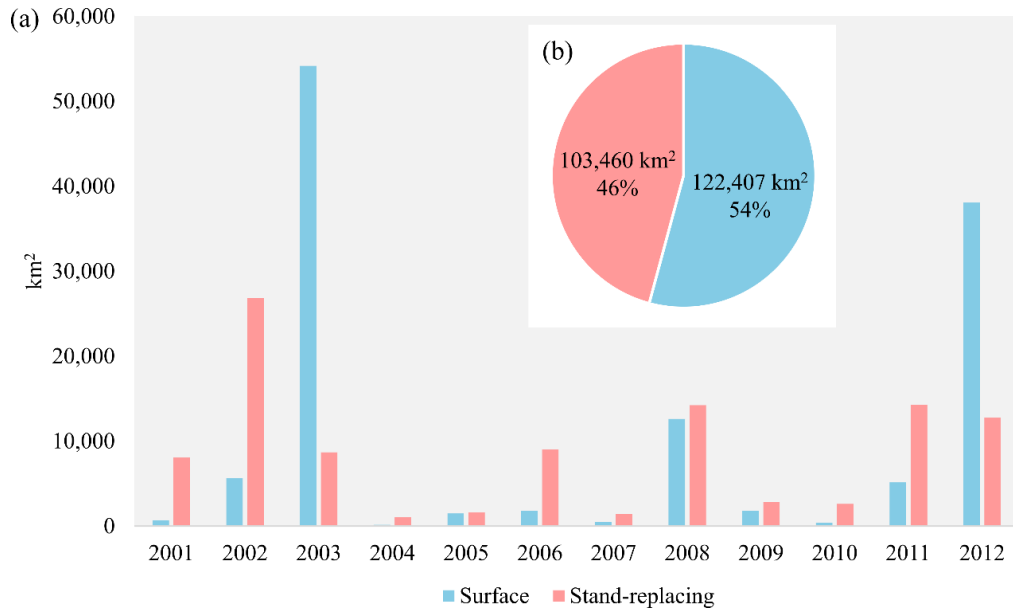


**Figure 4-1 Comparison of (a) annual area distribution and (b) total area between surface and stand-replacing fires between 2001 and 2011.**

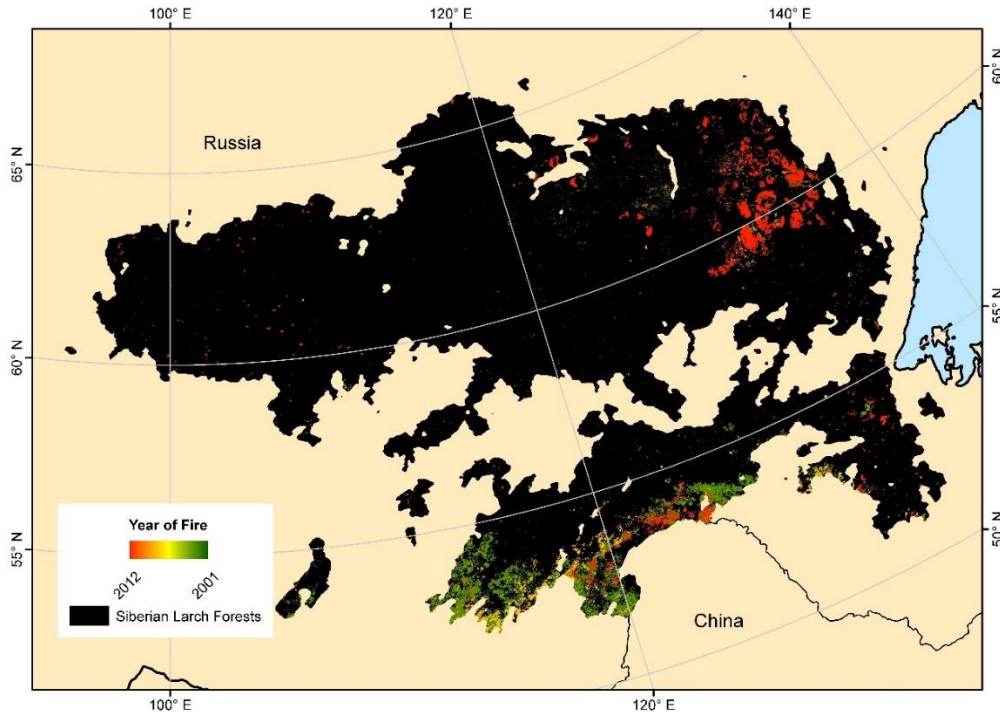


**Figure 4-2 Distribution of surface fires in the Siberian larch forests between 2001 and 2012.**

The results show mean SF of surface fires follows a similar trajectory as that of stand-replacing fires but the magnitude of the fire-induced forcing is considerably

smaller (Figure 4-3). In the first two years after fire, mean SF from both surface and stand-replacing fires is similar with the difference less than  $0.3 \text{ Wm}^{-2}$ . However, by year 3, the magnitude of SF of the stand-replacing fires increases at a much more rapid rate. The mean SF of surface fires grows at a mean rate of  $-0.16 \text{ year}^{-1}$  between years 2 and 6, after that the direction of the trajectory changes as the SF gradually moves towards the pre-fire state at a mean rate of  $0.13 \text{ year}^{-1}$  between years 6 and 14. The BSA trajectories constructed for surface fires (Figure 4-4) show that the cause of the mean cooling effect in the post-surface fire sites is the increases in albedo,

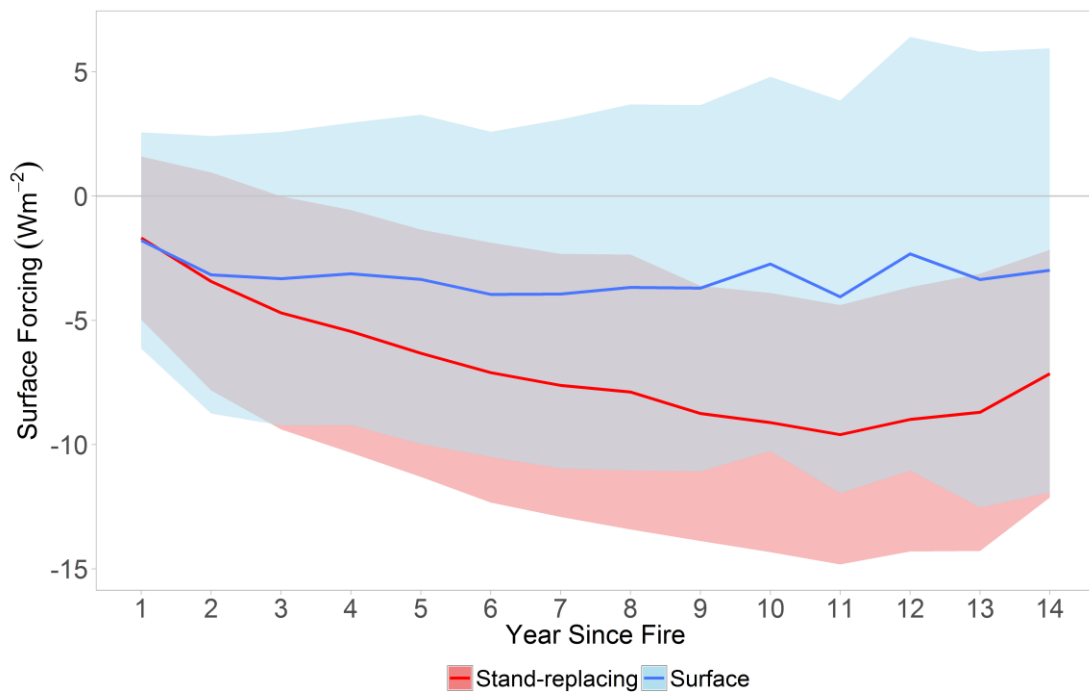


**Figure 4-3 Comparison of mean SF trajectories of surface (this chapter) and stand-replacing (see chapter 3 for details) fires. Solid red and blue lines represent the mean SF trajectories of stand-replacing and surface fires, respectively. Uncertainties are represented by shaded areas within  $\pm 1$  standard deviation.**



particularly during the snow season. The variability of SF of surface fires is much larger than that of the stand-replacing fires. After occurrence of a surface fire, forest stands can exhibit either warming or cooling effects within the 14 years after fire.

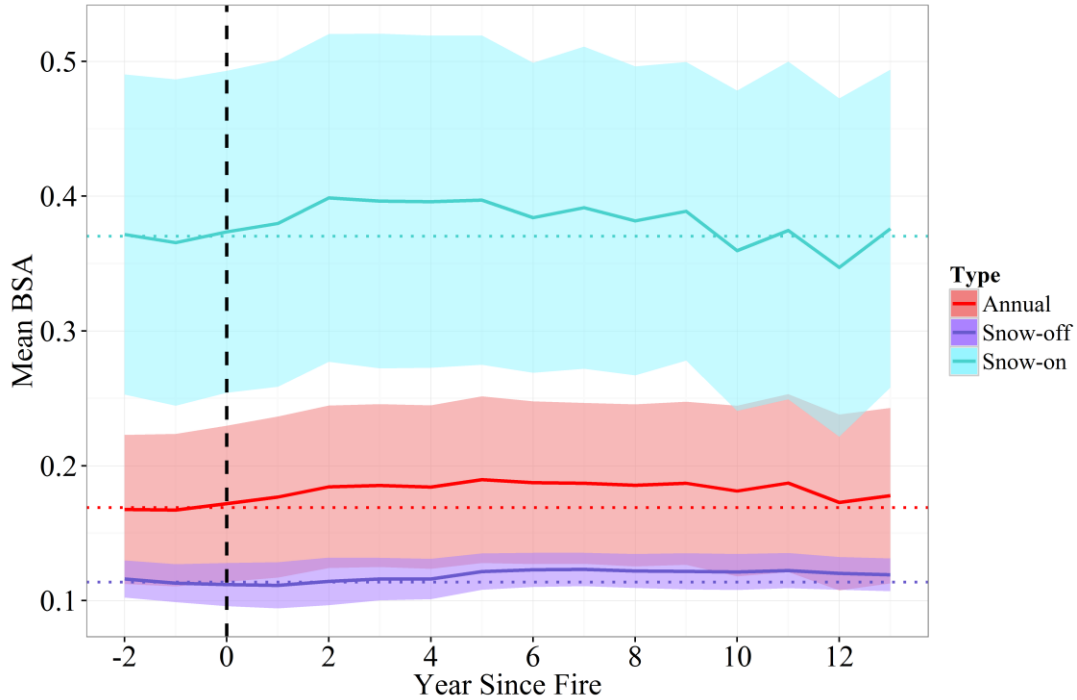


**Figure 4-4 Mean BSA trajectories for the burned forests generated using the MODIS albedo data for 2001-2015. The vertical dashed line represents the year of fire occurrence. The negative “year since fire” range presents pre-fire conditions over two years before fires. The horizontal dashed lines represent the mean pre-fire BSA for the corresponding trajectories. Uncertainties are represented by shaded areas within  $\pm 1$  standard deviation.**

The difference in post-fire forcing between surface fires and stand-replacing fires brings out the importance of separating the two fire types in any modeling activities that attempt to forecast the post-fire impacts on radiative budget regionally and likely globally. The results (Figure 4-5) show that summer dNBR provides the best classification accuracy (88%) achieved at 0.175 threshold. In contrast, snow

season dBSA and summer dNDVI performed poorly, with classification accuracy generally below 60%.

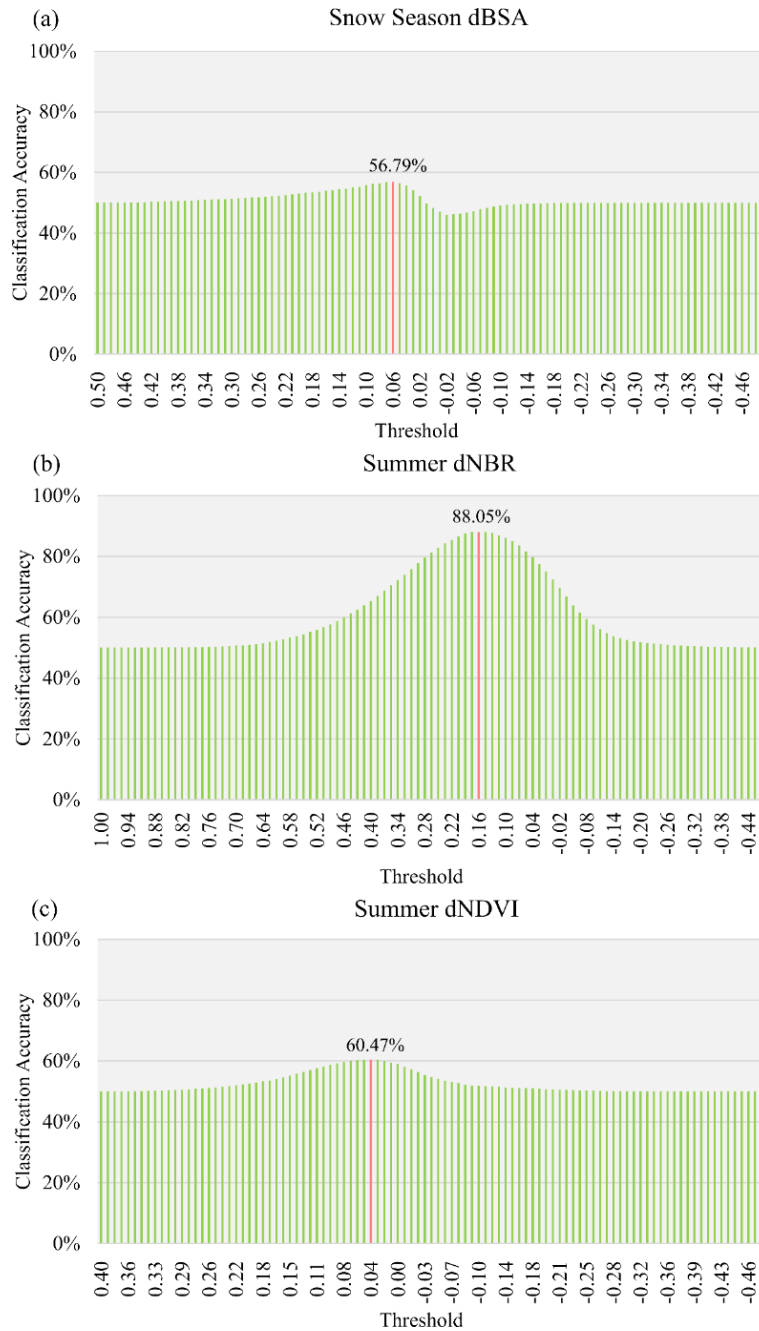


**Figure 4-5 Classification accuracy of first post-fire (a) snow season dBSA, (b) summer dNBR, and (c) summer dNDVI in differentiating surface fires from stand-replacing fires. Each bar represents the classification accuracy associated with a single threshold value. The red bar in each graph represents the threshold value with the most optimal classification accuracy for the corresponding index.**

## 4.4. Discussion

### *4.4.1. Temporal and spatial distribution of surface fires in the Siberian larch forests between 2001 and 2012*

Surface fires are a key element of the Siberian larch forest functioning. They support larch dominance by increasing soil temperature and drainage and eliminating competition (Kharuk et al. 2016; Schulze et al. 2012; Shorohova et al. 2009; Sofronov and Volokitina 2010). Because of the differences in spatial coverage, a direct comparison of the total burned area between this and other previous studies is not feasible. However, in terms of the proportion of surface fires, my result (54%) is consistent with those yielded by other studies, which almost uniformly suggested that surface fires cover more areas than stand-replacing fires (de Groot et al. 2013; Korovin 1996; Kukavskaya et al. 2017; Kukavskaya et al. 2012).

The large difference in mapping resolution of the MODIS-based burned area (500 m) and the forest loss dataset (30 m) presents a major source of uncertainty in defining surface fires within this study. The resampling of 30 m data to 500 m can lead to either underestimation or overestimation of stand-replacing fires in the resampled map, resulting in uncertainties being introduced to the mapped surface fires. Another major source of uncertainty could stem from the definition of stand-replacing fires used by the SRFM product, which considers a fire event to be stand-replacing if tree cover prior to fire is larger than 25% (Krylov et al. 2014). Since larch forests are generally open in terms of canopy closure (Babintseva and Titova 1996; Kharuk et al. 2010; Kharuk et al. 2011; Sofronov and Volokitina 2010), it is possible that many stand-replacing fires were not mapped because they occurred in the forests

that were deemed to be too sparse by the SRFM product, resulting in an overestimation of surface fires. Finally, the uncertainty of the surface fire map is also influenced by the mapping accuracy of the SRFM and the MODIS-based burned area products, especially the latter. The predominant method to identify surface fires based on remote sensing has been using the active fire observations from either AVHRR (Soja et al. 2004; Sukhinin et al. 2004) or MODIS (Kukavskaya et al. 2012) sensors. However, because of the low severity of surface fires, the heat signals emitted by surface fires are generally low. This, coupled with the relatively large footprints of both AVHRR and MODIS active fire observations (~1 km), makes mapping surface fires accurately quite difficult. With the successful launch of the Visible Infrared Imaging Radiometer Suite (VIIRS) sensor on board the Suomi National Polar-orbiting Partnership (Suomi NPP) satellite as well as the subsequent development of the VIIRS active fire product (Csiszar et al. 2014), it is expected that the accuracy in mapping surface fires can be increased significantly. With a higher spatial resolution (375 m) and better radiometric quality, the VIIRS active fire product possesses the potential to identify low severity surface fires much more accurately than its predecessors (Csiszar et al. 2014).

#### *4.4.2. Surface forcing trajectory of surface fires*

According to the established SF trajectory, surface fires in the region on average impose a cooling effect through the albedo changes within 14 years after fire. A further analysis on the post-fire annual and seasonal BSA trajectories shows that the cooling is attributable to the increased albedo in the burned forests, especially during snow-on season. This is similar to the mechanism for the albedo-induced

cooling observed in the forests that experienced stand-replacing fires, which may be indicative of the canopy damages caused by surface fires. Although surface fires have been known to be of lower severity than stand-replacing fires, they can still lead to a certain level of canopy loss by killing the juvenile trees which are less resistant to fires than the mature trees (Conard and Ivanova 1997; Kharuk et al. 2016; Schulze et al. 2012; Shorohova et al. 2009). This will also result in increases in forest albedo. Another potential reason which may be equally significant is that although surface fires do not cause significant damage to the canopy of mature trees, they consume shrubs in the understory which also create a shading effect similar to the tree canopy. This effect may be particularly important in the Siberian larch forests because of the lower canopy closure relative to other boreal forests (Babintseva and Titova 1996; Kharuk et al. 2010; Sofronov and Volokitina 2010).

Surface fire-induced SF exhibits higher variability than stand-replacing fires as indicated by the uncertainty intervals in Figure 4-3. Unlike stand-replacing fires, which consistently lead to cooling effects, a significant fraction of forests that experienced surface fires exerts a warming effect. I believe this is, at least partially, due to the darkening effect of surface fires. One of the immediate effects of wildfires is usually the darkening of the forest floor and tree boles caused by char deposition (Chambers and Chapin 2002; Randerson et al. 2006). This effect lowers the albedo of the burned forests and thus leads to a warming effect. Another reason which may contribute to the warming effect in some burned sites is the lengthening of snow-free season in Siberia. A considerable increase in mean annual temperature has been observed in Siberia over the past decades and it is widely expected to persist in the

region (Collins 2013; Hartmann 2013; Kirtman 2013). One of the consequences of this warming is an increase in duration of snow-free seasons, which, as demonstrated in Chapter 3, has been evident in spring and fall albedo changes within the Siberian larch forests since 2000. In addition to the ecological and climatic drivers of this variability, uncertainties within the MCD43A3 dataset also may explain the strong fluctuation of the snow-on BSA trajectory over 12-14 years since fire occurrence in Figure 4-4 as those estimates are based on the smaller number of fire events.

#### *4.4.3. Identifying surface and stand-replacing fires using remote sensing-based burn severity indices*

Surface fires and stand-replacing fires differ in burn severity and resultant post-fire impacts (Conard and Ivanova 1997; de Groot et al. 2013). Although there have been a host of studies showing the differences between the two fire types in the impacts on forest properties such as biomass accumulation and successional patterns in the field (Schulze et al. 2012; Sofronov and Volokitina 2010), the effective application of findings from in-situ studies at the regional scale is hindered by, at least partially, the challenge associated with our ability to map surface and stand-replacing fires reliably from satellite observations. As discussed previously, the identification of surface fires using remotely sensed data has been mostly linked to active fire observations primarily related to very coarse spatial resolution and comparatively weak thermal signals from creeping surface fires. A fraction of surface fires are captured by surface reflectance change-based burned area products along with nearly all stand-replacing fires. However, none of the burned area products currently routinely differentiate between the two fire types. In part this is a result of

the larger discourse in the scientific and management communities on what constitutes burn severity in different ecosystems (French et al. 2008; Hoy et al. 2008). For example, while tree mortality is commonly associated with burn severity, it is not an informative proxy for burn severity in the black spruce forests in Alaska, where in-situ studies show that burn severity in those forests are usually indicated by consumption of the surface organic layer (Hoy et al. 2008). And on the other hand, there has been an equally broad debate on how burn severity can be measured using remote sensing (French et al. 2008). More specifically, which remote sensing-based burn severity metrics can be used to properly represent the different gradients of burn severity in the Siberian larch forests has remained uncertain. Although a number of metrics have been proposed to measure burn severity within boreal biome, their performance is highly influenced by vegetation and terrain conditions and therefore their usage needs to be calibrated for specific applications (French et al. 2008). This study does not address the issue of defining and mapping burn severity in Siberian larch forests. Instead it focuses on a very specific aspect, which can be related to burn severity, and is specific for Siberian larch forests only. This study shows that for the purpose of separating surface fires from stand-replacing fires, dNBR presents the strongest metric among the three that were examined. Not only is dNBR capable of accurately differentiating the two fire types, it is also easy to be deployed, since the calculation of dNBR is straightforward and does not require any additional data inputs other than surface reflectance data in the near-infrared and shortwave infrared (SWIR) at  $\sim 2 \mu\text{m}$  range of the electro-magnetic spectrum. Due to its accuracy and cost-effectiveness, it has the potential to be readily adopted in a variety of large-scale



fire-based studies, including the work modeling post-fire energy budget and carbon budget, which have been shown to be significantly impacted by fires of different severity.

#### **4.5. Conclusion**

Surface fires are a key component of fire regime in the Siberian larch forests. In addition to their influence on the carbon budget through carbon emissions, surface fires also affect the energy budget through the resultant changes in surface albedo. This work, to my knowledge, is the first regional analysis focusing explicitly on the surface forcing of surface fires in the Siberian larch forests. The results show that similarly to stand-replacing fires, surface fires also impose an overall cooling effect through surface forcing due to increased snow-on albedo resulting from the partial canopy damage and the removal of shrub understory. The cooling effect of surface fires, however, is much weaker than that of stand-replacing fires over several years after the fire. This carries strong scientific implications because it highlights a potential need to differentiate the two fire types in various studies in which the impacts of wildfires are involved, including those modeling post-fire radiative budget. Based on the rationale that surface and stand-replacing fires differ in burn severity, this study identifies summer dNBR as a remote sensing-based index that can differentiate these two fire types reliably and cost-effectively. Our results suggest that dNBR-based threshold can be easily incorporated in existing and future coarse resolution burned area mapping products to provide reasonably accurate (88%) estimates of the extent of each fire type at least within the Siberian larch forests and

can likely be extended to other ecosystems using a similar approach of identifying most appropriate remote sensing indices and thresholds.

Expanding upon the findings of the current study, future research can be conducted in several directions. First, the spatial distribution of surface fires needs to be mapped with better accuracies. This can be achieved by incorporating the VIIRS active fires observations at 375 m resolution, which are more sensitive to low-severity surface fires than the 1-km MODIS product. Second, factors influencing the post-fire surface forcing of both surface and stand-replacing fires need to be identified. This will help us explain the variability associated with the post-fire surface forcing of both fire types and allow for a better prediction of future wildfire impacts. Third, other impacts that are imposed by the wildfires in the Siberian larch forests need to be located and quantified. This will likely require a better understanding of the fire-related processes at the stand level and of the spatial distribution of the forest conditions at the regional scale.

## Chapter 5: Conclusion

### 5.1. Major findings

The goal of this dissertation is to advance our understanding of the impacts wildfires impose on the Earth's energy budget through changes in albedo in the Siberian larch forests. The following paragraphs summarize the major findings of this dissertation work and their associated implications.

#### *5.1.1. Cooling effects of wildfires in the Siberian larch forests through fire-induced albedo changes*

The primary finding of this dissertation is that wildfires in the Siberian larch forests impose mean cooling effects through increased snow-on albedo, but the magnitude of the cooling differs between stand-replacing fires (detailed in Chapter 3) and surface fires (detailed in Chapter 4). For stand-replacing fires, the magnitude of their cooling effect is much larger than that of surface fires, and this is likely a consequence of higher levels of canopy openings after stand-replacing fires. At the maximum level, which occurs 11 years after fire, the cooling magnitude is similar to that of the North American boreal fires. The large magnitude of the cooling effect, accompanied with the wide occurrence of stand-replacing fires, leads to a net negative surface forcing over the entire region during 2002-2013. Based on the extended albedo trajectory which was made possible by incorporating a 24-year stand age map also produced in this dissertation project, it is shown that the cooling effect of stand-replacing fires lasts for more than 26 years, suggesting that forest canopy still has not recovered to the pre-fire condition after at least 26 years. For surface

fires, their smaller overall cooling effect is likely indicative of damages not only to the canopies, but also the shrubs in the understory. In addition, the post-fire surface forcing of the surface fires shows a much larger variability, with a considerable proportion showing warming effects. This likely reflects a broader range of fire severity impacts within forest stands that experienced surface fires ranging from minimal removal of surface litter to a partial damage to the canopy.

### *5.1.2. Effectiveness of dNBR as a measure differentiating stand-replacing fires from surface fires*

Another major finding of this dissertation is the identification of dNBR as an effective measure that can differentiate stand-replacing fires from surface fires reliably. As detailed in Chapter 4, the accuracy of dNBR in separating the two fire types in the Siberian larch forests is 88%. This finding suggests that the two types of fire can be effectively differentiated in a timely manner, based primarily on remote sensing inputs. Considering the differences in post-fire impacts between the two fire types, including the surface forcing patterns as revealed in this dissertation, accurate separation between them allows future climate models to parameterize two fire types differently with relative ease based on dNBR-based burn severity, thus achieving higher confidence in the fire-related projections. In addition, this finding reveals a new method that, when augmented by the active fire observations, can be used to map surface fires specifically. Mapping surface fires relying solely on active fire data has been proven to be challenging, because the thermal signals of both stand-replacing and surface fires are recorded and they are inseparable without further information. As a result, there have been large uncertainties in the area estimates of surface fires

offered by previous studies. Based on the results of this dissertation, dNBR can supplement the active fire observations with the burn severity information, allowing for the identification of surface fire specifically. This will greatly improve our overall understanding of fire regimes in the boreal zones.

### *5.1.3. The stand age dynamics of the Siberian larch forests*

In Chapter 2, a map showing the stand age dynamics of the Siberian larch forests over 24 years at the 30-m resolution is produced. It is a crucial component of the dissertation because by revealing the spatial-temporal distribution of stand-replacing fires between 1989 and 2012, it serves as the foundation based on which the subsequent analysis on post-fire forcing trajectory of stand-replacing fires is made possible. The importance of this stand age map, however, is not limited to this dissertation. It shows the pervasiveness of the stand-replacing fire events in the Siberian larch forests over a 24-year period, confirming the strong influences of wildfires over this region. The wall-to-wall, spatially detailed annual distribution of stand-replacing fires will allow knowledge about the relationships between stand age and a variety of forest parameters, such as biomass and vegetation structure, acquired through in-situ studies to be applied over the regional scale to the entire Siberian larch forests, benefitting the accurate representation of wild-based processes in various models.

## **5.2. Implications for climate science**

Over the past few decades, with the rapid advancements of climate models in terms of both variety and modeling details, there have been an increasing number of

climate models that incorporate wildfires (Flato 2013; Hantson et al. 2016). However, wildfires have been mostly considered by these models regarding their close relationships with emissions, while their surface forcing through changes in albedo has been largely overlooked. In my opinion, this has been the result of three factors. First, there has been a lack of awareness regarding the influences of wildfires imposed through albedo. Although wildfires have long been known to impose strong impacts on climate through aerosol and trace gas emissions (Ward et al. 2012), it is not until recently that their surface forcing through albedo changes in the high northern latitude boreal forests has been highlighted (Bonan 2008; Randerson et al. 2006). It has been shown that the cooling effect of wildfires in the boreal zone may overwhelm all major positive forcings, including long-lived greenhouse gases, ozone and black carbon over a long period of time (Randerson et al. 2006). This new yet significant understanding requires the climate modelers to adjust their models accordingly, which takes time. Second, there has been a lack of modeling capacity allowing for the details required by modeling wildfire. Due to their complex nature, climate models are highly computationally-intensive. Therefore climate models are usually operated at the relatively coarse spatial resolutions (Flato 2013), at which scales wildfires become less discernible. Fortunately, with continuous technological advancements, there have been climate models, especially regional ones, that run at the spatial resolutions that are comparable to remotely sensed datasets (Cubasch et al. 2013). Third, there has been a lack of understanding of fire-forest-climate interactions. In order for climate models to make projections accurately, the model parameters must be informed by strong scientific understanding of fire impacts

(Kantzas et al. 2013). For example, built upon the empirical relationship between albedo and forest stand age established through both field measurements (Amiro et al. 2006) and satellite observations (Randerson et al. 2006), Euskirchen et al. (2009) established models suggesting that the fire-induced cooling effect in the Alaskan boreal forests will be significant during the 21<sup>st</sup> century. While there have been extensive studies, both in-situ and remote sensing-based, focusing on wildfires in the North American and European boreal forests, information on Siberian forests in the English language literature has been more limited, due in part to both relatively higher inaccessibility and a lack of long term remote sensing observations. As a result, there are great uncertainties regarding many critical fire-related parameters, including post-fire energy budget.

In the context of the aforementioned challenges, this dissertation enhances our understanding of wildfire impacts in a major yet understudied component of the global boreal biome: the Siberian larch forests. It highlights the strong cooling effect of the fire-induced albedo changes in these forests, which had not been focused on and quantified previously. In addition, the primary cause of the cooling effect, which is the increased snow-on albedo, is identified. For the forests that experienced stand-replacing fires, when coupled with the 24-year stand age map which is also an output of this dissertation, the post-fire albedo dynamics over a longer span (26 years) is revealed. Surface fires summer dNBR differs strongly from dNBR of stand-replacing fires, based on which these two fire types can be reliably and cost-effectively differentiated. Moreover, in this dissertation a 30-m wall-to-wall stand age map of the Siberian larch forests is developed. This map provides the best estimates so far

regarding the spatial-temporal distribution of stand-replacing fire events in these forests for 1989-2012 at an unprecedented spatial resolution, which may be of help for climate models that need to upscale in-situ fire-based knowledge to the regional scale. Although by no means complete, these findings serve to boost our overall understanding of the influences imposed by wildfires in the Siberian larch forests, based on which future climate models with enhanced representation of wildfires in the Siberian larch forests or even the entire boreal biome can be developed.

### **5.3. Future work**

One immediate and natural extension of the work accomplished through this dissertation is the comparison of the radiative forcing of the fire-induced albedo changes with other forcing agents in the Siberian larch forests, based on which the regional net forcing of the wildfires, including surface fires and stand-replacing fires, can be determined. This comparison will require completion of several specific tasks. First, surface forcing estimated in this dissertation needs to be converted into radiative forcing, which allows for the direct comparison. Second, all forcing agents with strong influences need to be accounted for. This demands a comprehensive evaluation of the potential candidates whose contributions need to be quantified. Based on the previous studies (Randerson et al. 2006), carbon-related emissions (e.g. CO<sub>2</sub> and CH<sub>4</sub>) are expected to be a major agent and of particular interest. To estimate their forcing, how wildfires interact with aboveground biomass and soil-based carbon in the Siberian larch forests needs to be understood.

Another natural potential to expand the dissertation work is exploring the surface forcing trajectories over a longer time frame. This can be achieved by



incorporating the latest datasets once they become available. The surface forcing and albedo trajectories presented in the dissertation covers 14 years and 26 years, respectively, which was generated using stand-replacing fires identified to have occurred between 2001 and 2012 and the MODIS albedo product for 2001-2015. Theoretically, an increase in the temporal ranges of the stand-replacing fire mapping product and the albedo data for one more year will result in a 1-year increase in the corresponding surface forcing trajectory and a 2-year increase in the albedo trajectory. This means that our understanding of post-fire dynamics of surface forcing of wildfires in the region will be much improved with time.

One of the interesting phenomena that this dissertation revealed is the relatively large variation in the post-fire surface forcing of the burned forests, both after stand-replacing and surface fires. Although the uncertainties, including the errors in the data inputs and those introduced during conversions, inevitably played a role, I hypothesize that this is also the consequence of a series of factors, including weather, topography, fuel, burn severity, and soil conditions. Another similar and equally interesting phenomenon is the spatial aggregation of the fire events in the region over the past 12 years. An accurate identification of the influential factors contributing to the post-fire surface forcing distribution as well as the spatial distribution of the fires will no doubt boost our understanding of the role played by wildfires in the Siberian larch forests, leading to better predictions of the locations and impacts of the future fire events in the region, which will in turn allow for more effective and efficient, prioritized fire treatments.

## References

- Abaimov, A.P. (2010). Geographical Distribution and Genetics of Siberian Larch Species. In A. Osawa, O.A. Zyryanova, Y. Matsuura, T. Kajimoto, & R.W. Wein (Eds.), *Permafrost Ecosystems* (pp. 41-58): Springer Netherlands
- Abaimov, A.P., & Sofronov, M.A. (1996). The Main Trends of Post-Fire Succession in Near-Tundra Forests of Central Siberia. In J. Goldammer, & V. Furyaev (Eds.), *Fire in Ecosystems of Boreal Eurasia* (pp. 372-386): Springer Netherlands
- Alexander, H.D., Mack, M.C., Goetz, S., Loranty, M.M., Beck, P.S.A., Earl, K., Zimov, S., Davydov, S., & Thompson, C.C. (2012). Carbon Accumulation Patterns During Post-Fire Succession in Cajander Larch (*Larix cajanderi*) Forests of Siberia. *Ecosystems*, 15, 1065-1082. <http://dx.doi.org/10.1007/s10021-012-9567-6>
- Amiro, B.D., Orchansky, A.L., Barr, A.G., Black, T.A., Chambers, S.D., Chapin, F.S., Goulden, M.L., Litvak, M., Liu, H.P., McCaughey, J.H., McMillan, A., & Randerson, J.T. (2006). The effect of post-fire stand age on the boreal forest energy balance. *Agricultural and Forest Meteorology*, 140, 41-50. <http://dx.doi.org/10.1016/j.agrformet.2006.02.014>
- Babintseva, R.M., & Titova, Y.V. (1996). Effects of Fire on the Regeneration of Larch Forests in the Lake Baikal Basin. In J. Goldammer, & V. Furyaev (Eds.), *Fire in Ecosystems of Boreal Eurasia* (pp. 358-365): Springer Netherlands
- Bala, G., Caldeira, K., Wickett, M., Phillips, T.J., Lobell, D.B., Delire, C., & Mirin, A. (2007). Combined climate and carbon-cycle effects of large-scale deforestation. *Proceedings of the National Academy of Sciences of the United States of America*, 104, 6550-6555. <http://dx.doi.org/10.1073/pnas.0608998104>
- Balzter, H., Tansey, K., Kaduk, J., George, C., Gerard, F., Gonzalez, M.C., Sukhinin, A., & Ponomarev, E. (2010). Fire/Climate Interactions in Siberia. In H. Balzter (Ed.), *Environmental Change in Siberia* (pp. 21-36): Springer Netherlands
- Barnes, C.A., & Roy, D.P. (2008). Radiative forcing over the conterminous United States due to contemporary land cover land use albedo change. *Geophysical Research Letters*, 35, L09706. <http://dx.doi.org/10.1029/2008GL033567>
- Bathiany, S., Claussen, M., Brovkin, V., Raddatz, T., & Gayler, V. (2010). Combined biogeophysical and biogeochemical effects of large-scale forest cover changes in the MPI earth system model. *Biogeosciences*, 7, 1383-1399. <http://dx.doi.org/10.5194/bg-7-1383-2010>
- Berner, L.T., Beck, P.S.A., Loranty, M.M., Alexander, H.D., Mack, M.C., & Goetz, S.J. (2012). Cajander larch (*Larix cajanderi*) biomass distribution, fire regime

and post-fire recovery in northeastern Siberia. *Biogeosciences*, 9, 3943-3959.  
<http://dx.doi.org/10.5194/bg-9-3943-2012>

Betts, A.K., & Ball, J.H. (1997). Albedo over the boreal forest. *Journal of Geophysical Research-Atmospheres*, 102, 28901-28909.  
<http://dx.doi.org/10.1029/96jd03876>

Betts, R.A. (2000). Offset of the potential carbon sink from boreal forestation by decreases in surface albedo. *Nature*, 408, 187-190.  
<http://dx.doi.org/10.1038/35041545>

Bindoff, N.L., P.A. Stott, K.M. AchutaRao, M.R. Allen, N. Gillett, D. Gutzler, K. Hansingo, G. Hegerl, Y. Hu, S. Jain, I.I. Mokhov, J. Overland, J. Perlwitz, R. Sebbari and X. Zhang (2013). Detection and Attribution of Climate Change: from Global to Regional. In T.F. Stocker, D. Qin, G.-K. Plattner, M. Tignor, S.K. Allen, J. Boschung, A. Nauels, Y. Xia, V. Bex, & P.M. Midgley (Eds.), *Climate Change 2013: The Physical Science Basis. Contribution of Working Group I to the Fifth Assessment Report of the Intergovernmental Panel on Climate Change*. Cambridge, United Kingdom and New York, NY, USA: Cambridge University Press

Bonan, G.B. (2008). Forests and climate change: Forcings, feedbacks, and the climate benefits of forests. *Science*, 320, 1444-1449.  
<http://dx.doi.org/10.1126/science.1155121>

Bonan, G.B., Pollard, D., & Thompson, S.L. (1992). Effects of boreal forest vegetation on global climate. *Nature*, 359, 716-718.  
<http://dx.doi.org/10.1038/359716a0>

Bond-Lamberty, B., Wang, C., & Gower, S.T. (2004). Net primary production and net ecosystem production of a boreal black spruce wildfire chronosequence. *Global Change Biology*, 10, 473-487. <http://dx.doi.org/10.1111/j.1529-8817.2003.0742.x>

Bourgeau-Chavez, L.L., Alexander, M.E., Stocks, B.J., & Kasischke, E.S. (2000). Distribution of forest ecosystems and the role of fire in the North American boreal region. In E.S. Kasischke, & B.J. Stocks (Eds.), *Fire, Climate Change, and Carbon Cycling in the Boreal Forest* (pp. 111-131). New York, NY, USA: Springer

Breiman, L. (2001). Random Forests. *Machine Learning*, 45, 5-32.  
<http://dx.doi.org/10.1023/A:1010933404324>

Breiman, L., & Cutler, A. (2003). Manual—Setting Up, Using, and Understanding Random Forests V4.0. In.  
[https://www.stat.berkeley.edu/~breiman/Using\\_random\\_forests\\_v4.0.pdf](https://www.stat.berkeley.edu/~breiman/Using_random_forests_v4.0.pdf).

Bright, R.M., Astrup, R., & Strømman, A. (2013). Empirical models of monthly and annual albedo in managed boreal forests of interior Norway. *Climatic Change*, 1-14. <http://dx.doi.org/10.1007/s10584-013-0789-1>

Chambers, S.D., & Chapin, F.S. (2002). Fire effects on surface-atmosphere energy exchange in Alaskan black spruce ecosystems: Implications for feedbacks to regional climate. *Journal of Geophysical Research: Atmospheres*, 107, 8145. <http://dx.doi.org/10.1029/2001JD000530>

Chapin, F.S., McGuire, A.D., Randerson, J., Pielke, R., Baldocchi, D., Hobbie, S.E., Roulet, N., Eugster, W., Kasischke, E., Rastetter, E.B., Zimov, S.A., & Running, S.W. (2000). Arctic and boreal ecosystems of western North America as components of the climate system. *Global Change Biology*, 6, 211-223. <http://dx.doi.org/10.1046/j.1365-2486.2000.06022.x>

Chapin, F.S., Yarie, J., Cleve, K.V., & Viereck, L.A. (2006). The Conceptual Basis of LTER Studies in the Alaskan Boreal Forest. In I. F. Stuart Chapin (Ed.), *Alaska's Changing Boreal Forest* (p. 354). New York, NY, USA: Oxford University Press

Chen, D., Loboda, T.V., Krylov, A., & Potapov, P.V. (2016). Mapping stand age dynamics of the Siberian larch forests from recent Landsat observations. *Remote Sensing of Environment*, 187, 320-331. <http://dx.doi.org/10.1016/j.rse.2016.10.033>

Chen, D., Loboda, T.V., Krylov, A., & Potapov, P.V. (2017). Distribution of Estimated Stand Age Across Siberian Larch Forests, 1989-2012. In. Oak Ridge, Tennessee, USA: ORNL Distributed Active Archive Center. <http://dx.doi.org/10.3334/ORNLDAAC/1364>

Collins, M., R. Knutti, J. Arblaster, J.-L. Dufresne, T. Fichet, P. Friedlingstein, X. Gao, W.J. Gutowski, T. Johns, G. Krinner, M. Shongwe, C. Tebaldi, A.J. Weaver and M. Wehner (2013). Long-term Climate Change: Projections, Commitments and Irreversibility. In T.F. Stocker, D. Qin, G.-K. Plattner, M. Tignor, S.K. Allen, J. Boschung, A. Nauels, Y. Xia, V. Bex and P.M. Midgley (Ed.), *Climate Change 2013: The Physical Science Basis. Contribution of Working Group I to the Fifth Assessment Report of the Intergovernmental Panel on Climate Change*. Cambridge, United Kingdom and New York, NY, USA: Cambridge University Press

Conard, S., Sukhinin, A., Stocks, B., Cahoon, D., Davidenko, E., & Ivanova, G. (2002). Determining Effects of Area Burned and Fire Severity on Carbon Cycling and Emissions in Siberia. *Climatic Change*, 55, 197-211. <http://dx.doi.org/10.1023/A:1020207710195>

Conard, S.G., & Ivanova, G.A. (1997). Wildfire in Russian boreal forests - Potential impacts of fire regime characteristics on emissions and global carbon balance estimates. *Environmental Pollution*, 98, 305-313. [http://dx.doi.org/10.1016/s0269-7491\(97\)00140-1](http://dx.doi.org/10.1016/s0269-7491(97)00140-1)

Csiszar, I., Schroeder, W., Giglio, L., Ellicott, E., Vadrevu, K.P., Justice, C.O., & Wind, B. (2014). Active fires from the Suomi NPP Visible Infrared Imaging

Radiometer Suite: Product status and first evaluation results. *Journal of Geophysical Research: Atmospheres*, 119, 803-816. <http://dx.doi.org/10.1002/2013JD020453>

Cubasch, U., Wuebbles, D., Chen, D., Facchini, M.C., Frame, D., Mahowald, N., & Winther, J.-G. (2013). Introduction. In T.F. Stocker, D. Qin, G.-K. Plattner, M. Tignor, S.K. Allen, J. Boschung, A. Nauels, Y. Xia, V. Bex, & P.M. Midgley (Eds.), *Climate Change 2013: The Physical Science Basis. Contribution of Working Group I to the Fifth Assessment Report of the Intergovernmental Panel on Climate Change*. Cambridge, United Kingdom and New York, NY, USA: Cambridge University Press

de Groot, W.J., Cantin, A.S., Flannigan, M.D., Soja, A.J., Gowman, L.M., & Newbery, A. (2013). A comparison of Canadian and Russian boreal forest fire regimes. *Forest Ecology and Management*, 294, 23-34. <http://dx.doi.org/10.1016/j.foreco.2012.07.033>

Dixon, R.K., Brown, S., Houghton, R.A., Solomon, A.M., Trexler, M.C., & Wisniewski, J. (1994). Carbon Pools and Flux of Global Forest Ecosystems. *Science*, 263, 185-190. <http://dx.doi.org/10.1126/science.263.5144.185>

Euskirchen, E.S., McGuire, A.D., Rupp, T.S., Chapin, F.S., & Walsh, J.E. (2009). Projected changes in atmospheric heating due to changes in fire disturbance and the snow season in the western Arctic, 2003-2100. *Journal of Geophysical Research-Biogeosciences*, 114 <http://dx.doi.org/10.1029/2009jg001095>

Flato, G., J. Marotzke, B. Abiodun, P. Braconnot, S.C. Chou, W. Collins, P. Cox, F. Driouech, S. Emori, V. Eyring, C. Forest, P. Gleckler, E. Guilyardi, C. Jakob, V. Kattsov, C. Reason and M. Rummukainen (2013). Evaluation of Climate Models. In T.F. Stocker, D. Qin, G.-K. Plattner, M. Tignor, S.K. Allen, J. Boschung, A. Nauels, Y. Xia, V. Bex, & P.M. Midgley (Eds.), *Climate Change 2013: The Physical Science Basis. Contribution of Working Group I to the Fifth Assessment Report of the Intergovernmental Panel on Climate Change*. Cambridge, United Kingdom and New York, NY, USA: Cambridge University Press

French, N.H.F., Kasischke, E.S., Hall, R.J., Murphy, K.A., Verbyla, D.L., Hoy, E.E., & Allen, J.L. (2008). Using Landsat data to assess fire and burn severity in the North American boreal forest region: an overview and summary of results. *International Journal of Wildland Fire*, 17, 443-462. <http://dx.doi.org/10.1071/wf08007>

Friedl, M.A., McIver, D.K., Hodges, J.C.F., Zhang, X.Y., Muchoney, D., Strahler, A.H., Woodcock, C.E., Gopal, S., Schneider, A., Cooper, A., Baccini, A., Gao, F., & Schaaf, C. (2002). Global land cover mapping from MODIS: algorithms and early results. *Remote Sensing of Environment*, 83, 287-302. [http://dx.doi.org/10.1016/s0034-4257\(02\)00078-0](http://dx.doi.org/10.1016/s0034-4257(02)00078-0)

Friedl, M.A., Sulla-Menashe, D., Tan, B., Schneider, A., Ramankutty, N., Sibley, A., & Huang, X.M. (2010). MODIS Collection 5 global land cover:

Algorithm refinements and characterization of new datasets. *Remote Sensing of Environment*, 114, 168-182. <http://dx.doi.org/10.1016/j.rse.2009.08.016>

Fuentes, D., Gamon, J., Qiu, H.-l., Sims, D., & Roberts, D. (2001). Mapping Canadian boreal forest vegetation using pigment and water absorption features derived from the AVIRIS sensor. *Journal of Geophysical Research. D. Atmospheres*, 106, 33. <http://dx.doi.org/10.1029/2001JD900110>

Furyaev, V.V., Vaganov, E.A., Tchebakova, N.M., & Valendik, E.N. (2001). Effects of fire and climate on successions and structural changes in the Siberian boreal forest. *Eurasian Journal of Forest Research*, 2, 1-15.

Gao, B.-C. (1996). NDWI—A normalized difference water index for remote sensing of vegetation liquid water from space. *Remote Sensing of Environment*, 58, 257-266. [http://dx.doi.org/10.1016/S0034-4257\(96\)00067-3](http://dx.doi.org/10.1016/S0034-4257(96)00067-3)

Garcia, M.J.L., & Caselles, V. (1991). Mapping burns and natural reforestation using Thematic Mapper data. *Geocarto International*, 6, 31-37. <http://dx.doi.org/10.1080/10106049109354290>

Giglio, L., Descloitres, J., Justice, C.O., & Kaufman, Y.J. (2003). An enhanced contextual fire detection algorithm for MODIS. *Remote Sensing of Environment*, 87, 273-282. [http://dx.doi.org/10.1016/s0034-4257\(03\)00184-6](http://dx.doi.org/10.1016/s0034-4257(03)00184-6)

Goldammer, J.G., & Furyaev, V.V. (1996). Fire in Ecosystems of Boreal Eurasia: Ecological Impacts and Links to the Global System. In J.G. Goldammer, & V.V. Furyaev (Eds.), *Forestry Sciences; Fire in ecosystems of Boreal Eurasia* (pp. 1-20): Kluwer Academic Publishers, PO Box 989, 3300 AZ Dordrecht, Netherlands 101 Phillip Drive, Norwell, Massachusetts 02061, USA

Goulden, M.L., Winston, G.C., McMillan, A.M.S., Litvak, M.E., Read, E.L., Rocha, A.V., & Rob Elliot, J. (2006). An eddy covariance mesonet to measure the effect of forest age on land-atmosphere exchange. *Global Change Biology*, 12, 2146-2162. <http://dx.doi.org/10.1111/j.1365-2486.2006.01251.x>

Goward, S., Arvidson, T., Williams, D., Faundeen, J., Irons, J., & Franks, S. (2006). Historical Record of Landsat Global Coverage. *Photogrammetric Engineering & Remote Sensing*, 72, 1155-1169. <http://dx.doi.org/10.14358/PERS.72.10.1155>

Gower, S.T., McMurtrie, R.E., & Murty, D. (1996). Aboveground net primary production decline with stand age: potential causes. *Trends in Ecology & Evolution*, 11, 378-382. [http://dx.doi.org/10.1016/0169-5347\(96\)10042-2](http://dx.doi.org/10.1016/0169-5347(96)10042-2)

Groisman, P.Y., Sherstyukov, B.G., Razuvaev, V.N., Knight, R.W., Enloe, J.G., Stroumentova, N.S., Whitfield, P.H., Førlund, E., Hannsen-Bauer, I., Tuomenvirta, H., Aleksandersson, H., Mescherskaya, A.V., & Karl, T.R. (2007). Potential forest fire danger over Northern Eurasia: Changes during the 20th century.

*Global and Planetary Change*, 56, 371-386.  
<http://dx.doi.org/10.1016/j.gloplacha.2006.07.029>

Hall, D., Riggs, G., & Salomonson, V. (2006). MODIS/Terra Snow Cover Daily L3 Global 500m Grid V005, 2000–2011. *Boulder, Colo, USA, National Snow and Ice Data Center. Digital media*

Hall, D.K., Foster, J.L., Irons, J.R., & Dabney, P.W. (1993). Airborne bidirectional radiances of snow covered surfaces in Montana, U.S.A. *U.S.A.. Annals of Glaciology*, 17, 35-40.

Hansen, J., Sato, M., & Ruedy, R. (1997). Radiative forcing and climate response. *Journal of Geophysical Research: Atmospheres*, 102, 6831-6864.  
<http://dx.doi.org/10.1029/96JD03436>

Hansen, M.C., Potapov, P.V., Moore, R., Hancher, M., Turubanova, S.A., Tyukavina, A., Thau, D., Stehman, S.V., Goetz, S.J., Loveland, T.R., Kommareddy, A., Egorov, A., Chini, L., Justice, C.O., & Townshend, J.R.G. (2013). High-Resolution Global Maps of 21st-Century Forest Cover Change. *Science*, 342, 850-853. <http://dx.doi.org/10.1126/science.1244693>

Hantson, S., Arneeth, A., Harrison, S.P., Kelley, D.I., Prentice, I.C., Rabin, S.S., Archibald, S., Mouillot, F., Arnold, S.R., Artaxo, P., Bachelet, D., Ciais, P., Forrest, M., Friedlingstein, P., Hickler, T., Kaplan, J.O., Kloster, S., Knorr, W., Lasslop, G., Li, F., Mangeon, S., Melton, J.R., Meyn, A., Sitch, S., Spessa, A., van der Werf, G.R., Voulgarakis, A., & Yue, C. (2016). The status and challenge of global fire modelling. *Biogeosciences*, 13, 3359-3375. <http://dx.doi.org/10.5194/bg-13-3359-2016>

Harden, J.W., Trumbore, S.E., Stocks, B.J., Hirsch, A., Gower, S.T., O'Neill, K.P., & Kasischke, E.S. (2000). The role of fire in the boreal carbon budget. *Global Change Biology*, 6, 174-184. <http://dx.doi.org/10.1046/j.1365-2486.2000.06019.x>

Hartmann, D.L., A.M.G. Klein Tank, M. Rusticucci, L.V. Alexander, S. Brönnimann, Y. Charabi, F.J. Dentener, E.J. Dlugokencky, D.R. Easterling, A. Kaplan, B.J. Soden, P.W. Thorne, M. Wild and P.M. Zhai (2013). Observations: Atmosphere and Surface. In T.F. Stocker, D. Qin, G.-K. Plattner, M. Tignor, S.K. Allen, J. Boschung, A. Nauels, Y. Xia, V. Bex and P.M. Midgley (Ed.), *Climate Change 2013: The Physical Science Basis. Contribution of Working Group I to the Fifth Assessment Report of the Intergovernmental Panel on Climate Change*. Cambridge, United Kingdom and New York, NY, USA: Cambridge University Press

Herzschuh, U., Pestryakova, L.A., Savelieva, L.A., Heinecke, L., Böhmer, T., Biskaborn, B.K., Andreev, A., Ramisch, A., Shinneman, A.L.C., & Birks, H.J.B. (2013). Siberian larch forests and the ion content of thaw lakes form a geochemically functional entity. *Nat Commun*, 4 <http://dx.doi.org/10.1038/ncomms3408>

- Hoy, E.E., French, N.H.F., Turetsky, M.R., Trigg, S.N., & Kasischke, E.S. (2008). Evaluating the potential of Landsat TM/ETM+ imagery for assessing fire severity in Alaskan black spruce forests. *International Journal of Wildland Fire*, 17, 500-514. <http://dx.doi.org/10.1071/wf08107>
- Huang, C., Goward, S.N., Masek, J.G., Gao, F., Vermote, E.F., Thomas, N., Schleeweis, K., Kennedy, R.E., Zhu, Z., Eidenshink, J.C., & Townshend, J.R.G. (2009). Development of time series stacks of Landsat images for reconstructing forest disturbance history. *International Journal of Digital Earth*, 2, 195-218. <http://dx.doi.org/10.1080/17538940902801614>
- Huang, C., Goward, S.N., Masek, J.G., Thomas, N., Zhu, Z., & Vogelmann, J.E. (2010). An automated approach for reconstructing recent forest disturbance history using dense Landsat time series stacks. *Remote Sensing of Environment*, 114, 183-198. <http://dx.doi.org/10.1016/j.rse.2009.08.017>
- Isaev, A.S., Korovin, G.N., Bartalev, S.A., Ershov, D.V., Janetos, A., Kasischke, E.S., Shugart, H.H., French, N.H.F., Orlick, B.E., & Murphy, T.L. (2002). Using Remote Sensing to Assess Russian Forest Fire Carbon Emissions. *Climatic Change*, 55, 235-249. <http://dx.doi.org/10.1023/a:1020221123884>
- Jin, Y.F., Randerson, J.T., Goetz, S.J., Beck, P.S.A., Loranty, M.M., & Goulden, M.L. (2012a). The influence of burn severity on postfire vegetation recovery and albedo change during early succession in North American boreal forests. *Journal of Geophysical Research-Biogeosciences*, 117 <http://dx.doi.org/10.1029/2011jg001886>
- Jin, Y.F., Randerson, J.T., Goulden, M.L., & Goetz, S.J. (2012b). Post-fire changes in net shortwave radiation along a latitudinal gradient in boreal North America. *Geophysical Research Letters*, 39 <http://dx.doi.org/10.1029/2012gl051790>
- Kalnay, E., Kanamitsu, M., Kistler, R., Collins, W., Deaven, D., Gandin, L., Iredell, M., Saha, S., White, G., & Woollen, J. (1996). The NCEP/NCAR 40-year reanalysis project. *Bulletin of the American Meteorological Society*, 77, 437-471. [http://dx.doi.org/10.1175/1520-0477\(1996\)077<0437:TNYRP>2.0.CO;2](http://dx.doi.org/10.1175/1520-0477(1996)077<0437:TNYRP>2.0.CO;2)
- Kantzas, E., Lomas, M., & Quegan, S. (2013). Fire at high latitudes: Data-model comparisons and their consequences. *Global Biogeochemical Cycles*, 27, 677-691. <http://dx.doi.org/10.1002/gbc.20059>
- Kasischke, E., & Stocks, B. (2000). Introduction. In E. Kasischke, & B. Stocks (Eds.), *Fire, Climate Change, and Carbon Cycling in the Boreal Forest* (pp. 1-5): Springer New York
- Kasischke, E.S. (2000). Boreal ecosystems in the global carbon cycle. In E.S. Kasischke, & B.J. Stocks (Eds.), *Fire, Climate Change and Carbon Cycling in the Boreal Forest* (pp. 19-30). New York, NY, USA: Springer-Verlag



Kasischke, E.S., O'Neill, K.P., French, N.H.F., Richter, D.D., Bourgeau-Chavez, L.L., & Harrell, P.H. (2000). Influence of fire on long-term patterns of forest succession in Alaskan boreal forests. In E.S. Kasischke, & B.J. Stocks (Eds.), *Fire, Climate Change and Carbon Cycling in the Boreal Forest* (pp. 214-238). New York, NY, USA: Springer

Kato, S., Loeb, N.G., Rose, F.G., Doelling, D.R., Rutan, D.A., Caldwell, T.E., Yu, L., & Weller, R.A. (2013). Surface irradiances consistent with CERES-derived top-of-atmosphere shortwave and longwave irradiances. *Journal of Climate*, 26, 2719-2740. <http://dx.doi.org/10.1175/JCLI-D-12-00436.1>

Key, C.H., & Benson, N.C. (2006). Landscape Assessment: Ground measure of severity, the Composite Burn Index; and Remote sensing of severity, the Normalized Burn Ratio. In D.C. Lutes, R.E. Keane, J.F. Caratti, C.H. Key, N.C. Benson, S. Sutherland, & L.J. Gangi (Eds.), *FIREMON: Fire Effects Monitoring and Inventory System*. Ogden, UT: USDA Forest Service, Rocky Mountain Research Station.

Kharuk, V.I., Dvinskaya, M.L., Petrov, I.A., Im, S.T., & Ranson, K.J. (2016). Larch forests of Middle Siberia: long-term trends in fire return intervals. *Regional Environmental Change*, 1-9. <http://dx.doi.org/10.1007/s10113-016-0964-9>

Kharuk, V.I., Ranson, K.J., & Dvinskaya, M.L. (2010). Wildfire Dynamics in Mid-Siberian Larch Dominated Forests. In H. Balzter (Ed.), *Environmental Change in Siberia* (pp. 83-100): Springer Netherlands

Kharuk, V.I., Ranson, K.J., Dvinskaya, M.L., & Im, S.T. (2011). Wildfires in northern Siberian larch dominated communities. *Environmental Research Letters*, 6 <http://dx.doi.org/10.1088/1748-9326/6/4/045208>

Kim, D.-H., Sexton, J.O., Noojipady, P., Huang, C., Anand, A., Channan, S., Feng, M., & Townshend, J.R. (2014). Global, Landsat-based forest-cover change from 1990 to 2000. *Remote Sensing of Environment*, 155, 178-193. <http://dx.doi.org/10.1016/j.rse.2014.08.017>

Kirtman, B., S.B. Power, J.A. Adedoyin, G.J. Boer, R. Bojariu, I. Camilloni, F.J. Doblas-Reyes, A.M. Fiore, M. Kimoto, G.A. Meehl, M. Prather, A. Sarr, C. Schär, R. Sutton, G.J. van Oldenborgh, G. Vecchi and H.J. Wang (2013). Near-term Climate Change: Projections and Predictability. In T.F. Stocker, D. Qin, G.-K. Plattner, M. Tignor, S.K. Allen, J. Boschung, A. Nauels, Y. Xia, V. Bex and P.M. Midgley (Ed.), *Climate Change 2013: The Physical Science Basis. Contribution of Working Group I to the Fifth Assessment Report of the Intergovernmental Panel on Climate Change*. Cambridge, United Kingdom and New York, NY, USA: Cambridge University Press

Kobak, K.I., Turcmnovich, I.Y., Kondrasiheva, N.Y., Schulze, E.D., Schulze, W., Koch, H., & Vygodskaya, N.N. (1996). Vulnerability and adaptation of the larch

forest in eastern Siberia to climate change. *Water, Air, and Soil Pollution*, 92, 119-127. <http://dx.doi.org/10.1007/BF00175558>

Korovin, G.N. (1996). Analysis of the Distribution of Forest Fires in Russia. In J.G. Goldammer, & V.V. Furyaev (Eds.), *Fire in Ecosystems of Boreal Eurasia* (pp. 112-128). Dordrecht: Springer Netherlands

Kovalskyy, V., & Roy, D.P. (2013). The global availability of Landsat 5 TM and Landsat 7 ETM + land surface observations and implications for global 30 m Landsat data product generation. *Remote Sensing of Environment*, 130, 280-293. <http://dx.doi.org/10.1016/j.rse.2012.12.003>

Krylov, A., L. McCarty, J., Potapov, P., Loboda, T., Tyukavina, A., Turubanova, S., & C. Hansen, M. (2014). Remote sensing estimates of stand-replacement fires in Russia, 2002–2011. *Environmental Research Letters*, 9, 105007. <http://dx.doi.org/10.1088/1748-9326/9/10/105007>

Kukavskaya, E.A., Buryak, L.V., Kalenskaya, O.P., & Zarubin, D.S. (2017). Transformation of the ground cover after surface fires and estimation of pyrogenic carbon emissions in the dark-coniferous forests of Central Siberia. *Contemporary Problems of Ecology*, 10, 62-70. <http://dx.doi.org/10.1134/s1995425517010073>

Kukavskaya, E.A., Soja, A.J., Petkov, A.P., Ponomarev, E.I., Ivanova, G.A., & Conard, S.G. (2012). Fire emissions estimates in Siberia: evaluation of uncertainties in area burned, land cover, and fuel consumption. *Canadian Journal of Forest Research*, 43, 493-506. <http://dx.doi.org/10.1139/cjfr-2012-0367>

Larsen, J.A. (1980). *The Boreal Ecosystem*. New York, NY, USA: Academic Press

Liang, S.L. (2004). *Quantitative Remote Sensing of Land Surfaces*. Hoboken, NJ, USA: Wiley-Interscience

Linke, J., Fortin, M.-J., Courtenay, S., & Cormier, R. (2017). High-resolution global maps of 21st-century annual forest loss: Independent accuracy assessment and application in a temperate forest region of Atlantic Canada. *Remote Sensing of Environment*, 188, 164-176. <http://dx.doi.org/10.1016/j.rse.2016.10.040>

Liu, H.P., & Randerson, J.T. (2008). Interannual variability of surface energy exchange depends on stand age in a boreal forest fire chronosequence. *Journal of Geophysical Research-Biogeosciences*, 113 <http://dx.doi.org/10.1029/2007jg000483>

Loboda, T., O'Neal, K.J., & Csiszar, I. (2007). Regionally adaptable dNBR-based algorithm for burned area mapping from MODIS data. *Remote Sensing of Environment*, 109, 429-442. <http://dx.doi.org/10.1016/j.rse.2007.01.017>

Loboda, T.V., & Chen, D. (2016). Spatial distribution of young forests and carbon fluxes within recent disturbances in Russia. *Global Change Biology* <http://dx.doi.org/10.1111/gcb.13349>

Loboda, T.V., Hoy, E.E., Giglio, L., & Kasischke, E.S. (2011). Mapping burned area in Alaska using MODIS data: a data limitations-driven modification to the regional burned area algorithm. *International Journal of Wildland Fire*, 20, 487-496. <http://dx.doi.org/10.1071/wf10017>

Loboda, T.V., Zhang, Z., O'Neal, K.J., Sun, G., Csiszar, I.A., Shugart, H.H., & Sherman, N.J. (2012). Reconstructing disturbance history using satellite-based assessment of the distribution of land cover in the Russian Far East. *Remote Sensing of Environment*, 118, 241-248. <http://dx.doi.org/10.1016/j.rse.2011.11.022>

Loveland, T.R., Reed, B.C., Brown, J.F., Ohlen, D.O., Zhu, Z., Yang, L., & Merchant, J.W. (2000). Development of a global land cover characteristics database and IGBP DISCover from 1 km AVHRR data. *International Journal of Remote Sensing*, 21, 1303-1330. <http://dx.doi.org/10.1080/014311600210191>

Lucht, W., Schaaf, C.B., & Strahler, A.H. (2000). An algorithm for the retrieval of albedo from space using semiempirical BRDF models. *Ieee Transactions on Geoscience and Remote Sensing*, 38, 977-998. 10.1109/36.841980

Lyons, E.A., Jin, Y.F., & Randerson, J.T. (2008). Changes in surface albedo after fire in boreal forest ecosystems of interior Alaska assessed using MODIS satellite observations. *Journal of Geophysical Research-Biogeosciences*, 113 <http://dx.doi.org/10.1029/2007jg000606>

Malhi, Y., Baldocchi, D.D., & Jarvis, P.G. (1999). The carbon balance of tropical, temperate and boreal forests. *Plant Cell and Environment*, 22, 715-740. <http://dx.doi.org/10.1046/j.1365-3040.1999.00453.x>

Masek, J.G., Huang, C., Wolfe, R., Cohen, W., Hall, F., Kutler, J., & Nelson, P. (2008). North American forest disturbance mapped from a decadal Landsat record. *Remote Sensing of Environment*, 112, 2914-2926. <http://dx.doi.org/10.1016/j.rse.2008.02.010>

McMillan, A.M.S., & Goulden, M.L. (2008). Age-dependent variation in the biophysical properties of boreal forests. *Global Biogeochemical Cycles*, 22 <http://dx.doi.org/10.1029/2007gb003038>

Melillo, J.M., McGuire, A.D., Kicklighter, D.W., Moore, B., Vorosmarty, C.J., & Schloss, A.L. (1993). Global climate change and terrestrial net primary production. *Nature*, 363, 234-240. <http://dx.doi.org/10.1038/363234a0>

Murphy, K.A., Reynolds, J.H., & Koltun, J.M. (2008). Evaluating the ability of the differenced Normalized Burn Ratio (dNBR) to predict ecologically significant

burn severity in Alaskan boreal forests. *International Journal of Wildland Fire*, 17, 490-499. <http://dx.doi.org/10.1071/wf08050>

Myhre, G., D. Shindell, F.-M. Br ón, W. Collins, J. Fuglestvedt, J. Huang, D. Koch, J.-F. Lamarque, D. Lee, B. Mendoza, T. Nakajima, A. Robock, G. Stephens, T. Takemura and H. Zhang (2013). Anthropogenic and Natural Radiative Forcing. In T.F. Stocker, D. Qin, G.-K. Plattner, M. Tignor, S.K. Allen, J. Boschung, A. Nauels, Y. Xia, V. Bex and P.M. Midgley (Ed.), *Climate Change 2013: The Physical Science Basis. Contribution of Working Group I to the Fifth Assessment Report of the Intergovernmental Panel on Climate Change*. Cambridge, United Kingdom and New York, NY, USA: Cambridge University Press

Ni, W., & Woodcock, C.E. (2000). Effect of canopy structure and the presence of snow on the albedo of boreal conifer forests. *Journal of Geophysical Research: Atmospheres*, 105, 11879-11888. <http://dx.doi.org/10.1029/1999jd901158>

Nikolov, N., & Helmisaari, H. (1992). Silvics of the circumpolar boreal forest tree species. In H.H. Shugart, R. Leemans, & G.B. Bonan (Eds.), *A Systems Analysis of the Global Boreal Forest* (pp. 13-84). Cambridge, UK: Cambridge University Press

O'Neill, K.P., Kasischke, E.S., & Richter, D.D. (2003). Seasonal and decadal patterns of soil carbon uptake and emission along an age sequence of burned black spruce stands in interior Alaska. *Journal of Geophysical Research: Atmospheres*, 108, FFR 11-11-FFR 11-15. <http://dx.doi.org/10.1029/2001JD000443>

Olofsson, P., Foody, G.M., Herold, M., Stehman, S.V., Woodcock, C.E., & Wulder, M.A. (2014). Good practices for estimating area and assessing accuracy of land change. *Remote Sensing of Environment*, 148, 42-57. <http://dx.doi.org/10.1016/j.rse.2014.02.015>

Osawa, A., & Zyryanova, O.A. (2010). Introduction. In A. Osawa, O.A. Zyryanova, Y. Matsuura, T. Kajimoto, & R.W. Wein (Eds.), *Permafrost Ecosystems: Siberian Larch Forests* (pp. 3-15): Springer, 233 Spring Street, New York, Ny 10013, United States

Pedregosa, F., Varoquaux, G., Gramfort, A., Michel, V., Thirion, B., Grisel, O., Blondel, M., Prettenhofer, P., Weiss, R., & Dubourg, V. (2011). Scikit-learn: Machine learning in Python. *Journal of Machine Learning Research*, 12, 2825-2830.

Prasad, A.M., Iverson, L.R., & Liaw, A. (2006). Newer Classification and Regression Tree Techniques: Bagging and Random Forests for Ecological Prediction. *Ecosystems*, 9, 181-199. <http://dx.doi.org/10.1007/s10021-005-0054-1>

Randerson, J.T., Liu, H., Flanner, M.G., Chambers, S.D., Jin, Y., Hess, P.G., Pfister, G., Mack, M.C., Treseder, K.K., Welp, L.R., Chapin, F.S., Harden, J.W., Goulden, M.L., Lyons, E., Neff, J.C., Schuur, E.A.G., & Zender, C.S. (2006). The

impact of boreal forest fire on climate warming. *Science*, 314, 1130-1132.  
<http://dx.doi.org/10.1126/science.1132075>

Rogers, B.M., Soja, A.J., Goulden, M.L., & Randerson, J.T. (2015). Influence of tree species on continental differences in boreal fires and climate feedbacks. *Nature Geosci*, 8, 228-234. <http://dx.doi.org/10.1038/ngeo2352>

Schaaf, C.B., Gao, F., Strahler, A.H., Lucht, W., Li, X.W., Tsang, T., Strugnell, N.C., Zhang, X.Y., Jin, Y.F., Muller, J.P., Lewis, P., Barnsley, M., Hobson, P., Disney, M., Roberts, G., Dunderdale, M., Doll, C., d'Entremont, R.P., Hu, B.X., Liang, S.L., Privette, J.L., & Roy, D. (2002). First operational BRDF, albedo nadir reflectance products from MODIS. *Remote Sensing of Environment*, 83, 135-148.  
[http://dx.doi.org/10.1016/s0034-4257\(02\)00091-3](http://dx.doi.org/10.1016/s0034-4257(02)00091-3)

Schimel, D.S., House, J.I., Hibbard, K.A., Bousquet, P., Ciais, P., Peylin, P., Braswell, B.H., Apps, M.J., Baker, D., Bondeau, A., Canadell, J., Churkina, G., Cramer, W., Denning, A.S., Field, C.B., Friedlingstein, P., Goodale, C., Heimann, M., Houghton, R.A., Melillo, J.M., Moore, B., Murdiyarso, D., Noble, I., Pacala, S.W., Prentice, I.C., Raupach, M.R., Rayner, P.J., Scholes, R.J., Steffen, W.L., & Wirth, C. (2001). Recent patterns and mechanisms of carbon exchange by terrestrial ecosystems. *Nature*, 414, 169-172. <http://dx.doi.org/10.1038/35102500>

Schroeder, T.A., Wulder, M.A., Healey, S.P., & Moisen, G.G. (2011). Mapping wildfire and clearcut harvest disturbances in boreal forests with Landsat time series data. *Remote Sensing of Environment*, 115, 1421-1433.  
<http://dx.doi.org/10.1016/j.rse.2011.01.022>

Schulze, E.D., Wirth, C., Mollicone, D., von Lupke, N., Ziegler, W., Achard, F., Mund, M., Prokushkin, A., & Scherbina, S. (2012). Factors promoting larch dominance in central Siberia: fire versus growth performance and implications for carbon dynamics at the boundary of evergreen and deciduous conifers. *Biogeosciences*, 9, 1405-1421. <http://dx.doi.org/10.5194/bg-9-1405-2012>

Shorohova, E., Kuuluvainen, T., Kangur, A., & Jogiste, K. (2009). Natural stand structures, disturbance regimes and successional dynamics in the Eurasian boreal forests: a review with special reference to Russian studies. *Annals of Forest Science*, 66 <http://dx.doi.org/10.1051/forest/2008083>

Shuman, J.K., Shugart, H.H., & O'Halloran, T.L. (2011). Sensitivity of Siberian larch forests to climate change. *Global Change Biology*, 17, 2370-2384.  
<http://dx.doi.org/10.1111/j.1365-2486.2011.02417.x>

Shvidenko, A., & Nilsson, S. (2000). Extent, Distribution, and Ecological Role of Fire in Russian Forests. In E. Kasischke, & B. Stocks (Eds.), *Fire, Climate Change, and Carbon Cycling in the Boreal Forest* (pp. 132-150): Springer New York

Sofronov, M.A., & Volokitina, A.V. (2010). Wildfire Ecology in Continuous Permafrost Zone. In A. Osawa, O.A. Zyryanova, Y. Matsuura, T. Kajimoto, & R.W. Wein (Eds.), *Permafrost Ecosystems* (pp. 59-82): Springer Netherlands

Soja, A.J., Sukhinin, A.I., Cahoon, D.R., Shugart, H.H., & Stackhouse, P.W. (2004). AVHRR-derived fire frequency, distribution and area burned in Siberia. *International Journal of Remote Sensing*, 25, 1939-1960. <http://dx.doi.org/10.1080/01431160310001609725>

Stocks, B.J., Fosberg, M.A., Lynham, T.J., Mearns, L., Wotton, B.M., Yang, Q., Jin, J.Z., Lawrence, K., Hartley, G.R., Mason, J.A., & McKenney, D.W. (1998). Climate change and forest fire potential in Russian and Canadian boreal forests. *Climatic Change*, 38, 1-13. <http://dx.doi.org/10.1023/a:1005306001055>

Sukhinin, A.I., French, N.H.F., Kasischke, E.S., Hewson, J.H., Soja, A.J., Csizar, I.A., Hyer, E.J., Loboda, T., Conrad, S.G., Romasko, V.I., Pavlichenko, E.A., Miskiv, S.I., & Slinkina, O.A. (2004). AVHRR-based mapping of fires in Russia: New products for fire management and carbon cycle studies. *Remote Sensing of Environment*, 93, 546-564. <http://dx.doi.org/10.1016/j.rse.2004.08.011>

Thomas, N.E., Huang, C., Goward, S.N., Powell, S., Rishmawi, K., Schleeweis, K., & Hinds, A. (2011). Validation of North American Forest Disturbance dynamics derived from Landsat time series stacks. *Remote Sensing of Environment*, 115, 19-32. <http://dx.doi.org/10.1016/j.rse.2010.07.009>

Tucker, C.J. (1979). Red and photographic infrared linear combinations for monitoring vegetation. *Remote Sensing of Environment*, 8, 127-150. [http://dx.doi.org/10.1016/0034-4257\(79\)90013-0](http://dx.doi.org/10.1016/0034-4257(79)90013-0)

USDA (2014). Forest Inventory and Analysis National Core Field Guide, Version 6.1. In.

Verbyla, D.L., Kasischke, E.S., & Hoy, E.E. (2008). Seasonal and topographic effects on estimating fire severity from Landsat TM/ETM+ data. *International Journal of Wildland Fire*, 17, 527-534. <http://dx.doi.org/10.1071/WF08038>

Vermote, E.F., El Saleous, N.Z., & Justice, C.O. (2002). Atmospheric correction of MODIS data in the visible to middle infrared: first results. *Remote Sensing of Environment*, 83, 97-111. [http://dx.doi.org/10.1016/S0034-4257\(02\)00089-5](http://dx.doi.org/10.1016/S0034-4257(02)00089-5)

Viereck, L.A. (1973). Wildfire in the taiga of Alaska. *Quaternary Research*, 3, 465-495. [http://dx.doi.org/10.1016/0033-5894\(73\)90009-4](http://dx.doi.org/10.1016/0033-5894(73)90009-4)

Wallenius, T., Larjavaara, M., Heikkinen, J., & Shibistova, O. (2011). Declining fires in Larix-dominated forests in northern Irkutsk district. *International Journal of Wildland Fire*, 20, 248-254. <http://dx.doi.org/10.1071/wf10020>

Wang, D., Morton, D., Masek, J., Wu, A., Nagol, J., Xiong, X., Levy, R., Vermote, E., & Wolfe, R. (2012). Impact of sensor degradation on the MODIS NDVI time series. *Remote Sensing of Environment*, *119*, 55-61.

<http://dx.doi.org/10.1016/j.rse.2011.12.001>

Ward, D.S., Kloster, S., Mahowald, N.M., Rogers, B.M., Randerson, J.T., & Hess, P.G. (2012). The changing radiative forcing of fires: global model estimates for past, present and future. *Atmos. Chem. Phys.*, *12*, 10857-10886.

<http://dx.doi.org/10.5194/acp-12-10857-2012>

Wirth, C. (2005). Fire Regime and Tree Diversity in Boreal Forests: Implications for the Carbon Cycle. In M. Scherer-Lorenzen, C. Körner, & E.-D. Schulze (Eds.), *Forest Diversity and Function* (pp. 309-344): Springer Berlin Heidelberg

Zhang, Q., Pavlic, G., Chen, W., Latifovic, R., Fraser, R., & Cihlar, J. (2004). Deriving stand age distribution in boreal forests using SPOT VEGETATION and NOAA AVHRR imagery. *Remote Sensing of Environment*, *91*, 405-418.

<http://dx.doi.org/10.1016/j.rse.2004.04.004>

Zyryanova, O.A., Abaimov, A.P., Bugaenko, T.N., & Bugaenko, N.N. (2010). Recovery of Forest Vegetation After Fire Disturbance. In A. Osawa, O.A. Zyryanova, Y. Matsuura, T. Kajimoto, & R.W. Wein (Eds.), *Permafrost Ecosystems: Siberian Larch Forests* (pp. 83-96): Springer, 233 Spring Street, New York, Ny 10013, United States